



FEDERAL UNIVERSITY OF UBERLÂNDIA  
FACULTY OF ELECTRICAL ENGINEERING

JÚLIA TANNÚS DE SOUZA

“Free to Fly”: Development and evaluation of a novel exergame with a low-cost  
3D tracking method for post-stroke rehabilitation

Uberlândia, Brazil

2021

JÚLIA TANNÚS DE SOUZA

“Free to Fly”: Development and evaluation of a novel exergame with a low-cost  
3D tracking method for post-stroke rehabilitation

Dissertation presented to the Faculty of  
Electrical Engineering at the Federal University  
of Uberlandia as a partial requirement for  
obtaining the degree Master of Science

Concentration area: Computer Graphics

Advisor: Prof. Dr. Edgard Afonso Lamounier  
Júnior

Co-advisor: Prof. Dr. Eduardo Lázaro Martins  
Naves

Uberlandia, Brazil

2021

Ficha Catalográfica Online do Sistema de Bibliotecas da UFU  
com dados informados pelo(a) próprio(a) autor(a).

S729 2021	<p>Souza, Júlia Tannús de, 1995- "Free to Fly": Development and evaluation of a novel exergame with a low-cost 3D tracking method for post- stroke rehabilitation [recurso eletrônico] / Júlia Tannús de Souza. - 2021.</p> <p>Orientador: Edgard Afonso Lamounier Júnior. Coorientador: Eduardo Lázaro Martins Naves. Dissertação (Mestrado) - Universidade Federal de Uberlândia, Pós-graduação em Engenharia Elétrica. Modo de acesso: Internet. Disponível em: <a href="http://doi.org/10.14393/ufu.di.2021.462">http://doi.org/10.14393/ufu.di.2021.462</a> Inclui bibliografia. Inclui ilustrações.</p> <p>1. Engenharia elétrica. I. Lamounier Júnior, Edgard Afonso ,1964-, (Orient.). II. Naves, Eduardo Lázaro Martins,1970-, (Coorient.). III. Universidade Federal de Uberlândia. Pós-graduação em Engenharia Elétrica. IV. Título.</p> <p style="text-align: right;">CDU: 621.3</p>
--------------	--

Bibliotecários responsáveis pela estrutura de acordo com o AACR2:

Gizele Cristine Nunes do Couto - CRB6/2091

JÚLIA TANNÚS DE SOUZA

“Free to Fly”: Development and evaluation of a novel exergame with a low-cost  
3D tracking method for post-stroke rehabilitation

Dissertation presented to the Faculty of  
Electrical Engineering at the Federal University  
of Uberlandia as a partial requirement for  
obtaining the degree Master of Science

Concentration area: Computer Graphics

Uberlandia, Brazil, 2021

Examination Board:

Prof. Dr. Edgard Afonso Lamounier Júnior – Advisor (UFU)

Prof. Dr. Eduardo Lázaro Martins Naves – Co-advisor (UFU)

Prof. Dr. Adriano de Oliveira Andrade – (UFU)

Prof. Dr. Yann Morère – (Université de Lorraine - France)



**UNIVERSIDADE FEDERAL DE UBERLÂNDIA**  
 Coordenação do Programa de Pós-Graduação em Engenharia Elétrica  
 Av. João Naves de Ávila, 2121, Bloco 3N - Bairro Santa Mônica, Uberlândia-MG, CEP 38400-902  
 Telefone: (34) 3239-4707 - www.posgrad.feelt.ufu.br - copel@ufu.br



### ATA DE DEFESA - PÓS-GRADUAÇÃO

Programa de Pós-Graduação em:	Engenharia Elétrica				
Defesa de:	Dissertação de Mestrado Acadêmico, 762, PPGEELT				
Data:	Dezoito de agosto de dois mil e vinte e um	Hora de início:	08:00	Hora de encerramento:	11:00
Matrícula do Discente:	11922EEL016				
Nome do Discente:	Júlia Tannús de Souza				
Título do Trabalho:	"Free to Fly": Development and evaluation of a novel exergame with a low-cost 3D tracking method for post-stroke rehabilitation"				
Área de concentração:	Processamento da informação				
Linha de pesquisa:	Computação gráfica				
Projeto de Pesquisa de vinculação:	Integração Sensorio-Motora Como Estratégia Para Potencialização do Reaprendizado Motor de Pacientes Paréticos Pós-AVE Agência financiadora: Não se aplica. Número do processo do projeto de pesquisa na agência financiadora: Não se aplica.				

Reuniu-se por meio de videoconferência, a Banca Examinadora, designada pelo Colegiado do Programa de Pós-graduação em Engenharia Elétrica, assim composta: Professores Doutores: Eduardo Lázaro Martins Naves - FEELT/UFU, Adriano de Oliveira Andrade - FEELT/UFU, Yann Morère - UNIVERSITÉ DE LORRAINE – FRANÇA, Edgard Afonso Lamounier Júnior - FEELT/UFU, orientador(a) do(a) candidato(a).

Iniciando os trabalhos o(a) presidente da mesa, Dr(a). Edgard Afonso Lamounier Júnior, apresentou a Comissão Examinadora e o candidato(a), agradeceu a presença do público, e concedeu ao Discente a palavra para a exposição do seu trabalho. A duração da apresentação do Discente e o tempo de arguição e resposta foram conforme as normas do Programa.

A seguir o senhor(a) presidente concedeu a palavra, pela ordem sucessivamente, aos(às) examinadores(as), que passaram a arguir o(a) candidato(a). Ultimada a arguição, que se desenvolveu dentro dos termos regimentais, a Banca, em sessão secreta, atribuiu o resultado final, considerando o(a) candidato(a):

Aprovado(a).

Esta defesa faz parte dos requisitos necessários à obtenção do título de Mestre.

O competente diploma será expedido após cumprimento dos demais requisitos, conforme as normas do Programa, a legislação pertinente e a regulamentação interna da UFU.

Nada mais havendo a tratar foram encerrados os trabalhos. Foi lavrada a presente ata que após lida e achada conforme foi assinada pela Banca Examinadora.



Documento assinado eletronicamente por **Adriano de Oliveira Andrade, Professor(a) do Magistério Superior**, em 18/08/2021, às 10:15, conforme horário oficial de Brasília, com fundamento no art. 6º, § 1º, do [Decreto nº 8.539, de 8 de outubro de 2015](#).

---



Documento assinado eletronicamente por **MORERE, Usuário Externo**, em 18/08/2021, às 10:16, conforme horário oficial de Brasília, com fundamento no art. 6º, § 1º, do [Decreto nº 8.539, de 8 de outubro de 2015](#).

---



Documento assinado eletronicamente por **Edgard Afonso Lamounier Junior, Professor(a) do Magistério Superior**, em 18/08/2021, às 10:16, conforme horário oficial de Brasília, com fundamento no art. 6º, § 1º, do [Decreto nº 8.539, de 8 de outubro de 2015](#).

---



Documento assinado eletronicamente por **Eduardo Lazaro Martins Naves, Professor(a) do Magistério Superior**, em 18/08/2021, às 10:17, conforme horário oficial de Brasília, com fundamento no art. 6º, § 1º, do [Decreto nº 8.539, de 8 de outubro de 2015](#).

---



A autenticidade deste documento pode ser conferida no site [https://www.sei.ufu.br/sei/controlador\\_externo.php?acao=documento\\_conferir&id\\_orgao\\_acesso\\_externo=0](https://www.sei.ufu.br/sei/controlador_externo.php?acao=documento_conferir&id_orgao_acesso_externo=0), informando o código verificador **2967584** e o código CRC **A54C3589**.

---

## ACKNOWLEDGEMENTS

All my gratitude to those who made this achievement possible.

To Professor Eduardo: you are a great supervisor, give me creative freedom, but still accompanies me in everything. You are a great motivator and your incentive was crucial for this project to come true. You direct me to the right path in my career and project success, and has genuine interest in helping people through technology and that inspires me. You don't let us lose focus and dedicate your time to all students. You value my work and gives me several opportunities. You take it out of your own pocket to help us buy what we need. You are very accessible, very supportive and always gives great advices.

To Professor Edgard: you never denied me an opportunity. You introduced me to research on rehabilitation technologies and encouraged me to be independent. You are a great example of a professional and inspires respect in everyone. You help whenever you can, with wise placements, always. Thank you for always believing in me.

To the multidisciplinary team at the Assistive Technology Laboratory, for being so receptive towards me, being so kind and helping me. You are very inspiring and make me proud.

To my work partner, MSc. Caroline Valentini, for her contributing ideas, willingness to apply the tests and supply the post-stroke volunteers in the future. It has been a pleasure to work with your collaboration.

To the Federal University of Uberlandia and the National Council for Scientific and Technological Development (CNPq), for all the opportunities and financial support.

To my parents, the greatest blessing of my life.

Thank you!

## ABSTRACT

Stroke is one of the main causes of long-term disability worldwide. Conventional upper limb physiotherapy programs can be tedious, expensive and require physical transportation. Video games can help solve these problems. In fact, recent studies show that health professionals are increasingly interested in using computer games for post-stroke rehabilitation. However, commercial possibilities can be inaccessible and inadequate to the needs of patients and therapists. Also, among academic research solutions, there is a prevalence of: exoskeletons, inertial, magnetic and ultrasonic sensors, all electronics of significant cost and difficult to obtain (imported). In Brazil, it is important to remember that financial conditions can be minimal. In this work, a solution for the following problems: time (for the proper set up of every session; lack of time of the therapist to accompany the rehabilitation sessions), space (for equipment to be stored; for some camera systems to capture the full movement properly), and cost (for private clinicians and patients themselves, some systems can be inaccessible, because they can require sophisticated electronic devices) was attempted, trying to develop a very accessible post-stroke rehabilitation exergame alternative. Thus, a video game with an innovative alternative for tracking the 3D movement of the upper limb was made, after reviewing the bibliographic and patent literature and identifying the needs directly from an occupational therapist and her stroke patients, which uses optical capture with a regular camera and colored sphere markers, while maintaining lightweight real-time processing on mobile devices. The game has 2D and 3D versions, for both Windows and Android, simplified interface and progress monitoring. The fact that the controller can be handcrafted by the users makes the game very low-cost, possible to be distributed worldwide, reaching a large number of people, and possible to be played and monitored remotely. The proposed system was tested in order to find out how accurate it can be, compared to a gold standard system (a goniometer). It has been found that the system has limitations, such as low accuracy at obtuse angles, illumination variation, small spheres (the type of marker utilized), occlusions, camera distortions and motion blur. Still, it can be faster than using fiducial markers or Deep Learning, since it is a simpler algorithm, leading to a higher frame rate, which was demonstrated in this work, and can be very accurate when respecting the aforementioned problems. In conclusion, the system seems promising, due to its accessibility, very low cost, customization to the needs of patients and therapists and good tests results, as a complementary alternative for post-stroke rehabilitation.

**Keywords:** Stroke. Rehabilitation. Camera. Computer Vision. Video games



## LIST OF FIGURES

<b>Figure 1</b> – The system developed previously was expensive to some private practitioners and patients.....	16
<b>Figure 2</b> – Motion tracking device categories. ....	20
<b>Figure 3</b> – (a) Kinect sensor and (b) depth map with skeletal estimation. ....	20
<b>Figure 4</b> – Five typical arm spasticity patterns.....	22
<b>Figure 5</b> – PRISMA flow diagram of study selection. ....	27
<b>Figure 6</b> – Devices employed in selected studies by year (some studies used more than one device). ....	28
<b>Figure 7</b> – Commercial devices categories and frequencies.....	30
<b>Figure 8</b> – Related work by Schweighofer (2019).....	38
<b>Figure 9</b> – Projection tracking using colored bands. ....	38
<b>Figure 10</b> – Schematics of the intended application: the movement of an object, held by the patient, is captured by a camera and, through a tracking algorithm, translated into game commands.....	40
<b>Figure 11</b> – Color tracking thresholding works by defining an upper and lower range in a given color space, in this case, HSV, (left) and then masking this color (right) from the original image, detecting the object (center). ....	41
<b>Figure 12</b> – Schematic of the algorithm test.....	43
<b>Figure 13</b> – Success chart. ....	45
<b>Figure 14</b> – Precision chart. ....	45
<b>Figure 15</b> – Time per frame chart. ....	46
<b>Figure 16</b> – The controller of the game consists of spheres, which can be made out of craft materials and placed to measure the angle of any joint in the body.....	49
<b>Figure 17</b> – Original image (left) and corrected (right).....	50
<b>Figure 18</b> – Before (left) and after (right) the morphological opening operation. ....	51
<b>Figure 19</b> – Detected sphere and its 2D pixel coordinates. Observe that the tests were done in a common room without a special background. ....	52
<b>Figure 20</b> – Field of view of a camera. ....	52
<b>Figure 21</b> – A change in the z axis (3D) (a) when the object is near the center of the camera and (b) when the object is dislocated from the center of the camera: the x axis of the 2D projection is also dislocated.....	53
<b>Figure 22</b> – The Perspective-n-Point problem.....	54

<b>Figure 23</b> – The angle of the elbow joint can be found by the law of cosines. ....	55
<b>Figure 24</b> – System usage flow.....	56
<b>Figure 25</b> – Initial questionnaire screen: (a) consent form and (b) general information collection. ....	57
<b>Figure 26</b> – Initial interface of the game in the (a) 2D and (b) 3D versions. ....	58
<b>Figure 27</b> – Camera calibration interface – 3D version.....	58
<b>Figure 28</b> – Color calibration panel – 2D version. ....	59
<b>Figure 29</b> – Configuration panel – 3D version. ....	59
<b>Figure 30</b> – The difficulty adjustment panel captures the current angle range and extension velocity. This information is used to adjust the difficulty of the game and in the progress report. ....	60
<b>Figure 31</b> – Difficulty choice panel. ....	60
<b>Figure 32</b> – Exergame - 2D version.....	61
<b>Figure 33</b> – Exergame – 3D version. ....	62
<b>Figure 34</b> – Drawing coordination test. ....	63
<b>Figure 35</b> – Example of progress report generated by the game. ....	67
<b>Figure 36</b> – Goniometer with spheres attached. ....	68
<b>Figure 37</b> – Angle readings chart. ....	73
<b>Figure 38</b> – Distance readings chart. ....	73
<b>Figure 39</b> – $42\sin\left(\frac{\theta}{2}\right)$ plot from chord length formula.....	73
<b>Figure 40</b> – Experimental results of measuring the distance (in red) between angles in a protractor. ....	74
<b>Figure 41</b> – Error of the mean of each angle. ....	74
<b>Figure 42</b> – Interference of number of photos on the accuracy. ....	74
<b>Figure 43</b> – Influence of the sphere x and y coordinates on the angle error.....	77
<b>Figure 44</b> – Original (left) and corrected (right) images. ....	77
<b>Figure 45</b> – Influence of the speed on the angle error. ....	78

**LIST OF TABLES**

<b>Table 1</b> – Search strategy.....	24
<b>Table 2</b> – Keywords for the patent search. ....	25
<b>Table 3</b> – Websites screened for the patent search. ....	25
<b>Table 4</b> – Summary of related studies – first review. ....	30
<b>Table 5</b> – Summary of related studies – second review.....	32
<b>Table 6</b> – Comparison study. ....	33
<b>Table 7</b> – Classification of device tracking types of the selected studies. ....	35
<b>Table 8</b> – List of problems for tracking algorithms. ....	43
<b>Table 9</b> – All precision results. ....	47
<b>Table 10</b> – Variables that are used to adjust the difficulty. ....	63
<b>Table 11</b> – Influence of sphere diameter and distance from camera on accuracy. ....	75

## CONTENTS

<b>1 INTRODUCTION .....</b>	<b>14</b>
<b>1.1 Context.....</b>	<b>14</b>
<b>1.2 Justification .....</b>	<b>15</b>
<b>1.3 Objective.....</b>	<b>17</b>
1.3.1 General Objective .....	17
1.3.2 Specific Objectives .....	17
<b>1.4 Chapter Organization .....</b>	<b>18</b>
<b>2 THEORETICAL FOUNDATION .....</b>	<b>19</b>
<b>2.1 Exergames .....</b>	<b>19</b>
<b>2.2 Computer Vision.....</b>	<b>19</b>
<b>2.3 OpenCV .....</b>	<b>21</b>
<b>2.4 Post-stroke Recovery Stages .....</b>	<b>21</b>
<b>2.5 Final Considerations.....</b>	<b>23</b>
<b>3 LITERATURE REVIEW .....</b>	<b>24</b>
<b>3.1 Sources and Search Strategy .....</b>	<b>24</b>
<b>3.2 Inclusion Criteria.....</b>	<b>26</b>
<b>3.3 Data Extraction.....</b>	<b>27</b>
<b>3.4 Correlated Work.....</b>	<b>28</b>
<b>3.5 Final Considerations.....</b>	<b>36</b>
<b>4 MATERIALS AND METHODS .....</b>	<b>39</b>
<b>4.1 Determination of the Tracking Algorithm .....</b>	<b>39</b>
4.1.1 OpenCV tracking algorithms .....	39
4.1.2 Algorithm testing methods .....	42
4.1.3 Algorithm tests results .....	44
<b>4.2 System Development.....</b>	<b>47</b>
4.2.1 Theoretical base .....	47
4.2.2 Software development tools .....	55
4.2.3 System architecture and interface .....	55
4.2.4 Difficulty adjustment .....	63
4.2.5 Collected data and progress report .....	66
<b>4.3 System Tests .....</b>	<b>68</b>
<b>4.4 Final Considerations.....</b>	<b>70</b>

<b>5 RESULTS AND DISCUSSION .....</b>	<b>71</b>
<b>5.1 Final Considerations.....</b>	<b>79</b>
<b>6 CONCLUSIONS AND FUTURE WORK.....</b>	<b>80</b>
<b>6.1 Research Conclusions .....</b>	<b>80</b>
<b>6.2 Future Works .....</b>	<b>81</b>
<b>BIBLIOGRAPHY .....</b>	<b>83</b>

---

# INTRODUCTION

---

## 1.1 Context

Stroke is a major cause of long-term disability. In Brazil, in 2013, it has been estimated that 568,000 people had very severe limitations after a stroke, with the prevalence of post-stroke disability being 29.5% in men and 21.5% in women (Bensenor et al., 2015). In addition, this number was not statistically different according to sociodemographic data, being able to reach any part of the population (Bensenor et al., 2015).

Despite encouraging data on the recent decline in the incidence of stroke, on a global level, the aging population and the accumulation of risk factors contribute to an increasing risk of stroke throughout life (Feigin et al., 2018). According to the Global Burden of Disease 2016 Lifetime Risk of Stroke Collaborators, the mean global lifetime risk of stroke has increased from 22.8% in 1990 to 24.9% in 2016 (Feigin et al., 2018). In 2020, on average, every 40 seconds, someone in the United States suffered a stroke (Virani et al., 2020). In addition, studies indicate that in 30% (Heller et al., 1987) to 66% of patients (Sunderland et al., 1989; Wade et al., 1983), the affected arm remains without function for at least 6 months later, while only 5% to 20% demonstrate complete functional recovery (Heller et al., 1987; Nakayama et al., 1994), which has a highly negative impact on the quality of life, social and daily activities.

A physical therapy routine can improve motor function of the upper limb. However, conventional programs can be time-consuming, labor- and resource-intensive, and dependent on patient compliance. They also can have limited availability depending on geography, modest and delayed effects, be tedious, expensive and require physical transportation (Saposnik & Levin, 2011). Video games can help solving these problems, as they are engaging for players, generate entertainment, motivation, in addition of being able to be played at home, without the need for transportation of the patient (Pyae et al., 2015; Saposnik, 2016). In 2011, a meta-analysis of randomized and observational clinical studies concluded that, indeed, these applications are potentially useful and can be combined with conventional rehabilitation for the

functional improvement of the arm, cognition and quality of life after stroke (Saposnik & Levin, 2011).

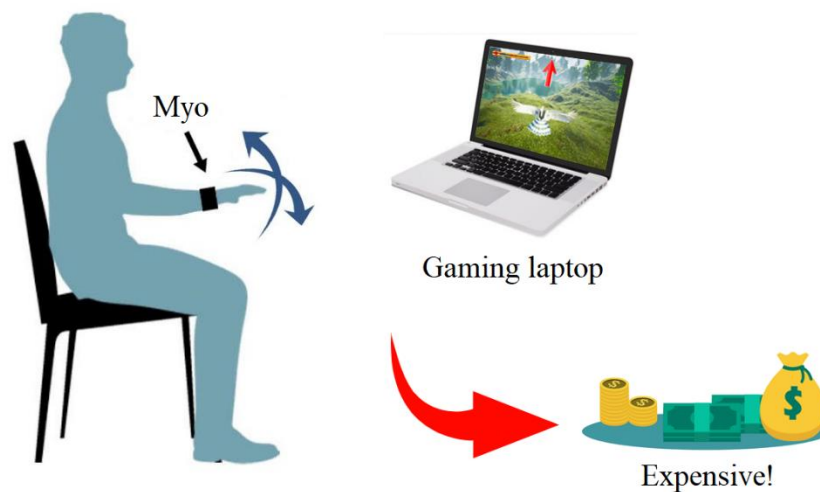
## 1.2 Justification

For these reasons, recent studies show that health professionals are increasingly interested in using computer games for post-stroke rehabilitation. To this end, commercial alternatives, such as games that use the Wii Remote and Kinect sensors, which capture the physical movement of players, are the most sought after, due to their relatively accessible hardware and exercise games (Thomson et al., 2016). Regarding the difficulties of transferring these technologies to the public, a 2016 study found that gaming was currently used by only 18% of therapists, but 61% (68/112) stated that they would use this intervention should equipment be available and other barriers, such as time (for the proper set up of every session; lack of time of the therapist to accompany the rehabilitation sessions), space (for equipment to be stored; for some camera systems to capture the full movement properly), and cost (for private clinicians and patients themselves, in Brazil, some systems can be inaccessible, since they can require sophisticated electronic devices) (Thomson et al., 2016). These barriers were also observed in Brazil after a previous study (Cyrino et al., 2018), when it was tried to distribute the developed gaming system to local clinicians and patients. As it was necessary to have a computer device with gaming specifications to play the heavy processing video game and an inertial sensor device for 3D orientation tracking of the arm, it was not possible to transfer it to the public, since all the equipment ended up being too expensive ([Figure 1](#)). For comparison between the cited devices, a full Nintendo Wii system “can easily cross the magic US\$1,000 mark” (Guina, 2020), an Azure Kinect (sensor only) had an official price tag of US\$399 in 2019 (Warren, 2019), cheap gaming laptop options usually run between \$700 and \$1,000 (Goldman, 2020) and the Myo inertial sensor armband, currently out of production, had an official cost of US\$199 in 2015 (Mack, 2015). In addition to the conversion of the currency to Brazilian Real, which is more devalued, heavy taxes on imports also apply, on a population with a low purchasing power already. These costs can be inaccessible to private practitioners and patients that do not have access to more expensive solutions, taking in consideration all financial conditions.

Also, although commercial games, for being readily accessible, are used in clinical rehabilitation by therapists around the world, most of them are not well-designed for stroke

patients and their motivational needs in rehabilitation (Pyae et al., 2015), for it should be noticed that they are designed for young and healthy people and for entertainment purposes only. In this way, there are some problems in using commercial games for rehabilitation, which can be defined: the difficulty of the game can be excessive and is not adjustable for different levels of disability; games do not transmit feedback on motor progress; the therapist's participation in the follow-up is not considered; the theme and motivational content are not directed at stroke patients; and the movements required may not be suitable for post-stroke physical therapy (Pyae et al., 2015). Regarding post-stroke rehabilitation games developed in research, even though they generally access the previous needs, it is also found a prevalence of reasonably complex electronic devices, which can be high-cost, and the fact that these systems have a low probability to be worldwide available, thus, oftentimes, not reaching the final customers (Y. Chen et al., 2019).

**Figure 1** – The system developed previously was expensive to some private practitioners and patients.



Source: The author.

Therefore, these gaps between rehabilitation and motivational needs of stroke patients and existing game technologies must be bridged. To this end, a new alternative for tracking the 3D movement of the upper limb was developed, using optical capture with a regular camera and a special algorithm that enables real-time capture on mobile devices, for use in a custom-made game taking into account the needs of post-stroke patients and their therapists. The main advantage of this system is the fact that it is very low or zero cost, since it uses artifacts that the patient already has at home or are easily obtainable, that is, either a smartphone, tablet or computer with a webcam, even some of the most basic models, which 79.3% of the Brazilian



population has access to (IBGE, 2018), and small colored spheres, which can be made using craft materials. Also, the developed system requires a low set up time for each session; allows the patient to do a higher number of exercises, at any moment, anywhere he/she desires, without the therapist being present at every training session; does not need a big space to store equipment; does not need the patient to be standing; does not need a large distance to be captured by the camera; can be used in a large range of processing devices, even without specific gaming specifications, i.e. a graphics card; and does not need any wearable electronics.

Therefore, this work describes the development and preliminary tests of this system, hoping it can achieve a good tracking accuracy, simplified use, practicality to private practitioners and patients, and a greater accessibility than commercial solutions.

### **1.3 Objective**

#### 1.3.1 General Objective

The general objective of this work is to develop a post-stroke physiotherapy video game system, seeking a high accessibility, and an improvement in terms of time (for the proper set up of every session; lack of time of the therapist to accompany the rehabilitation sessions), space (for equipment to be stored; for some camera systems to capture the full movement properly), and cost (for private clinicians and patients themselves, in Brazil, some systems can be inaccessible, since they can require sophisticated electronic devices), in order to effectively reach a large number of users, and test its accuracy and performance.

#### 1.3.2 Specific Objectives

In order to achieve the main objective, some specific objectives were stipulated. They are:

- Research applications for post-stroke rehabilitation using Virtual Reality;
- Define the 3D tracking method that best suits the requirements of the application;
- Define the Virtual Reality game requirements for patients and therapists;
- Investigate techniques, currently adopted, that use similar 3D tracking methods;
- Develop improvements in this type of tracking, following the requirements of the application;

- Develop a software that uses the developed tracking method, to command a custom-made game;
- Test the technical accuracy of the developed system;
- Analyze the results obtained in the applied tests.

## 1.4 Chapter Organization

The methodology used to achieve the main objective of this work is described in the subsequent chapters, which follow the structure below:

In Chapter 1, an introduction and general contextualization of the topic is presented, highlighting the current reality of the application of rehabilitation technologies using Virtual Reality and exercise games to assist in post-stroke rehabilitation.

In Chapter 2, a theoretical foundation is presented on 3D tracking of the upper limb, concepts of computer vision tools and post-stroke motor rehabilitation stages.

Chapter 3 discusses the bibliographic and patent revision, which brings together a set of works that were selected and consulted, according to their relevance and contribution regarding the topic under study.

Chapter 4 presents the materials, tools and technologies used to develop the system, including the methodology adopted, its theoretical explanation and how the final application was tested.

Chapter 5 shows the result of the technical testing process, exposing the advantages and limitations of the system, with a graphical analysis of the results obtained.

Chapter 6 presents the final considerations, concluding the research on the proposal to create an application for post-stroke rehabilitation through an exercise game with a new form of 3D motion capture, bringing possible improvements and adaptations for future works.



---

## THEORETICAL FOUNDATION

---

In this chapter, some theoretical foundations that are the basis for the correct understanding of the development of this work will be presented and briefly commented, namely the concepts of exergames, Computer Vision, OpenCV and post-stroke recovery stages.

### 2.1 Exergames

“Exergame” is a term used to define a video game which integrates exercise and gaming (Reis et al., 2016). Examples of exergames popular with the general public include "Just Dance" for Xbox 360 Kinect (Xbox, 2021) and "Wii Sports" for Nintendo Wii (Wii, 2021). These games, besides providing entertainment, can generate health benefits and also positive effects in increasing the recovery process in some diseases, such as after a stroke (Reis et al., 2016).

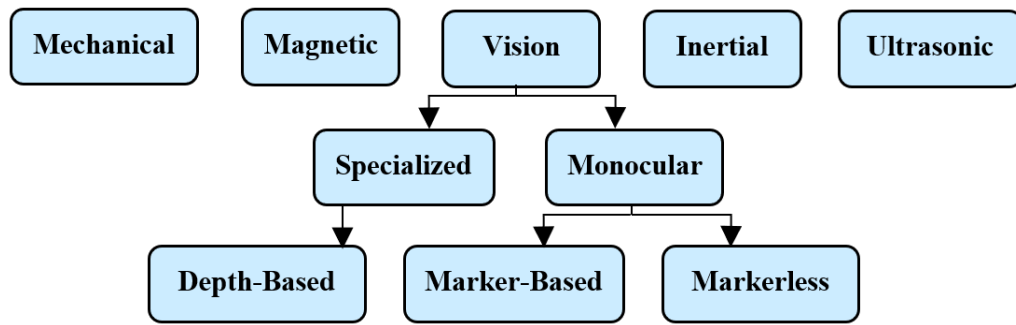
### 2.2 Computer Vision

For an exergame (exercise through a video game), it is necessary to use some form of motion tracking as input. Many technologies and devices have been tested in recent years in post-stroke rehabilitation games (da Silva Cameirão et al., 2011; GestureTek, 2016; Kwon et al., 2012; Pyae et al., 2015; Q. Wang et al., 2017). They can be summarized in mechanical, magnetic, vision, inertial and ultrasonic trackers (Billinghurst, 2013) ([Figure 2](#)).

Bearing in mind all the possible motion tracking categories, it is necessary to choose one that fits a research objective. All categories use electronic sensors, as follows:

- Mechanical: potentiometers, exoskeletons;
- Magnetic: magnetic transmitters and receivers;
- Vision: some type of camera, infrared, stereoscopic, retro-reflective;
- Inertial: inertial sensors, accelerometers, compasses, GPS;
- Ultrasonic: ultrasonic sensors.

**Figure 2** – Motion tracking device categories.



Source: The author.

Undoubtedly, all these categories of sensors add higher or lower cost to the system. However, in one of these categories, there is an opportunity. In the Vision category, there is the possibility of using only one regular RGB camera, which is a device that most people probably have in their homes (IBGE, 2018). Furthermore, the video game could be made lighter to process, in order to run on a regular computer or smartphone, which is already integrated with such a camera, resulting in a potential zero cost to the system.

Vision trackers depend on capturing a video frame through an optical system, such as a regular monocular RGB (color) camera, an infrared (IR) camera or a more specialized depth camera, such as Microsoft Kinect, which has a software to estimate the pose, based on the depth map generated by the RGB camera and IR sensors (Figure 3). To help the tracking, a marker can be used as a specific texture pattern, IR diodes or a distinct colored object. Yet, the tracking can be markerless, depending on Artificial Intelligence techniques, by detecting edges, shapes and other interest points. Then, the computer processes the captured frame and estimates the upper limb position in space. This technology of detecting position through camera frames is called Computer Vision.

**Figure 3** – (a) Kinect sensor and (b) depth map with skeletal estimation.



Source: (a) Evan-Amos, Public domain, via Wikimedia Commons;  
 (b) Sang1938, CC BY-SA 3.0 license, via Wikimedia Commons.

## 2.3 OpenCV

After choosing to develop a 3D tracking method with only a 2D regular camera, it was necessary to select a Computer Vision algorithm. As a result, the OpenCV library was used, since it is the most complete and popular library to have the searched algorithm. OpenCV (Open Source Computer Vision Library) is an open source Computer Vision and Machine Learning software library, that has a permissive license and more than 2500 optimized algorithms, both classic and state-of-the-art (OpenCV, 2020b). These algorithms can be used to detect and recognize faces, identify objects, classify human actions in videos, track camera movements, track moving objects, extract 3D models of objects, produce 3D point clouds from stereo cameras, follow eye movements, etc. (OpenCV, 2020a). However, every use case can be very particular, so it is nearly impossible to develop a universal tracking algorithm. Therefore, before developing the system, all the OpenCV algorithms that can track gross movements of the upper limbs and are suitable for post-stroke rehabilitation exergames were briefly tested, and a deeper comparison was made between the three most promising, as part of the research prior to the development of this work, the results of which will be presented in the next chapters.

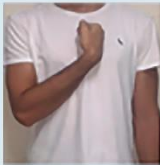
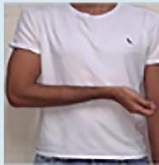

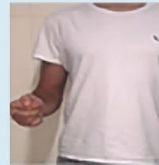

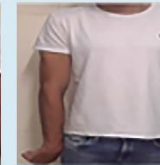






## 2.4 Post-stroke Recovery Stages

After a stroke, survivors go through recovery stages, which Brunnstrom (1966) classified as follows:

1. Flaccidity.
2. Dealing with the appearance of spasticity.
3. Increased spasticity.
4. Decreased spasticity.
5. Complex movement combinations.
6. Spasticity disappears.
7. Normal function returns (Brunnstrom, 1966).

Spasticity or hypertonia is an abnormal increase in muscle tone and stiffness. It is present in most of the recovery stages (2 to 5). It frequently affects the flexor muscles in the arm area, producing 5 stereotypical postural patterns, as observed by Hefter et al. (2012) ([Figure 4](#)):

**Figure 4** – Five typical arm spasticity patterns.

Hefter's classification	I	II	III		IV	V
Observed frequency	2% (1)	2% (1)	67.7% (33)		21.6% (11)	9.8% (5)
			Internal 76% (25)	External 24% (8)		
Described patterns						
Observed patterns						

Source: (Gomes et al., 2019) – CC-BY license.

1. Internal rotation and adduction of the shoulder, flexion at the elbow, supination in the forearm, and flexion at the wrist resulting in the arm being fixed in a posture across the chest.
2. Internal rotation and adduction of the shoulder, flexion at the elbow, supination in the forearm, and extension at the wrist.
3. Internal rotation and adduction of the shoulder and flexion at the elbow coupled with a neutral positioning of the forearm and the wrist. The neutral position of the wrist potentially results from simultaneous contracture of the flexor and extensor muscles.
4. Internal rotation and adduction of the shoulder, flexion at the elbow, pronation in the forearm, and flexion at the wrist. Some variation in the degree of elbow flexion may occur.
5. Internal rotation and retroversion of the shoulder, extension at the elbow, pronation of the forearm, and flexion at the wrist resulting in the arm being fixed in a position behind the body. This pattern of spasticity was frequently observed in connection with a dystonic component (Hefter et al., 2012).

Therefore, it should be taken into account, for the movement tracking algorithm, that patients generally do not open their hands easily and cannot sustain the arm up for a long time, tending to always keep it close to the torso.

## **2.5 Final Considerations**

This chapter presented the theoretical foundation and the main concepts necessary to understand this work, namely: exergames, Computer Vision, OpenCV and post-stroke recovery stages.

---



---

## LITERATURE REVIEW

---

In order to identify the state-of-art in post-stroke rehabilitation video games using Computer Vision and regular RGB cameras, a systematic literature and patent review has been made.

### 3.1 Sources and Search Strategy

For the literature review, two searches were made. One before the system was developed and other after. They will be referred to as “first” and “second” reviews. The first review was performed to identify what has been achieved before in games for post-stroke rehabilitation using regular RGB cameras. The second one was a patent review, to check whether the developed system was patentable or not, and produced more refined results.

Therefore, firstly, a systematic search was carried out, using PRISMA (Preferred Reporting Items for Systematic Reviews and Meta-Analyses) protocol (Moher et al., 2009). The IEEE Xplore, PubMed and ACM Digital Library databases online were screened using a keyword combination ([Table 1](#)). It is understood that there are more databases to be consulted, however, it was considered that a sufficient number of works was selected for this preliminary assessment.

**Table 1** – Search strategy.

<b>Stroke</b>	stroke
<b>Games</b>	AND (game OR gaming OR "virtual reality" OR "augmented reality" OR "mixed reality")
<b>Upper limbs</b>	AND (arm OR upper OR motor OR forearm OR shoulder OR elbow)



<b>Excluding factors:</b>	NOT
<b>other body parts,</b>	(trunk OR finger OR lower OR legs OR knee OR ankle OR spine OR gait OR balance
<b>other types of</b>	OR haptic OR robot OR exoskeleton OR inertial OR magnetic OR accelerometer OR
<b>tracking, reviews</b>	"meta-analysis" OR review)

Source: the author.

The search terms in the “games” category were chosen trying to include all types of games, even Augmented Reality ones, as the search focus was on motion capture strategies currently in use, regardless of game type. The “excluding factors” search terms were chosen because they returned better quality of results than very specific including factors, such as when trying to use “color”, “camera” or “Kinect” as search terms. The only search term restriction was to be in the English language. The beginning of the search time frame was not restricted, because this is a fairly recent paradigm. The search time frame ended on April 16, 2020. The questions to be answered were: Q1: What are the most popular devices and technologies used for Computer Vision gross upper limb motion tracking in post-stroke rehabilitation exergames? Q2: In what categories can they be classified? Q3: Is regular RGB one of the popular devices? Q4: Are the commercial ones still widely available?

For the patent review, a regular search for anteriority was carried, using keywords that identified the creation, both in English and Portuguese. The chosen words are in [Table 2](#). The search string was formed with a Boolean addition of the words.

**Table 2** – Keywords for the patent search.

<b>Keyword in Portuguese</b>	<b>Keyword in English</b>
1. Cor	1. Color
2. Rastreamento de movimento	2. Motion tracking
3. Derrame/AVC	3. Stroke
4. Reabilitação	4. Rehabilitation
5. Câmera	5. Camera

Source: The author.

The Websites screened were ([Table 3](#)):

**Table 3** – Websites screened for the patent search.

<b>Institution</b>	<b>Website</b>
1. INPI - Instituto Nacional de Propriedade Industrial	<a href="https://gru.inpi.gov.br/pePI/servlet/LoginController?action=login">https://gru.inpi.gov.br/pePI/servlet/LoginController?action=login</a>

2. EPO – European Patent Office	<a href="https://worldwide.espacenet.com/advancedSearch?locale=en_EP">https://worldwide.espacenet.com/advancedSearch?locale=en_EP</a>
3. Derwent Innovations Index	<a href="http://apps-webofknowledge.ez34.periodicos.capes.gov.br/DIIDW_AdvancedSearch_input.do?SID=1AjQhvLIVrSkN6IT1W2&amp;product=DIIDW&amp;search_mode=AdvancedSearch">http://apps-webofknowledge.ez34.periodicos.capes.gov.br/DIIDW_AdvancedSearch_input.do?SID=1AjQhvLIVrSkN6IT1W2&amp;product=DIIDW&amp;search_mode=AdvancedSearch</a>
4. Google Patents	<a href="https://patents.google.com/advanced">https://patents.google.com/advanced</a>
5. USPTO: United States Patent and Trademark Office	<a href="https://www.uspto.gov/patents/search">https://www.uspto.gov/patents/search</a>

Source: the author. Links last checked on 2/14/2021.

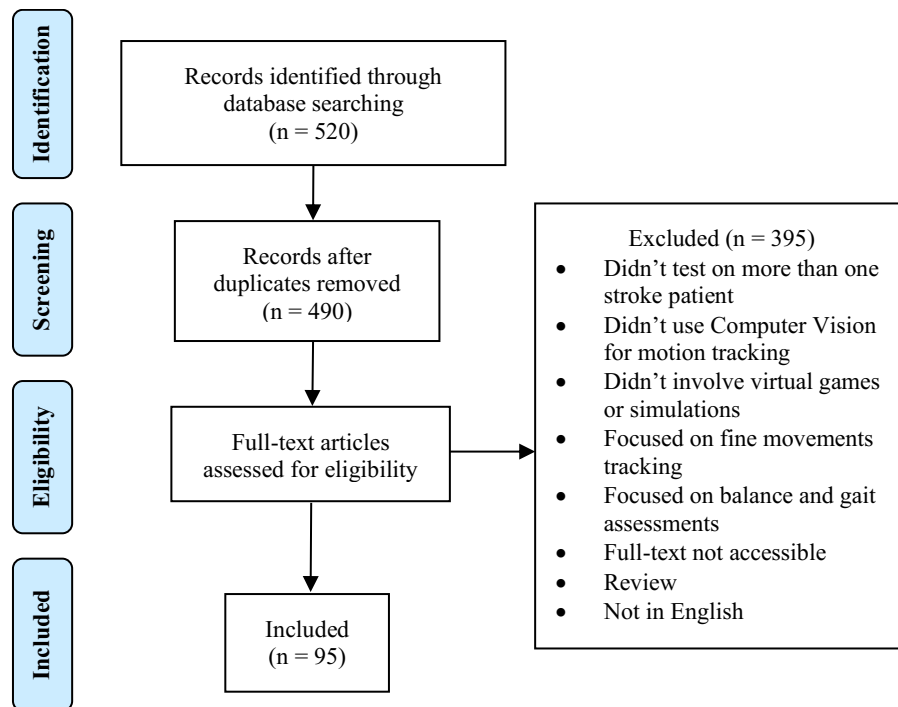
### 3.2 Inclusion Criteria

Studies included in the first review should be about post-stroke rehabilitation exergames or simulations and use Computer Vision motion tracking, that is, with some sort of camera. Assessment or product evaluation studies were also considered if they offered motor tests and outcomes. Only were included studies that tested on more than one stroke subject. Only gross upper limb movement assessment was considered, therefore balance and gait assessments were excluded, as well as hands and fingers. A PICOS (Population, Intervention, Control, Outcome and Study Design) approach was used (Moher et al., 2009):

- 1) Population: Patients enrolled in post-stroke rehabilitation video games or simulations.
- 2) Intervention: Computer Vision gross upper limb motion tracking in these games or simulations.
- 3) Control: Not taken into account, because several studies with good ideas do not make controlled clinical trials.
- 4) Outcome: Any measurements related to physical activity and motor control before and after intervention were included.
- 5) Study design: Randomized controlled trial, cohort and single-session studies.

A flow diagram of the selection process is shown in [Figure 5](#).

In the patent review, all patents, patent applications and utility models found on the websites were screened, and those with the most similar claims to the proposed system were chosen.

**Figure 5** – PRISMA flow diagram of study selection.

Source: the author.

### 3.3 Data Extraction

In the first review, the following information was extracted from the selected studies: country, conference or journal, year, device brand or model and tracking type. Then, the devices found were classified into 5 categories:

- 1) Depth skeletal tracking: RGB-D cameras;
- 2) RGB object tracking: RGB cameras that track object or marker features, such as color and texture pattern;
- 3) IR marker tracking: IR (infra-red) detecting cameras with markers;
- 4) LeapMotion tracking: unique device technology; and
- 5) RGB markerless body tracking: RGB cameras for movement tracking without markers (using Artificial Intelligence).

LeapMotion was placed in a separate category, because it has a unique technology that is not fully disclosed by its manufacturer, therefore not being able to be categorized properly, but it involves IR stereo markerless tracking and a monochrome camera, and does not generate depth maps.

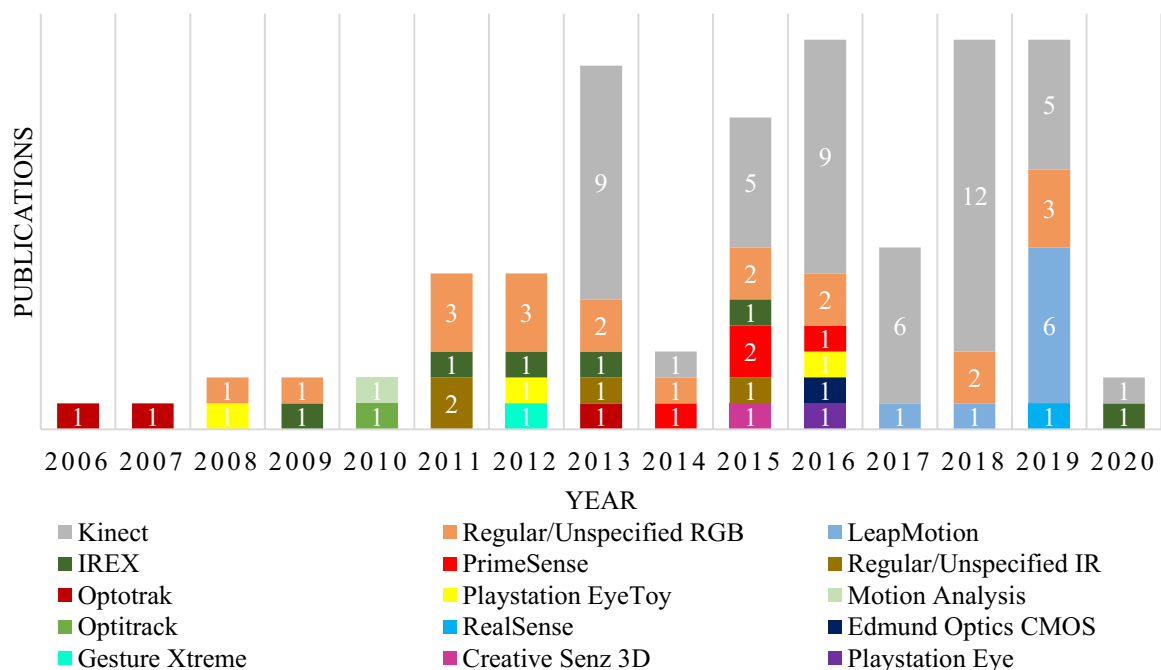
All the studies that used any regular RGB camera were detailed in a table, regardless of specific brands.

### 3.4 Correlated Work

After the PRISMA process, 95 articles were obtained, citing devices 103 times. These studies were from different parts of the world: America (n = 42), Asia (n = 29), Europe (n = 20) and Oceania (n = 4). Twenty-seven percent (26/95) of the studies were from the USA. Moreover, 63 of them came from journals and 32 from conferences. Regarding the year of publication, the first study was published in 2006. Since then, the number of publications had increased from one publication in 2006 to 15 in 2018 and 2019, followed by a slight decrease in 2014 and 2017 (3 and 7 publications, respectively).

The brands or models of optical devices found each year are shown in [Figure 6](#). Thirteen different commercial optical systems or devices for motion capture were found. The most widely used was Kinect, an RGB-D camera that has a markerless skeletal tracking SDK (Software Development Kit), corresponding to 47% (48/103) of all study devices, of which 71% (34/48) were from journals. In second place, unspecified or regular RGB (color) cameras, with 19% (20/103). It is also possible to note that Kinect has been found in studies every year for the past 8 years and RGB cameras for 10 non-consecutive years, while some systems, such as Optotrak, PrimeSense and PlayStation Eye stopped being found in later studies, due to the evolution of these technologies or their withdrawal from the market by their manufacturer.

**Figure 6** – Devices employed in selected studies by year (some studies used more than one device).



Source: The author.

The categories of devices found, as described previously, ended up having the following commercial devices:

- 1) Depth skeletal tracking: Intel RealSense, PrimeSense, Kinect and Creative Senz 3D;
- 2) RGB object tracking: regular/unspecified RGB and IREX;
- 3) IR marker tracking: regular/unspecified IR, Optotrak, Optitrack, Edmund Optics CMOS and Motion Analysis;
- 4) LeapMotion;
- 5) RGB markerless body tracking: regular/unspecified RGB, Playstation EyeToy, Playstation Eye and GestureXtreme.

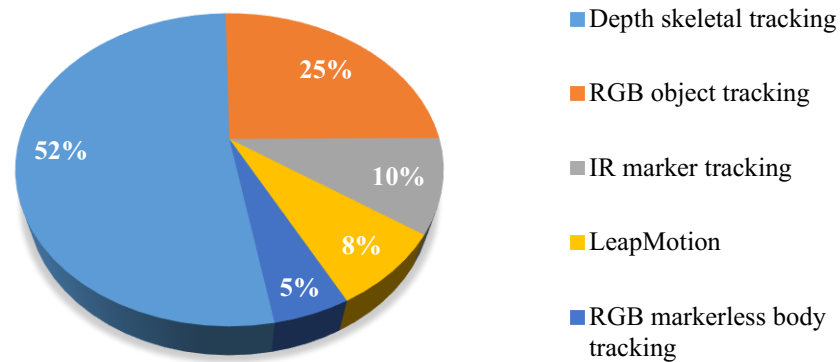
The devices categories and frequencies can be seen in [Figure 7](#). It has been identified that most studies used depth skeletal tracking (52% - 54/103), mainly due to Kinect. This is far more than the second placed category, RGB object tracking (25% - 26/103) and third, IR marker tracking (10% - 10/103).

Initially, a generalized search was made to understand the state of the art in games for post-stroke rehabilitation using Computer Vision. After that, the regular RGB object tracking category, which is the one that generated the most interest for future investigation, was exposed, with all 26 studies in [Table 4](#), from the first review.

Moreover, the patent review revealed the studies from [Table 5](#). Also, in [Table 6](#), the differences from the proposed method and the related studies are shown. Three comparison categories were chosen:

- 1) 3D position tracking using only one regular RGB camera;
- 2) In-game progress monitoring; and
- 3) Real-time joint angle measurement by one regular RGB camera.

These categories were chosen because it is considered that they are the main innovations of the developed system, in relation to other studies in the games category using a common RGB camera, which would compare precisely to the system proposed here. For instance, if games that utilize depth cameras, that provide joint angle measurements much more easily, were included in this comparison, it would not be fair to compare them with the proposed system.

**Figure 7** – Commercial devices categories and frequencies.

Source: The author.

**Table 4** – Summary of related studies – first review.

No.	Reference	Tracking method
1	AHMED et al., 2020	A commercial system called IREX (Interactive Rehabilitation and Exercise System) was tested, which consists of an RGB camera that tracks a colored glove.
2	CIDOTA; BANK; LUKOSCH, 2019	In one of the games, the game controller is a haptic device with five markers on top, held by the player, that determines the position of a virtual basket.
3	JAYASREE-KRISHNAN et al., 2019	A cup was decorated with contrasting color and extra features, such as a distinctive base. The 3D position and orientation of the cup was estimated via neural networks and pose estimation algorithms.
4	SEYEDEBRAHIMI; KHOSROWABADI; HONDORI, 2019	A webcam was used to capture the subject's hand movements through a color marker.
5	BANK et al., 2018	The virtual world was aligned to the real world using the Vuforia tracking library and a webcam. However, the 3D hand and arm coordinates were captured by LeapMotion and Kinect.
6	FARIA, Ana L et al., 2018	A handle with an AR tracking marker was used.
7	ASSIS et al., 2016	Participants wore a glove on the injured arm and AR markers on the shoulders.
8	CAMEIRÃO et al., 2016	The interaction with the computer was made through 2D arm movements with a camera-based 2D color tracking software (AnTS) and a colored glove.
9	HONDORI et al., 2016	Subjects were seated at a table and asked to perform reaching tasks while holding a small plastic cup, which served as a color marker that was tracked by the camera.

10	FARIA et al., 2015	Same as CAMEIRÃO et al., 2016.
11	HUNG; CROFT; VAN DER LOOS, 2015	The PlayStation Move controllers were used, one on each hand, one controlling the cursor's vertical movements and the other, the horizontal movements. The PlayStation Move motion controller features an orb at the head which can glow in any of a full range of colors using RGB LEDs. The colored light serves as an active marker, the position of which can be tracked along the image plane by the camera.
12	LEE, 2015	Same as AHMED et al., 2020.
13	LEE, Sook Joun; CHUN, 2014	Same as AHMED et al., 2020.
14	SUCAR et al., 2014	Same as GUTIÉRREZ-CELAYA et al., 2011.
15	LIN; KELLEHER; ENGSBERG, 2013	The Wii Remote was used to detect the participants' shoulder and arm motions. A webcam and a colored tracking object were also used to detect and track the participants' shoulder and arm movements.
16	VOURVOPOULOS et al., 2013	Same as CAMEIRÃO et al., 2016.
17	KWON et al., 2012	Same as AHMED et al., 2020.
18	RUBIO BALLESTER; BERMÚDEZ I BADIA; VERSCHURE, 2012	Same as DA SILVA CAMEIRÃO et al., 2011.
19	SAMPSON; SHAU; KING, 2012	The movement of the affected arm is picked up via a color patch which the computer vision software uses for real-time matching of the hand to the games.
20	SHIRI et al., 2012	The patient wears a black sleeveless vest over a white robe and sits against a blue background. His real arm is segmented out of the frame and replaced by a virtual one, which he controls by using a mouse, trackball or a joystick.
21	AUNG; AL-JUMAILY, 2011	A colored marker was used to track the current position of the patient's hand.
22	DA SILVA CAMEIRÃO et al., 2011	This vision-based tracking system detects color patches located on the wrists and elbows of the patients. A biomechanical model of the upper body allows the reconstruction of the patient's movements.
23	GUTIÉRREZ-CELAYA et al., 2011	Webcam tracks hand/gripper movements, through a colored ball, and translate that into commands to control the games. The 2D tracking is based on particle filters. The variance of the distribution of the particles is used to estimate the distance of the object to the camera, that is the depth, z.
24	KIM et al., 2011	Same as AHMED et al., 2020.

25	RAND; KATZ; WEISS, 2009	Same as AHMED et al., 2020.
26	SUCAR et al., 2009	Same as GUTIÉRREZ-CELAYA et al., 2011.

Source: the author.

**Table 5** – Summary of related studies – second review.

<b>Patents</b>			
<b>No.</b>	<b>Reference</b>	<b>Patent number and status</b>	<b>Tracking method</b>
1	SCHWEIGHOFER, 2019	US 20200197744 A1 (pending); WO 2020132415 A1 (application)	The user wears three passive fiducial markers, on the arm, forearm and torso, which enable the detection of 3D motions using a regular RGB camera, aided by Kalman and other predictive algorithms.
2	MAURO et al., 2014	WO 2015/139750 A1 (pending); US 10,092,220 B2 (active)	A glove with a different color at each fingertip is tracked by a normal RGB camera and a depth camera. A processing unit processes both color frames and depth frames for reconstructing the 3D positions of the markers.
3	SUCAR-SUCCAR et al., 2011	CA 2731775 A1 (active)	The user moves around a handling element with 2 distinguishable spheres. The author claims that a regular 2D uncalibrated camera is capable of tracking this handle in 3D, but doesn't describe how.
4	WILLMANN et al., 2007	US 20090259148 A1 (abandoned)	The user wears three sensors or markers on the upper limbs. Then, a series of calculations is used to estimate to position in 3D space and angle joints.
<b>Research articles, dissertations and theses</b>			
<b>No.</b>	<b>Reference</b>	<b>Tracking method</b>	
1	WANG, Robert; PARIS; POPOVIĆ, 2011	The system is for full upper body motion capture. It uses one or more RGB cameras and a colored shirt. The processing pipeline consists of several steps. First, the multi-colored shirt is located and cropped from the frame using its histogram. Then, a robust pose estimation process is performed, using Deep Learning from several photos from a database.	
2	YAQIN TAO; HUOSHENG HU, 2004	Belts of different colors are attached to different body joints of the subject. The estimated centers of these belts are regarded as the 2D joint positions.	
3	HIENZ; GROBEL; OFFNER, 1996	The user wears a glove with multiple colors, and colored markers on the upper limb. The missing third dimension is calculated using a geometric model of the human hand-arm arrangement, based on the 2D projection of upper and lower arms on the screen.	

Source: The author.



Table 6 – Comparison study.

Studies from first review				
No.	Study	3D position tracking using only one regular RGB camera	In-game progress monitoring	Real-time joint angle measurement by one regular RGB camera
1	AHMED et al., 2020	X	X	X
2	ASSIS et al., 2016	✓	X	X
3	AUNG; AL- JUMAILY, 2011	X	X	X
4	BANK et al., 2018	X	X	X
5	CAMEIRÃO et al., 2016	X	X	X
6	CIDOTA; BANK; LUKOSCH, 2019	✓	X	X
7	DA SILVA CAMEIRÃO et al., 2011	X	✓	✓
8	FARIA et al., 2015	X	X	X
9	FARIA, Ana L et al., 2018	✓	✓	X
10	GUTIÉRREZ- CELAYA et al., 2011	✓	X	X
11	HONDORI et al., 2016	X	X	X
12	HUNG; CROFT; VAN DER LOOS, 2015	X	X	X
13	JAYASREE- KRISHNAN et al., 2019	✓	X	X
14	KIM et al., 2011	X	X	X
15	KWON et al., 2012	X	X	X
16	LEE, 2015	X	X	X
17	LEE, Sook Joung; CHUN, 2014	X	X	X
18	LIN; KELLEHER; ENGSBERG, 2013	X	X	X

19	RAND; KATZ; WEISS, 2009	X	X	X
20	RUBIO BALLESTER; BERMÚDEZ I BADIA; VERSCHURE, 2012	X	✓	✓
21	SAMPSON; SHAU; KING, 2012	X	X	X
22	SEYEDEBRAHIMI; KHOSROWABADI; HONDORI, 2019	X	X	X
23	SHIRI et al., 2012	X	X	X
24	SUCAR et al., 2009	✓	X	X
25	SUCAR et al., 2014	✓	X	X
26	VOURVOPOULOS et al., 2013	X	✓	X
<b>Studies from second review</b>				
<b>Patents</b>				
1	MAURO et al., 2014	X	✓	X
2	SCHWEIGHOFER, 2019	X	✓	✓
3	SUCAR-SUCCAR et al., 2011	✓	✓	X
4	WILLMANN et al., 2007	✓	X	✓
<b>Research articles, dissertations and theses</b>				
1	HIENZ; GROBEL; OFFNER, 1996	✓	X	X
2	WANG, Robert; PARIS; POPOVIĆ, 2011	✓	X	✓
3	YAQIN TAO; HUOSHENG HU, 2004	X	X	✓

Source: The author.

All the articles found and their respective category according to the brands or models of optical devices are specified in [Table 7](#). It is important to note that some of these studies used more than one type of tracking device.

**Table 7** – Classification of device tracking types of the selected studies.

Category	Motion tracking device category	Camera brand or model	Selected studies
1	RGB-D skeletal tracking	RealSense, PrimeSense, Kinect, Creative Senz 3D	(Richard J Adams et al., 2019; Afsar et al., 2018; Askin et al., 2018; Belen Rubio Ballester et al., 2015, 2016; Bank et al., 2018; Boone et al., 2019; Borstad et al., 2018; Brokaw et al., 2015; Cameirao et al., 2016; Cargnin et al., 2015; Castano et al., 2014; C. Chen et al., 2017; Cidota et al., 2019; M Demers et al., 2017; Marika Demers et al., 2019; Ding et al., 2018; Dukes et al., 2013; Funabashi et al., 2017; Gauthier et al., 2017; George et al., 2017; Hoermann et al., 2017; Huang & Chen, 2016; Ji & Lee, 2016; Johnson et al., 2018; Kairy et al., 2016; Kato et al., 2016; Kelly et al., 2018; Kizony et al., 2013; Kutlu et al., 2016, 2015; Lauterbach et al., 2013; G. Lee, 2013; M. Lee et al., 2016; Mobini et al., 2015; N Norouzi-Gheidari et al., 2013; Nahid Norouzi-Gheidari et al., 2020; Proffitt et al., 2018; Roy et al., 2013; Schaham et al., 2018; Schüller et al., 2013; Shin et al., 2014, 2015; Sin & Lee, 2013; Thielbar et al., 2020; Vourvopoulos et al., 2013; Wairagkar et al., 2017; Yang et al., 2018; Yeh et al., 2019)
2	RGB object tracking	Regular/unspecified RGB, IREX	(Ahmed et al., 2020; Aung & Al-Jumaily, 2011; B Rubio Ballester et al., 2012; Cidota et al., 2019; da Silva Cameirão et al., 2011; A L Faria et al., 2015; Gutiérrez-Celaya et al., 2011; Hondori, Khademi, Dodakian, McKenzie, Lopes, & Cramer, 2016; Hung et al., 2015; Kim et al., 2011; Kwon et al., 2012; K.-H. Lee, 2015; S. J. Lee & Chun, 2014; Lin et al., 2013; D Rand et al., 2009; Sampson et al., 2012; Seyedebrahimi et al., 2019; Shiri et al., 2012a; Sucar et al., 2009; Vourvopoulos et al., 2013)

3	IR marker tracking	Regular/unspecified IR, Optotrak, Optitrack, Edmund Optics CMOS, Motion Analysis	(R J Adams et al., 2018; Assis et al., 2016; Baniña et al., 2013; Bank et al., 2018; Baran et al., 2015; X. Chen et al., 2007; M Duff, Chen, Attygalle, Herman, et al., 2010; M Duff, Chen, Attygalle, Sundaram, et al., 2010; Margaret Duff et al., 2013; Faith et al., 2011; Ana L Faria et al., 2018; House et al., 2016; Prange et al., 2008; Rabin et al., 2011; Subramanian et al., 2006)
4	LeapMotion	LeapMotion	(Bank et al., 2018; Choi et al., 2019; Cidota et al., 2019; J. Dias et al., 2019; P. Dias et al., 2019; McDermott & Himmelbach, 2019; Ogun et al., 2019; D Rand et al., 2009; Vanbellingen et al., 2017)
5	RGB markerless body tracking	Regular/unspecified RGB, Playstation EyeToy and Eye, GestureXtreme	(Cameirao et al., 2016; Jayasree-Krishnan et al., 2019; Levin et al., 2012; Debbie Rand et al., 2017; Reinthal et al., 2012; Yavuzer et al., 2008)

Source: the author.

### 3.5 Final Considerations

Even though the use of games in post-stroke rehabilitation is relatively new, this review shows that it has already been tested using diverse types of Computer Vision movement tracking devices. Most published studies used Kinect in tests, but RGB object tracking had 25% of all studies, being the second most popular device category. Kinect's popularity may be due to its relatively low cost, broad availability, ready-to-test commercial games and relatively good tracking accuracy (Karbasi et al., 2016), including angle joint estimation, while not depending on markers, any additional objects or special setups. The main drawbacks of Kinect are: limited distance to detect depth, inability to capture reactions of less than 0.5 seconds, sensitivity to sunlight and unsuitability for outdoor applications (Karbasi et al., 2016).

Regarding the availability of commercial devices found, some of them are still being manufactured as they were or in newer versions. LeapMotion and PrimeSense companies were sold to other companies, but redesigned versions of the same products are still on the market. Kinect ended production in October 2017, but a newer version, called Azure Kinect, was introduced in March 2020 by Microsoft, for a different target audience: "developers, not consumers", according to the Microsoft team (Microsoft, 2021).

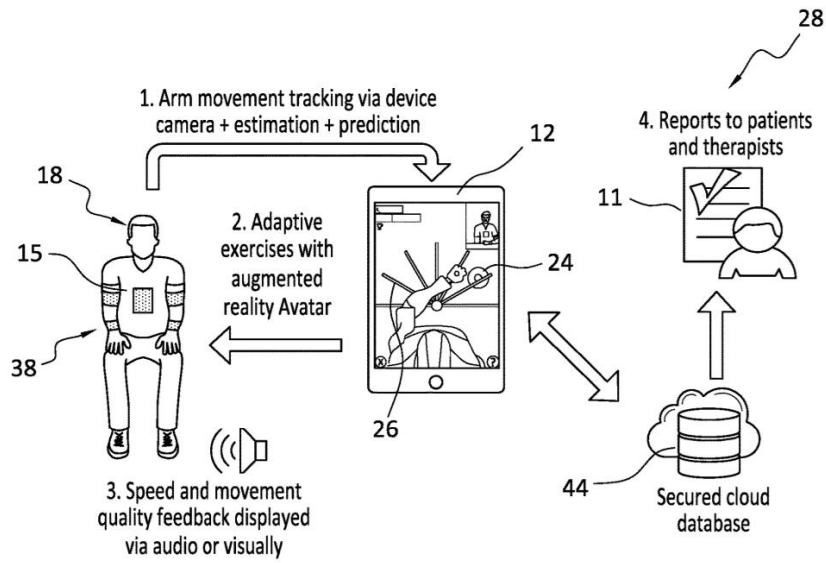
Moreover, positive and negative points were found for all devices, several of them qualitative remarks that did not specifically address the quality of motion capture, making it impossible to generalize if one device is better than the other.

Analyzing the related studies, the most similar one to the present application was the one by Schweighofer (2019) ([Figure 8](#)). Fiducial markers provide 3D position and orientation. However, the problem with this approach is that it is a detection algorithm, not a tracking one, therefore, it is not optimized to be used with video. As the author marks himself, “relatively long periods of marker loss can occur relatively frequently”. This is due to motion blur of the camera. The person wearing the markers must move incredibly slow for it to work. To minimize that, the author used Kalman filter and other prediction algorithms, which adds several calculations to the processing, since both Kalman filter and regular fiducial marker tracking algorithms are heavy to process. The author claims that the system performs real-time on a mobile device. Milovanovic (2019) said that this approach may be capable of operating at a frame rate of 30 frames per second (fps) with input images having a resolution of 640x480, which will be reduced much further when adding Kalman filter and graphics game processing, corroborated by this author personal experiments. It is commonly known around programmers that games should, ideally, maintain the fps above 30, because, a bit below that, the human eye perceives a video as a sequence of images.

Also worth mentioning are the solutions that use projection tracking through colored bands on the upper limb (Hienz et al., 1996; Willmann et al., 2007) ([Figure 9](#)). They don't mention taking camera distortions into account. Also, the armband center can be estimated incorrectly, if partially occluded or if they are different sizes, so this probably produces a flawed estimate when not in the center of the camera and with all bands fully visible.

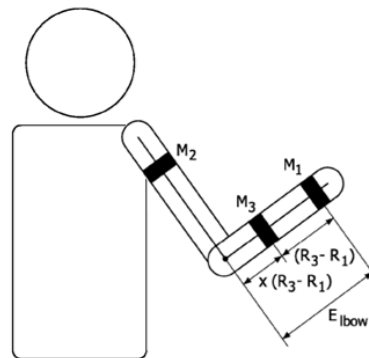
Therefore, there is a lack of an economically viable alternative in motion capture games for post-stroke rehabilitation with a regular RGB camera, but at the same time, that fulfills the requirements presented above, that is, 3D position tracking, not detection; in-game progress monitoring; and real-time joint angle measurement by one regular RGB camera at the same time. It is also important to remember about the game performance and angle, which must be efficiently read without performance lapses and sufficiently precise, also without losing game display performance, to effectively be a widely accepted and used low-cost game.

**Figure 8** – Related work by Schweighofer (2019).



Source: (Schweighofer, 2019) - Public domain.

**Figure 9** – Projection tracking using colored bands.



Source: (Willmann et al., 2007) - Public domain.



---

## MATERIALS AND METHODS

---

This chapter deals with the materials and methods used for the complete development of the system proposed here. First, the section "Determination of the Tracking Algorithm" is presented, which shows the investigation that was carried out in several motion tracking algorithms of OpenCV, in order to choose the most suitable one for this application. Furthermore, in the "System Development" section, the actual development of the system is presented, starting with the theory that supports the operation of this new motion capture device, passing through the software tools used, then explaining step-by-step the interface with the user and how the difficulty settings, data collection and other interactions are given. Finally, the "System Tests" section presents the tests that were performed on the system, in order to verify the preliminary values of the main variables influencing its functioning, accuracy and usability.

### 4.1 Determination of the Tracking Algorithm

#### 4.1.1 OpenCV tracking algorithms

As previously discussed, all OpenCV algorithms that needed only a single RGB camera were briefly tested. The findings are discussed in this subsection. The three chosen ones for a deeper comparison are explained below.

In the OpenCV library, several different approaches to object or body tracking can be found. They have evolved substantially in the past two decades, from traditional statistical or Machine Learning approaches to Deep Learning approaches based on Convolutional Neural Networks (OpenCV, 2020a).

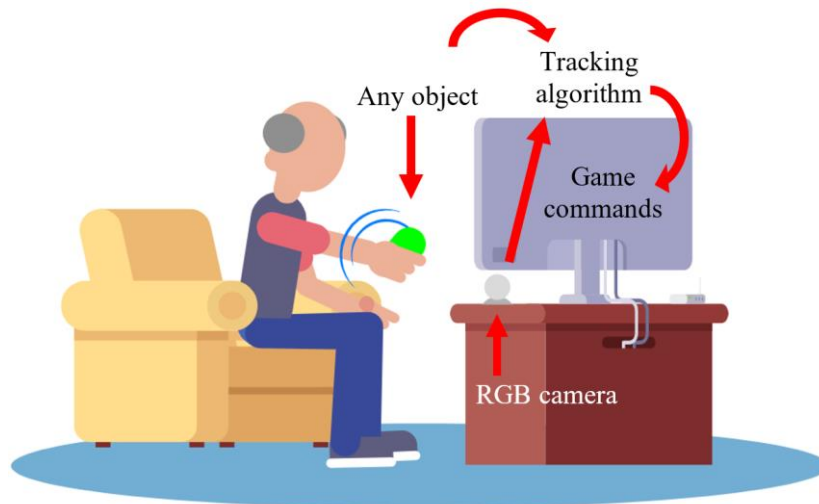
Object tracking is not the same as object detection. In object detection, each frame is processed independently and the objective is to identify and classify the objects in that particular frame. Object tracking, on the other hand, needs to follow a specific object throughout the video, in subsequent frames. Therefore, it is necessary to gather space-time features (Maiya,

2019). Thus, algorithms meant for object detection tend to be much slower and are not ideal for object tracking. An example of this is ArUco fiducial markers (i.e., Augmented Reality markers) detection algorithm, present in the OpenCV library. The slow response was verified, during a rapid test. As a result, no further investigation was pursued in this approach.

In addition, OpenCV approaches based on Deep Learning can be adapted for both object tracking and detection. For example, they can be trained to track a hand, some object or a complete 2D skeleton, without using markers. However, they require several calculations and, therefore, a very powerful and expensive machine to run at an acceptable frame rate (Dibia, 2019; Kimyoon-young, 2020). In general, markerless body tracking algorithms have a very high processing cost and need high-cost machines. This breaks the low-cost requisite intended here, so they were considered unsuitable for the application to be developed.

With that in mind, other approaches to real-time, lightweight and effective object tracking algorithms were searched. The objective is that any holdable or wearable objects in the user's home makes them capable of interacting with the post-stroke exergame ([Figure 10](#)).

**Figure 10** – Schematics of the intended application: the movement of an object, held by the patient, is captured by a camera and, through a tracking algorithm, translated into game commands.



Source: The author.

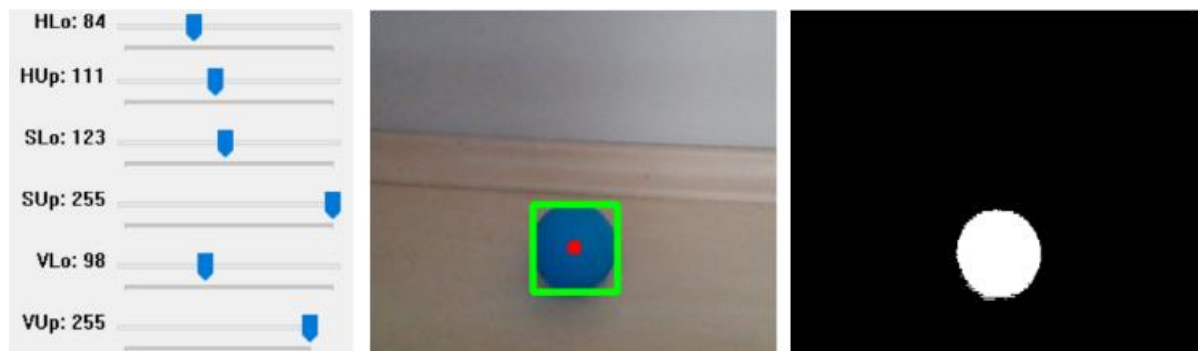
So, first of all, the most basic options for object tracking were surveyed:

1. *HSV color threshold*: Among all the features of an object, color is one of the most widely used for tracking (Yilmaz et al., 2006). In fact, such technique is even found in commercial post-stroke rehabilitation gaming solutions (GestureTek, 2016). It relies strictly on basic image processing concepts, namely color thresholding. First, it is necessary to define an upper and lower range in a given color space (such as



RGB and HSV). After that, several functions are used to generate a mask in which only the pixels with the desired color are white and all background pixels are black. Then, the white pixels can be tracked through the frames by restricting the area of the object, searching for a closed contour or fitting a rectangle over it, as shown in [Figure 11](#). This algorithm is very fast and can run in super real-time even on resource constrained devices (Rosebrock, 2020). Drawbacks include the necessity to recalibrate the exact colors once in a while, sensibility to illumination variation and the color of the object should not be present anywhere else in the frame.

**Figure 11** – Color tracking thresholding works by defining an upper and lower range in a given color space, in this case, HSV, (left) and then masking this color (right) from the original image, detecting the object (center).



Source: The author.

Moreover, in OpenCV, there is a long-term optical tracking API, which is a unique interface useful to plug several tracking algorithms and compare them. They provide eight already implemented algorithms: Boosting, CSRT, GOTURN, KCF, MedianFlow, MIL, MOSSE and TLD (OpenCV, 2020b). All of those were coded and a quick pretest was conducted with a variety of objects. When there was fast motion, all algorithms lost track at some point, except the CSRT, which was the only one that generated interest in further testing:

2. *Discriminative Correlation Filter with Channel and Spatial Reliability (CSRT):*

This is an algorithm introduced in 2018 that joins the channel and spatial reliability concepts to discriminative correlation filters tracking. The spatial reliability map adjusts the filter support to the part of the object suitable for tracking. Consequently, both allow to enlarge the search region and improves tracking of non-rectangular objects. Reliability scores reflect channel-wise quality of the learned filters and are used as feature weighting coefficients in localization. The authors claim that this algorithm can run in real-time on a CPU (Lukezic et al., 2017).

Besides those algorithms, in the “Video Analysis” module of the OpenCV library, more object tracking algorithms can be found, such as Mean shift and Cam shift. When testing them quickly, it was decided to further test the Mean shift algorithm. This algorithm was proposed in 1975, but had been ignored until Cheng’s revisit (Cheng, 1995), developing a more general formulation and demonstrating its potential uses in clustering and global optimization. Over the years, the Mean shift algorithm received more improvements (Yilmaz et al., 2006):

3. *Mean shift*: Mean shift tracking requires that a portion of the object is inside the circular region of interest (ROI) when the tracker is initialized. Then, a histogram is generated with the first frame information of the object, such as spatial and color information. For histogram generation, a weighting scheme defined by a spatial kernel gives higher weights to the pixels closer to the object center. Then, the algorithm compares the histograms of the object and the window around the hypothesized object location. At each iteration, the Mean shift vector is computed such that the histogram similarity is increased, thus moving the window closer to the object. This process is repeated until convergence is achieved (Yilmaz et al., 2006).

In the next session, the tests with these three algorithms are described.

#### 4.1.2 Algorithm testing methods

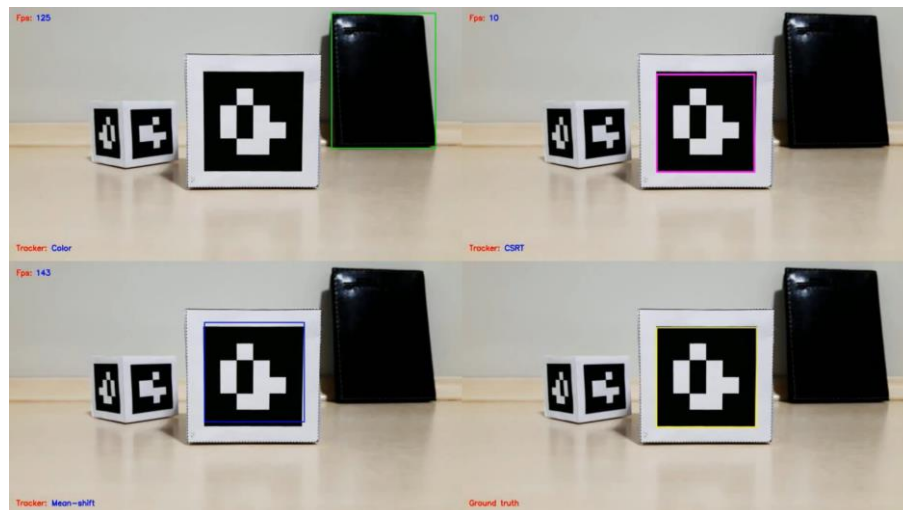
As tracking can be used for various different purposes, in many different environments and situations, doing a deep comparison of tracking algorithms can be tricky. There are also several variables that can influence results on tracking comparison, such as rotation or partial occlusion of tracked object, changing light conditions, blurred frame due to a fast camera movement, etc. Large standardized datasets exist and can be used to test new algorithms in relation to existing ones (Wu et al., 2013). However, the color algorithm is not suitable for these benchmarks, because it needs color calibration for each video and a background free of the same color to be tracked. Thus, a small dataset was created specially to test the three trackers analyzed in this study: Color, CSRT and Mean shift. A total of nine videos were produced, each representing one of the major problems that have to be dealt with when implementing a good tracking algorithm ([Table 8](#)), as described in the standard benchmarks (Wu et al., 2013). Therefore, each algorithm was tested through nine variables, during the exact same video reproduction. Even though a large standardized dataset would be more reliable, this preliminary test was already fitted for its purpose, which is to help in the development of the system.

**Table 8** – List of problems for tracking algorithms.

Abbr.	Name	Description
BC	Background Clutters	The background near the target has similar color or texture as the target.
IPR	In-Plane Rotation	The target rotates in the image plane.
IV	Illumination Variation	The illumination in the target region is significantly changed.
LR	Low Resolution	The number of pixels inside the ground-truth bounding box is below limit.
MB/FM	Motion Blur/ Fast Motion	The target region is blurred due to the motion of target or camera/ The motion of the ground truth is larger than limit.
OCC	Occlusion	The target is partially or fully occluded.
OPR	Out-of-Plane Rotation	The target rotates out of the image plane.
OV	Out-of-View	Some portion of the target leaves the view.
SV	Scale Variation	The ratio of the bounding boxes of the first frame and the current frame is out of the range.

Source: The author.

In all videos, the same object was used, in the same location. The chosen object was an ArUco marker, due to its very defined black square with a very distinguishable white pattern, which would facilitate the ROI visualization. A paper cube was used as support for the marker ([Figure 12](#)).

**Figure 12** – Schematic of the algorithm test.

Source: The author.

After filming every video, the ground truth, that is, the desired ROI output, was generated through the multi-paradigm numerical computing environment MATLAB Ground Truth Labeler application (MatLab, 2021), with some manual adjustments. Then, the three

algorithms were tested on each of the nine videos and evaluated in relation to ground truth, starting all of them with the same exact ROI as the ground truth in the first frame and using the following metrics:

1. *Success evaluation*: Following (Janku et al., 2016) and (Wu et al., 2013) evaluation metrics, a success plot was made. Given the ROI rectangle of the tracking algorithm ( $r_t$ ) and the ground truth ( $r_g$ ), the area of the intersection between them was divided by the area of the union between them. The number of successful frames in which this ratio was larger than a threshold, in this case, 0.5, was counted and divided by the total number of frames. The formula can be summarized as:  $n_{sf}$  = number of frames in which  $\frac{|A(r_t \cap r_g)|}{|A(r_t \cup r_g)|} > 0.5$ , where  $n_{sf}$  is the number of successful frames and A is the area of the rectangle. Then,  $S = \frac{n_{sf}}{n_f}$ , where S is the success and  $n_f$  is the total number of frames.
2. *Precision evaluation*: To evaluate the precision, it was decided to use the arithmetic mean of the intersection over union value of each frame,  $IoU = \frac{|A(r_t \cap r_g)|}{|A(r_t \cup r_g)|}$ , because it takes into account the scale of the bounding boxes and not just their centers. When there is a perfect overlap, the score is equal to 1.
3. *Time per frame evaluation*: In order to check how fast the algorithms were, the arithmetic mean of the time taken to process every frame was calculated for each video.

The notebook used to process the frames had a i7-9750H CPU, with 32 GB of RAM and a NVIDIA GTX 1660 Ti graphics card. The Python programming language was used. To display the results, the box-and-whisker plot was used. The box identifies where 50% of the most likely values are located, the line inside it is the median of the values and the extreme values are delimited by the whiskers.

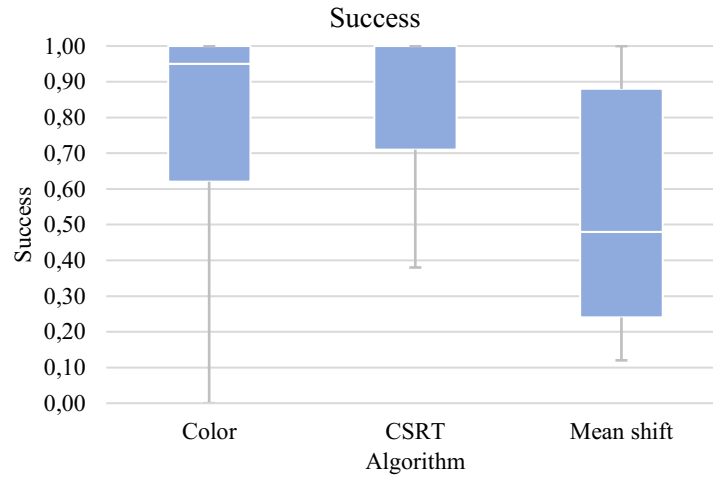
#### 4.1.3 Algorithm tests results

##### 1. *Success*

The total success plot can be seen in [Figure 13](#). It represents the percentage of frames that had a tracked and ground truth ROI overlap over 50%. The values are between 0.00 and 1.00, the higher the better. It can be seen that the CSRT algorithm had a median success of 1.00, or perfect, followed by the color algorithm, which scored 0.95 and the Mean shift, with 0.48.

Nevertheless, the minimum success of CSRT was lower, with 0.38, but it was still the best of the minimum values. Overall, it was significantly better than the Mean shift algorithm. Both the color and the CSRT algorithms achieved good results, with the color algorithm being more inconsistent.

**Figure 13** – Success chart.

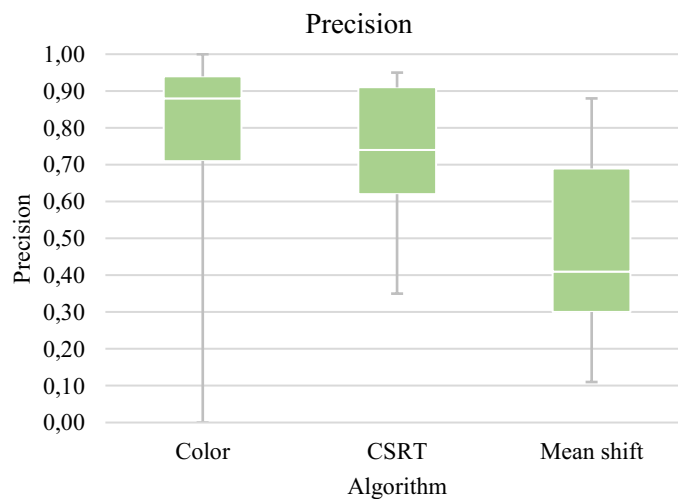


Source: The author.

## 2. Precision

The precision plot is shown in [Figure 14](#). It shows that the color algorithm was the most precise of all, with 0.88 median, followed closely by the CSRT algorithm, with 0.74, both good results. The color algorithm had a bit more consistent results inside the box than the CSRT algorithm this time, but a very dispersed result in the extremes, scoring a 0.00 in the BC test and 1.00 in the OPR test. Mean shift had a low median of 0.41.

**Figure 14** – Precision chart.

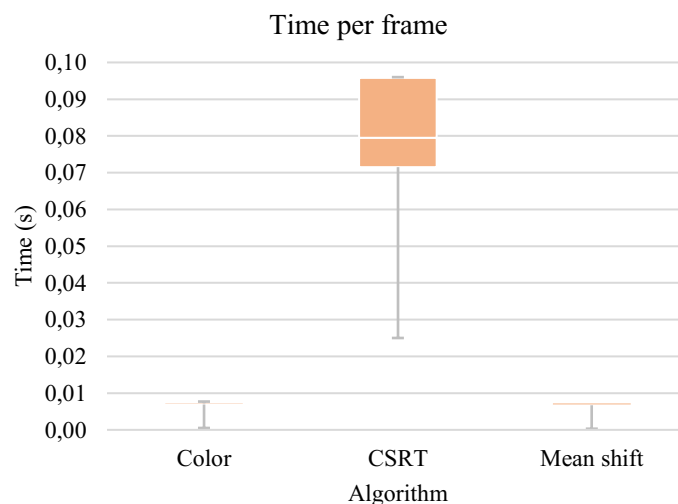


Source: The author.

### 3. Time per frame

The time per frame chart is shown in [Figure 15](#). It shows that that the color and the Mean shift algorithms were really fast, with the first having an average of 0.0071 seconds to process each frame, which results in a fps (frames per second) of  $1/0.0071 = 140.8$  fps, and the Mean shift, 0.0069 seconds, that is,  $1/0.0069 = 144.9$  fps, thus achieving the real-time requirement for the game. It was desired at least 30 fps. The CSRT algorithm did not achieve real-time in the i7 notebook, having an average of  $1/0.0795 = 12.6$  fps, because, at this framerate, the human eye can distinguish the different frames of the video. The fps value obtained with the CSRT is similar to the one the authors claimed in the original paper, 13 fps on a i7 processor (Lukezic et al., 2017).

**Figure 15** – Time per frame chart.



Source: the author.

[Table 9](#) displays all the 27 precision results, for each type of problem and solution tested. It can be seen that the color algorithm presented a better performance in five opportunities: in the In-Plane Rotation, Motion Blur/Fast Motion, Out-of-Plane Rotation, Out-of-View and Scale Variation. The color algorithm won in the rotation tests because it was able to change the ROI scale exactly like the actual scale change, while the other two algorithms varied the scale beyond the limits of the object. Some algorithms were completely lost, such as the Mean shift during the Out-of-Plane rotation, which was not expected, as this algorithm also uses color for tracking.

The fact that the color algorithm won in most of the tests was expected, because, even with great motion blur, the color is still there, while the other features that the other trackers generally depend on, such as texture pattern, can no longer be trusted. Therefore, the tests have

**Table 9** – All precision results.

<b>Problem</b>	<b>Color</b>	<b>CSRT</b>	<b>Mean shift</b>
BC	0.00	<b>0.95</b>	0.88
IV	0.77	<b>0.90</b>	0.30
IPR	<b>0.94</b>	0.74	0.74
LR	0.92	<b>0.95</b>	0.69
MB/FM	<b>0.71</b>	0.70	0.24
OCC	0.54	0.35	<b>0.59</b>
OPR	<b>1.00</b>	0.62	0.39
OV	<b>0.88</b>	0.62	0.11
SV	<b>0.97</b>	0.91	0.41

Source: The author.

shown that color is the most reliable feature to be tracked. It also, as a bonus, has the lowest processing cost, and, therefore, was chosen for the application to be developed. A video of the tests can be seen at <https://youtu.be/ICYYaRB9apU>.

## 4.2 System Development

### 4.2.1 Theoretical base

An exergame rehabilitation system consists of its software, the game itself, and the hardware, the device that will assist in capturing body movement and translating it into virtual movements. Seeking system accessibility (low cost and wide availability), the following requirements were considered:

1. The software must be easily distributed. This is only possible if the software is made for popular operating systems, such as Windows and Android, and for devices that people usually have at home, such as a smartphone (IBGE, 2018). For this reason, the system was developed for both Android and Windows platforms, being possible to be used on smartphones, tablets, notebooks and desktops;
2. The hardware should have the lowest possible implementation cost, and the most accessible materials. For this, a hardware totally free of electronic devices and

possible to be reproduced with handmade materials (e.g., Styrofoam, paints, fabric) has been chosen.

Based on these requirements, it was decided that the 3D tracking, the main innovation of this system, would be done as follows: two colored spheres, of the same diameter, of uniform color and distinct from the surrounding environment, would be affixed to the body of the user, using masking tape, for instance, so that they are at the same distance from a central joint. For example, if this joint is the elbow, one ball should be affixed to the hand and the other to the user's shoulder. Then, the software will turn on the webcam or front camera of the device used to display the game, capturing frame by frame. In each frame, the software will segment each sphere of the rest of the environment, through its colors, calibrated by the user. Then it will identify the 3D position of each sphere for calculating the angle of the joint, which is used to control the game ([Figure 16](#)).

This is achieved as follows:

### 1. *Compensating for camera distortions*

First, it should be noted that all traditional cameras will produce distortions in their images. Since the lens is curved, the center of the photo is slightly enlarged more than the edges. This makes the straight lines appear to curve around the edge of the image. The wider the lens, the more extreme the optical distortion. This is due to the physical shape of the lens glass. However, a camera lens from the same device, in the same position, will always create the same type of lens distortion. Therefore, it is possible to reverse this effect, by using a correction algorithm based on the specific lens model. The two main types of distortion are radial distortion and tangential distortion. Radial distortion makes straight lines look curved. The radial distortion becomes greater as the most distant points are from the center of the image. Radial distortion can be represented through the following formulas:

$$x_{distorted} = x(1 + k_1r^2 + k_2r^4 + k_3r^6)$$

$$y_{distorted} = y(1 + k_1r^2 + k_2r^4 + k_3r^6)$$

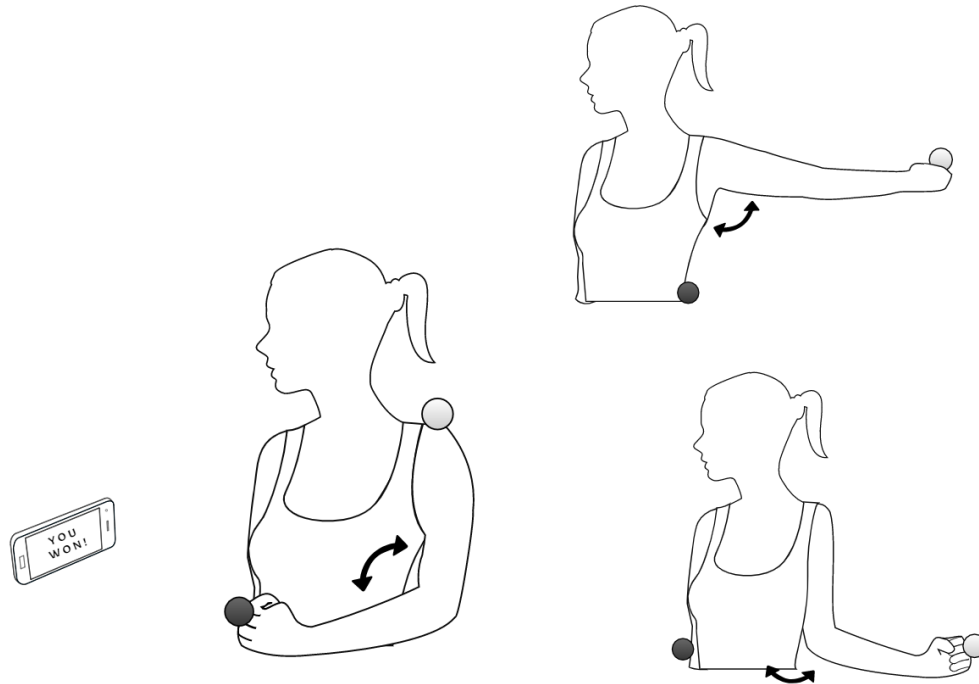
Likewise, tangential distortion occurs because the image captured by the lens is not perfectly aligned parallelly to the image plane. Therefore, some areas of the image may appear closer than expected. The amount of tangential distortion can be represented as follows:

$$x_{distorted} = x + [2p_1xy + p_2(r^2 + 2x^2)]$$

$$y_{distorted} = y + [p_1(r^2 + 2y^2) + 2p_2xy]$$



**Figure 16** – The controller of the game consists of spheres, which can be made out of craft materials and placed to measure the angle of any joint in the body.



Source: The author.

In short, it is necessary to find five parameters, known as distortion coefficients, given by:

$$\text{Distortion coefficients} = (k_1 \quad k_2 \quad p_1 \quad p_2 \quad k_3),$$

where  $r$  is the Euclidean distance between the distorted image point and the distortion center. The above formulas are derived from the Brown distortion model (Brown, 1966), also known as the Brown-Conrady model, based on previous work by Conrady (Conrady, 1919). The Brown-Conrady model corrects radial and tangential distortions, caused by physical elements in a lens that are not perfectly aligned.

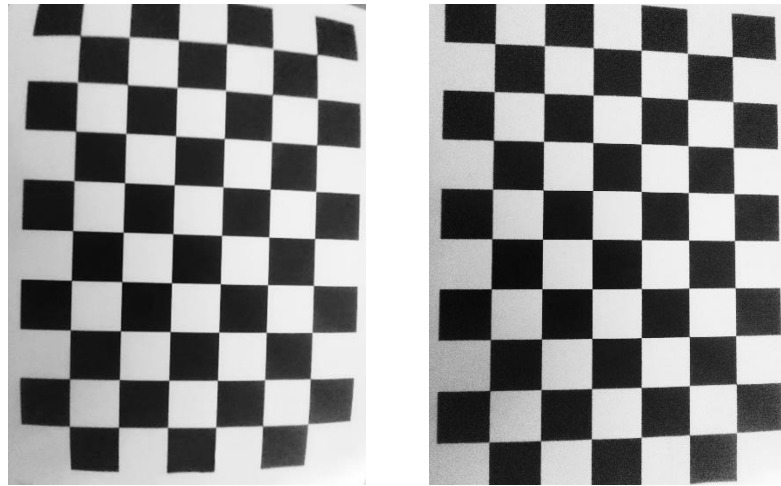
In addition, in Math, the transformation from 3D object points to 2D image points and vice-versa is done by a transformative matrix called the camera matrix. This contains some information exclusive to the camera, which is called the camera's intrinsic parameters, focal length ( $f_x, f_y$ ) and optical centers ( $c_x, c_y$ ):

$$\text{camera matrix} = \begin{bmatrix} f_x & 0 & c_x \\ 0 & f_y & c_y \\ 0 & 0 & 1 \end{bmatrix}$$

Also, there are the extrinsic parameters, which correspond to the rotation and translation vectors, that translate the coordinates of a 3D point to a 2D coordinate system (and vice-versa). To find them, one must provide some sample images of a well-defined pattern (for example, a

chessboard). The coordinates of the chessboard square corners, in image space, are calculated for every image and correlated to the real-world space coordinates. Therefore, calculating the distortion coefficients, which can be used to obtain an undistorted image from the camera ([Figure 17](#)) (Zhang, 2014).

**Figure 17** – Original image (left) and corrected (right).



Source: The author.

## 2. *Segmentation of the spheres*

After calibrating the camera, each camera frame is obtained and its distortions are corrected. It is now necessary to track the 3D position of the spheres. First, they need to be segmented from the rest of the image. This is done by searching, in each frame of the video, for the color of the sphere in the HSV space, which is the color system formed by the components Hue, Saturation and Value. For this, the user is asked to specify the maximum and minimum values of the desired sphere color. So, first, each pixel is analyzed, converted from the RGB space: Red, Green and Blue, which is the default, to HSV. Afterwards, the pixels that have an HSV value between the specified maximum and minimum are separated from the rest of the image, generating a binary mask ([Figure 11](#)).

However, the sphere has imperfections: it reflects light, produces shadow, and undergoes occlusions. Also, there may be another small object in the background of the same color as the sphere. In this way, to improve the image, morphological operations can be performed on it, which are image processing techniques. In this system, the morphological opening operation is performed, which is useful to remove small objects from an image while preserving the shape and size of larger objects in the image ([Figure 18](#)).

**Figure 18** – Before (left) and after (right) the morphological opening operation.



Source: The author.

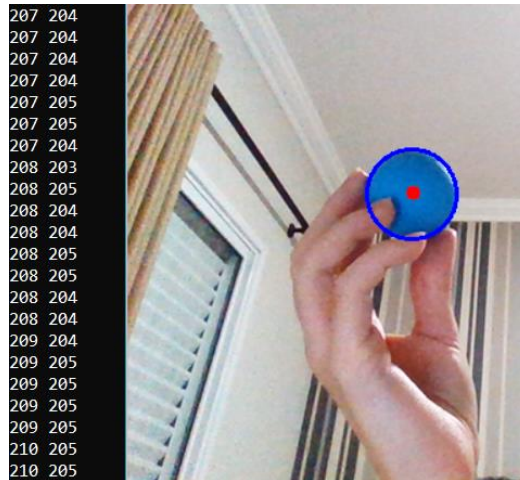
After the morphological operation, the contours of the white spots remaining on the mask are calculated. The largest contour found should be that of the sphere, if there is no larger object of the same color in the scene. If there is a larger object of the same color in the scene, the color of the spheres should be switched. Once the contour of the sphere is found, the circle circumscribed to this contour, with its center and its radius are calculated, which is the estimation of the center of the sphere in the image, in 2D pixel coordinates, with the point (0,0) being the top left pixel of the image ([Figure 19](#)).

### 3. *Real-time 3D position estimation*

From the 2D image obtained with the camera, the distortions of the lens are corrected, the sphere is segmented by means of its color and the center of the circle circumscribed to its outline is found. Now, it is necessary to transform the 2D coordinates of the center of the sphere into a real-world 3D position in centimeters.

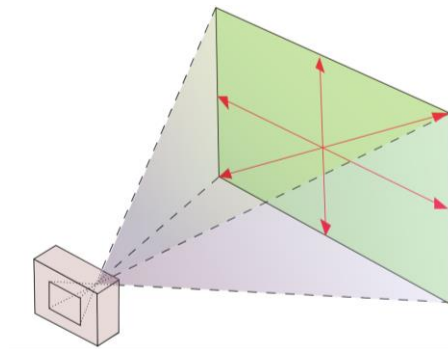
A first attempt to estimate the missing dimension, which is the distance between the object and the camera, or the z axis, could be by the variation of the diameter of the 2D projection of the sphere when it approaches or moves away from the camera. However, there is a problem with this, since the camera's field of view is not  $180^\circ$  ([Figure 20](#)). This causes the problem in [Figure 21](#): when the object is far from the center of the camera, a variation in the z axis (3D) causes a shift in the x axis of the 2D projection. This would make the 3D position estimation wrong.

**Figure 19** – Detected sphere and its 2D pixel coordinates. Observe that the tests were done in a common room without a special background.



Source: The author.

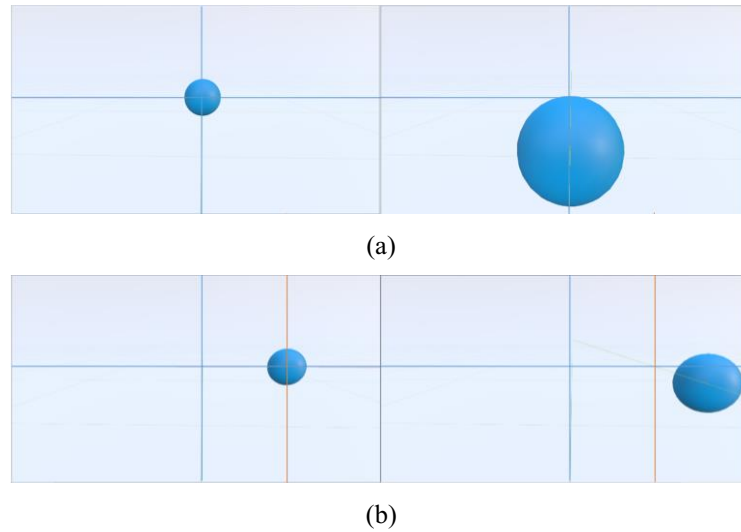
**Figure 20** – Field of view of a camera.



Source: Dicklyon at English Wikipedia, Public domain, via Wikimedia Commons.

In the field of Computer Vision, problems such as this (camera or object pose estimation) are fundamental and well understood. They have been studied for over a century (Lu, 2018). In the early 1980s, Fishler proposed the Perspective-n-Point problem (Fischler & Bolles, 1981), whose goal is to estimate the position and orientation of a calibrated camera from known 3D-to-2D point correspondences between a 3D model and their image projections, which is fundamental for many applications. The most general version of the problem requires estimating the 6 degrees-of-freedom (DOF) which are made up of the rotation (roll, pitch, and yaw) and 3D translation of the camera and five calibration parameters: focal length, principal point, aspect ratio and skew. The Perspective-n-Point is the most common simplification to the camera pose problem, by assuming known calibration parameters.

**Figure 21** – A change in the z axis (3D) (a) when the object is near the center of the camera and (b) when the object is dislocated from the center of the camera: the x axis of the 2D projection is also dislocated.



Source: The author.

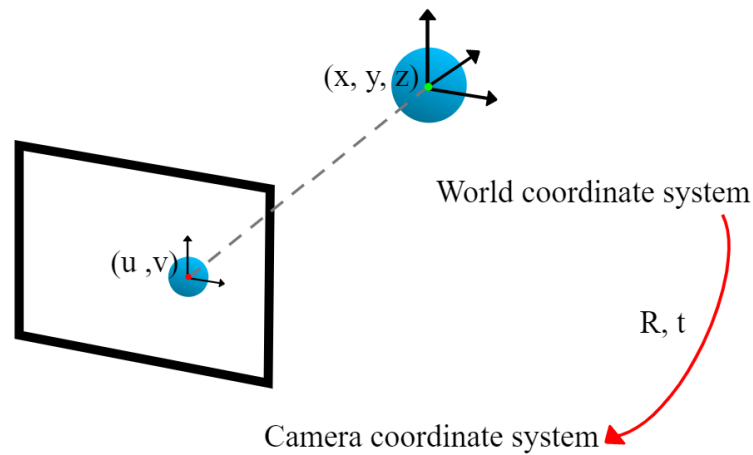
This problem can be formulated as: given a correspondence between a 3D point with  $(x, y, z)$  coordinates expressed in a world reference frame, and its 2D projection  $(u, v)$  onto the image, seek to retrieve the pose  $(R, t)$  of the camera with respect to the world and the camera's intrinsic parameters: focal length  $(f_x, f_y)$  and optical centers  $(c_x, c_y)$  (Figure 22).

This means that, with the following formula, it is possible to project 3D points on the image plane:

$$s \begin{bmatrix} u \\ v \\ 1 \end{bmatrix} = \begin{bmatrix} f_x & 0 & c_x \\ 0 & f_y & c_y \\ 0 & 0 & 1 \end{bmatrix} \begin{bmatrix} r_{11} & r_{12} & r_{13} & t_1 \\ r_{21} & r_{22} & r_{23} & t_2 \\ r_{31} & r_{32} & r_{33} & t_3 \end{bmatrix} \begin{bmatrix} x \\ y \\ z \\ 1 \end{bmatrix}$$

Note that the intrinsic parameters can be calculated in the camera calibration step. By replacing them in the equation, the coefficients  $R$  (rotation) and  $t$  (translation) of the sphere centers can be found. As a sphere has no intrinsic orientation, only the translation coefficients  $t_1, t_2, t_3$  can be used. They give the position of the center of the sphere in real-world coordinates.

**Figure 22** – The Perspective-n-Point problem.



Source: The author.

After obtaining the real 3D position of the center of both the spheres, the angle of the joint can be calculated, as this is an important parameter for measuring the spasticity of the upper limb and, therefore, the clinical progress of the patient. The angle of the elbow joint is calculated as follows:

- 1) The user is asked to measure the distance between his shoulder and elbow, which will be the same distance, approximately, between his fist and his elbow ( $d_1 = d_2$ ). This doesn't have to be very anatomically precise, as long as the distance between each sphere and the joint is the same.
- 2) From the 3D positions of each sphere, one on the wrist ( $X_2, Y_2, Z_2$ ) and other on the shoulder ( $X_3, Y_3, Z_3$ ), the distance ( $d_3$ ) between them can be calculated using the Euclidean distance formula:

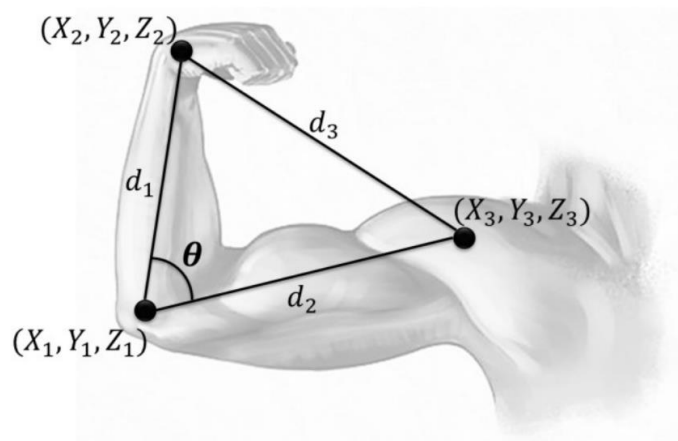
$$d_3 = \sqrt{(X_2 - X_3)^2 + (Y_2 - Y_3)^2 + (Z_2 - Z_3)^2}$$

- 3) Now, having  $d_1$ ,  $d_2$  and  $d_3$ , the value of the three sides of a triangle formed by the patient's arm is determined, in which  $d_3$  is the distance opposite the angle of the elbow (Figure 23). Then, the elbow angle ( $\theta$ ) can be obtained by the law of cosines:

$$\cos \theta = \frac{d_1^2 + d_2^2 - d_3^2}{2d_1d_2}$$

The same principle can be extended for similar body joints. Now, the elbow angle was found in 3D space without camera distortions. That is, the user can rotate the arm in all three dimensions and this angle will continue to be read correctly.

**Figure 23** – The angle of the elbow joint can be found by the law of cosines.



Source: (Freire Bastos Filho et al., 2017) – Public domain.

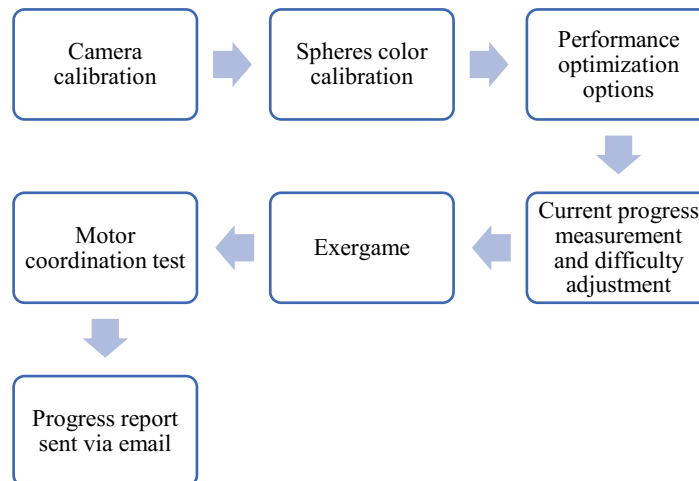
#### 4.2.2 Software development tools

The system was developed using Unity (Unity, 2021b) game engine. Three-dimensional modelling, texturing and animation was done with Blender (Blender, 2021). The vegetation was procedurally generated using TreeIt (TreeIt, 2021). The 2D vectors were created using the Vectr web editor (Vectr, 2021) and GIMP image manipulation software (GIMP, 2021). It was used the free version of all these tools. The 3D models for the scenery were adapted from Unity team demonstration projects. The OpenCV-Unity integration was done using the OpenCV plus Unity free plugin (Unity, 2021a). The main audio theme of the games is from Kevin MacLeod (FreeMusicArchive, 2021).

#### 4.2.3 System architecture and interface

The system has the usage flow of [Figure 24](#), which will be described in this subsection. As previously explained, the 3D elbow angle is known, as well as the 3D position of the patient's shoulder and wrist. This information will now be used in the exergame.

Two versions of the game were made. One with 2D graphics and one with 3D graphics. They have some differences. The 2D graphics version is much lighter to storage and process. Also, it has only one controllable axis of movement, which is the y axis (up and down). Therefore, it works only one joint at a time, being an easier game. The 3D graphics version is for devices that have a better hardware and can reproduce 3D semi-realistic games. It has 2 axes

**Figure 24** – System usage flow.

Source: The author.

of character movement, x and y (up and down, left and right), therefore, is a bit harder to play. Both versions are for Android and Windows.

When first opening the game on a new device, the user sees a questionnaire screen. This was done in case of need to collect data remotely for research. In the first page of the questionnaire, there is the consent form of this eventual research and, in the second page, some general information of the participant can be collected ([Figure 25](#)). Afterwards, the user sees the initial screen ([Figure 26](#)). From there, he can choose what he wants to do, from the menu options.

When playing for the first time, the user must perform the camera and color calibrations. This calibration will only be necessary again if the device camera or the device position or the illumination of the room is greatly changed. To calibrate the camera, the user should click on “Set Camera”. When entering this option, the panel in [Figure 27](#) appears.

Also, the user must print a checkerboard pattern, supplied with the system, and paste it on a rigid surface (a book, for example). Then, he must take some pictures of this object, from several different angles. It is possible to do a calibration with very few photos, however, the more photos are taken, the better. To take photos, the user must press the “Take Picture” button, which will count for five seconds and capture a photo from the camera, recognizing the checkerboard pattern. If the pattern is recognized correctly, colored lines will be seen over the image. When finishing the calibration, the user must click on “Calibrate and Apply”, to calculate the matrix with the calibration parameters. He can also clear the photos and what was calculated, in “Clear”, save for future sessions, in “Save”, or leave this panel, in “Back”. This panel was done with a simplified interface, for the post-stroke user to be able to do it with one hand.



**Figure 25** – Initial questionnaire screen: (a) consent form and (b) general information collection.

**CONSENT FORM**

This game is part of a research project, conducted by the Assistive Technology Lab at Federal University of Uberlândia, Brazil. We are testing the usability of this game and if it improves motor skills of impaired subjects. If so, it will be available for the community to use. You are invited to participate in this research if you have a upper limb gross motor impairment caused by stroke.

Your participation in this research study is voluntary. If you decide to participate, you may withdraw at any time. The procedure involves filling the brief survey on the next page. We will also collect your progress data, such as angle range, velocity, test scores and session duration. Your responses will be confidential and we will not collect identifying information such as your name, email address, IP address, video or audio inputs.

The results of this study will be used for scholarly purposes only. This research has been

agree

disagree

(a)

**INITIAL QUESTIONNAIRE**

Hello! Please answer the following information about you:

Sex (male/female):  male  female

Age (years):

Time post stroke (months):

Type of stroke (ischemic/hemorrhagic):  ischemic  hemorrhagic

Affected body side (right/left):  right  left

Dominant arm (right/left):  right  left

**SAVE**

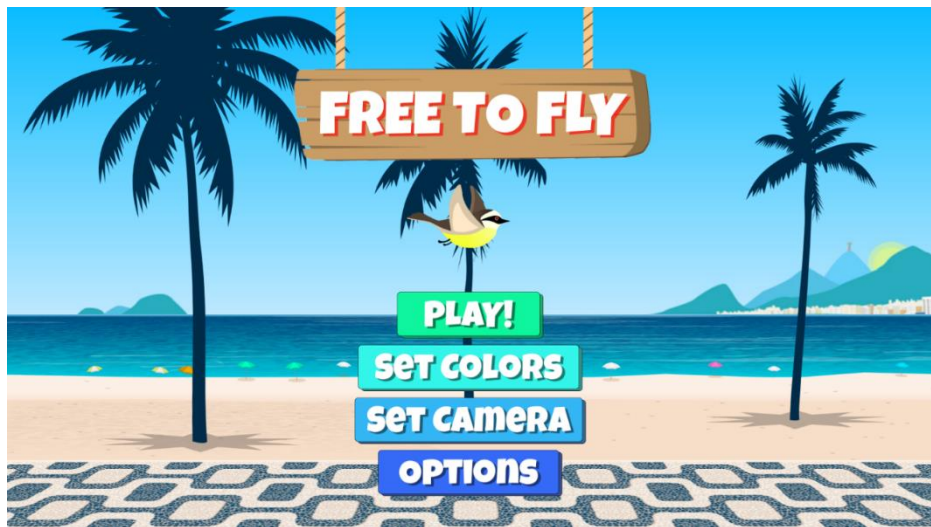
(b)

Source: The author.

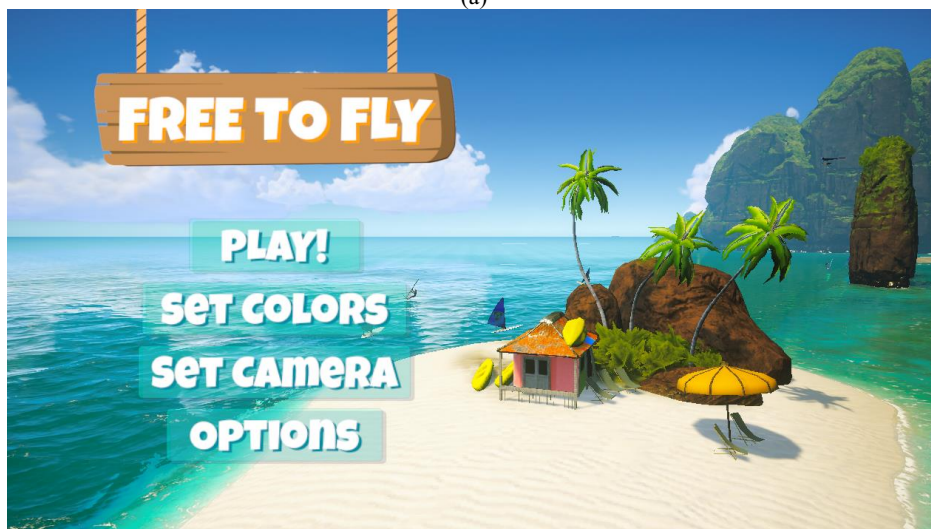
Now, the user must calibrate the colors of the spheres that he has, in relation to his environment. For this, he should enter the “Set Colors” panel ([Figure 28](#)).

In this panel, the user should move the arrows, choosing the maximum and minimum limit of the colors he wants to calibrate, according to their hue, saturation and value. To help, the user can click on “Change View” to view the mask produced. Calibrating correctly, he will see his spheres surrounded by a line. The user must also set his half arm length on “Half Arm Length (cm)” and the diameter of his sphere on “Ball Size (cm)”. In the lower left corner, he will see the angle of his elbow that the system is accusing. The user can then save in “Save” or return to the menu in “Back”.

**Figure 26** – Initial interface of the game in the (a) 2D and (b) 3D versions.



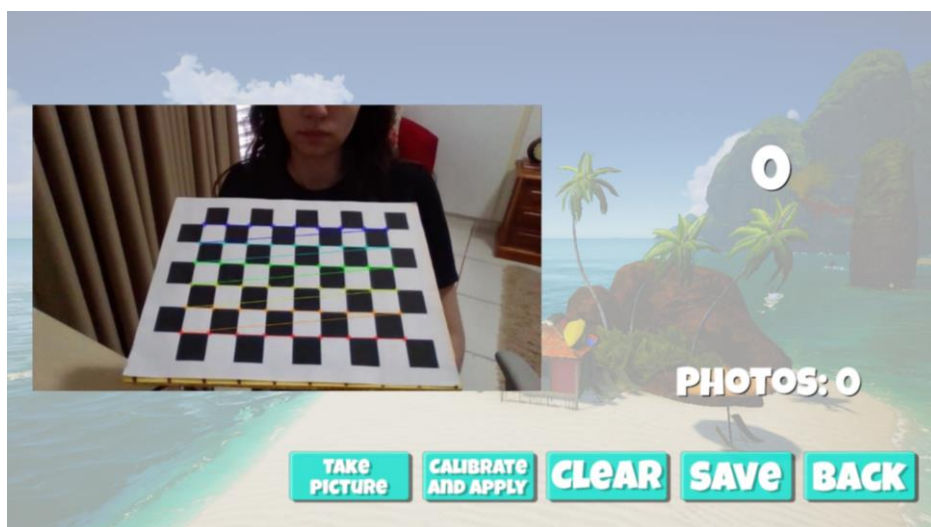
(a)



(b)

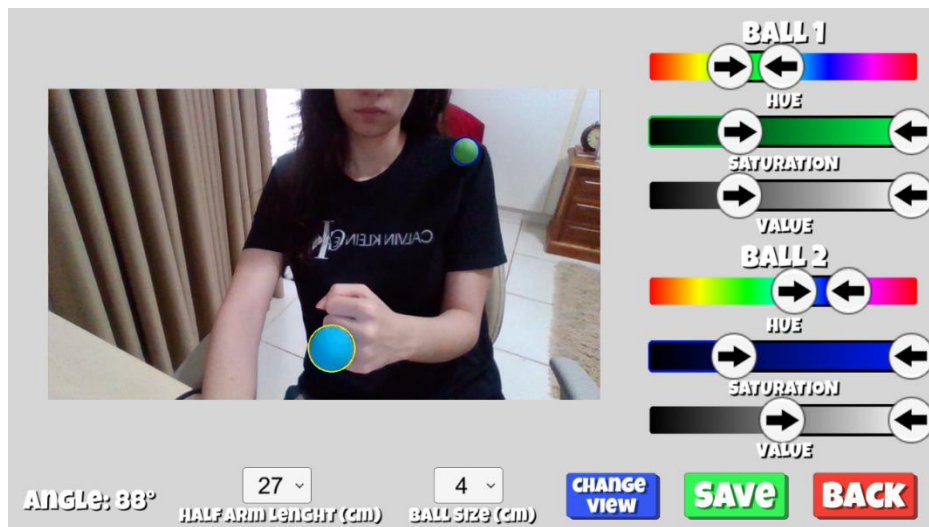
Source: the author.

**Figure 27** – Camera calibration interface – 3D version.



Source: The author.

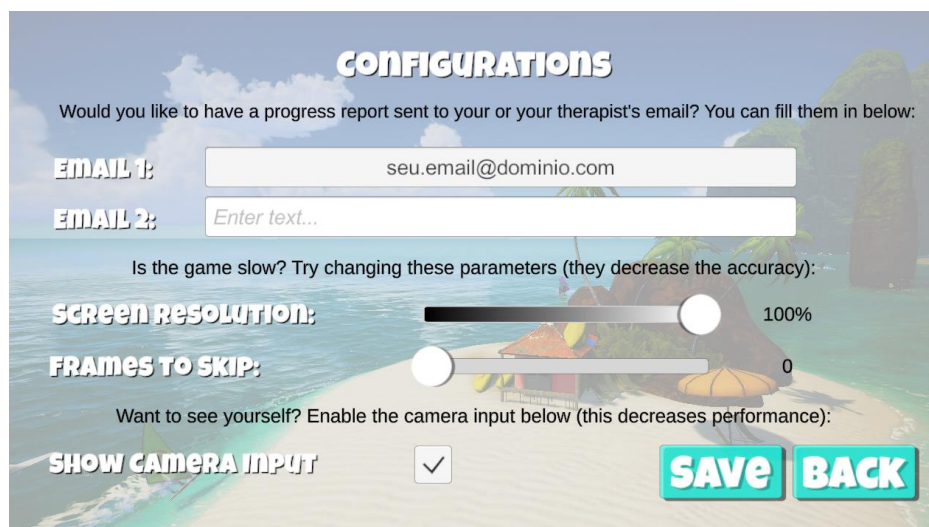
**Figure 28** – Color calibration panel – 2D version.



Source: the author.

Once the calibrations are done, the user can change some game settings in "Options". In this panel, he can place two emails, to which his progress report will be sent (it is suggested that one email is from the patient and the other from the therapist). In addition, the patient can change performance options, if the game is too slow on his device, by reducing the capture resolution in "Screen Resolution", and asking the system to skip the capture of some frames, in "Frames to Skip". This decreases the accuracy of the capture. The patient can also choose to see himself or not during the game, in "Show Camera Input", which also slows down the game (Figure 29).

**Figure 29** – Configuration panel – 3D version.

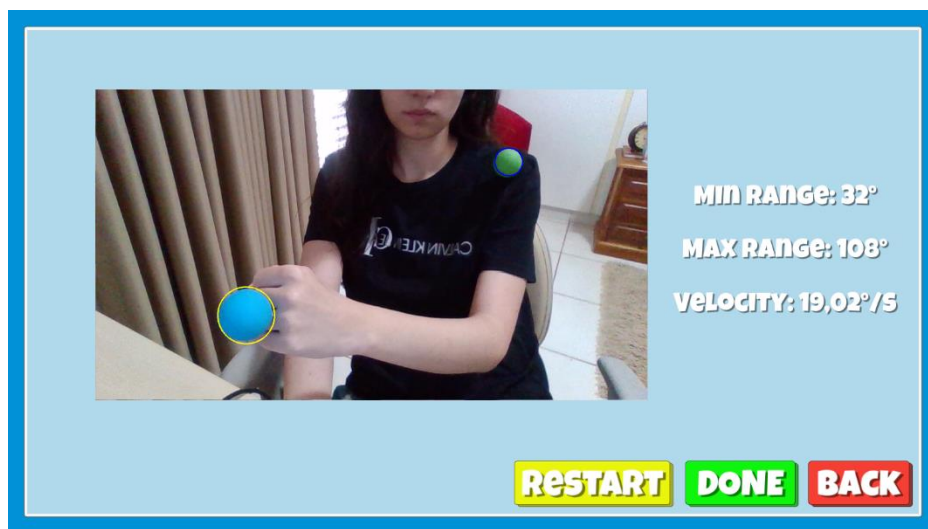


Source: The author.

Again, the patient can save or exit this panel. After that, he can play by clicking on the "Play!" button of the main menu. Then, the user enters the difficulty adjustment panel, which collects data on his current joint range and speed of movement. For this, he should flex the arm

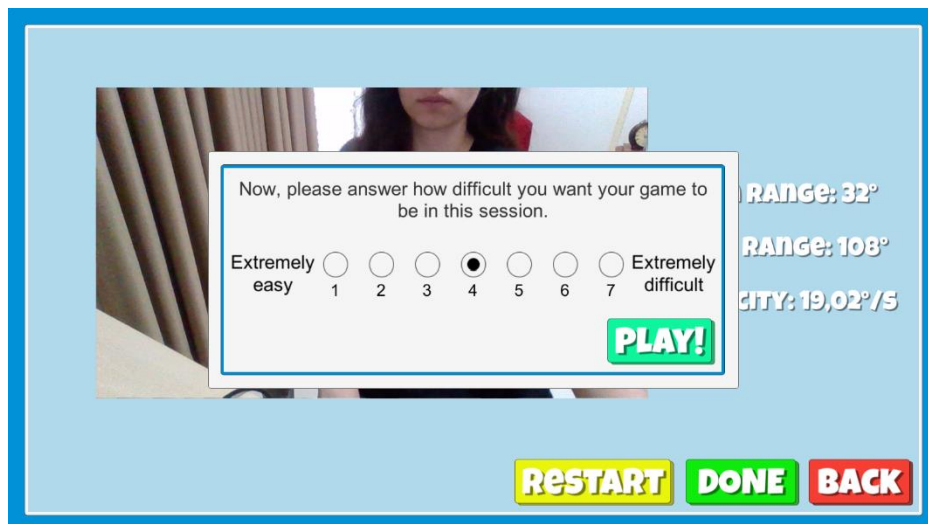
as much as possible and then extend it as much as possible, as fast as he can. Then, minimum and maximum angles and the joint extension speed will be captured. The user can restart this test, if desired, in “Restart”. He can return to the menu, in “Back”, or end the test, in “Done” (Figure 30). When clicking on “Done”, a question will appear, in the form of a scale from 1 to 7 (Likert scale), of how difficult the patient wants the system to be. He must choose the difficulty and click on “Play” (Figure 31).

**Figure 30** – The difficulty adjustment panel captures the current angle range and extension velocity. This information is used to adjust the difficulty of the game and in the progress report.



Source: the author.

**Figure 31** – Difficulty choice panel.

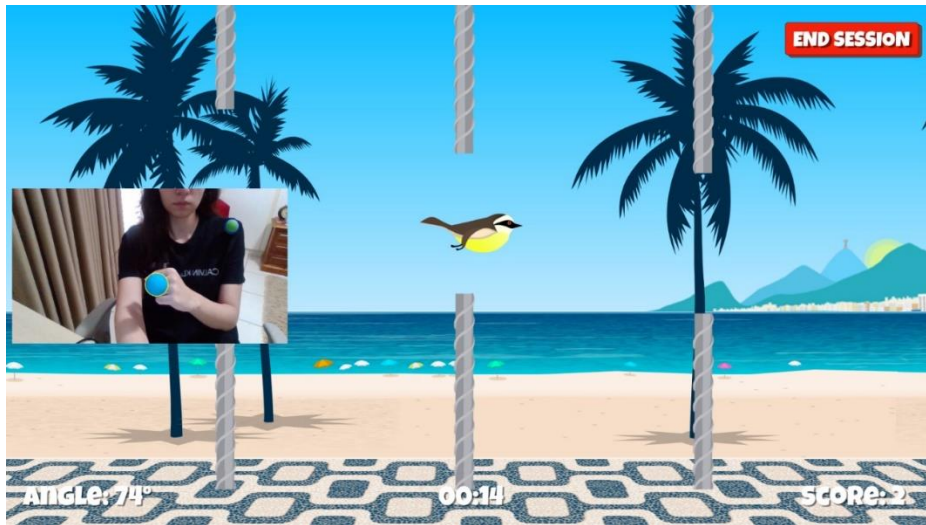


Source: The author.



By clicking "Play!", the game will start. Both versions take place on a beach, a scenario chosen because the advanced age of most post-stroke patients is expected by the author to translate into a preference for nature scenarios. In the 2D version, the angle of the patient's elbow will be used to move the bird character (a great kiskadee) upwards (by flexing) and downwards (by extending) (Figure 32). In the 3D version, there is the addition of the left-right movement of the green-winged macaw by rotating the shoulder joint internally or externally (Figure 33).

Figure 32 – Exergame - 2D version.



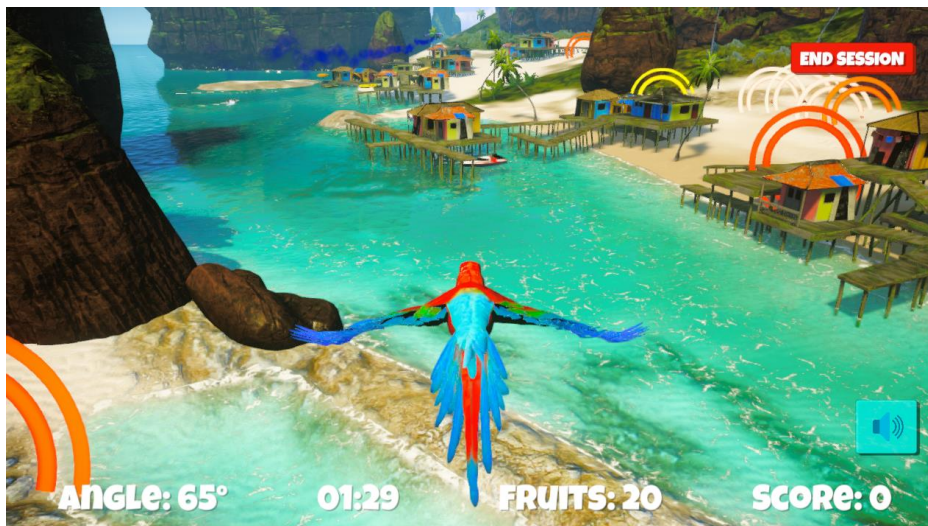
Source: The author.

The game versions have different narratives. In the 2D version, the bird must pass through the obstacles, which are metal columns. The information of time, “Score” in number of columns, and elbow angle can be seen. If the user has chosen this option in the options panel, he will see himself during the game. The user can end the session in “End Session”. In the 3D version, the bird must capture all fruits randomly distributed on the scenery. There is the information of fruits left to capture on the screen.

At the end of the session, the user will be asked to do a drawing test, to check whether his motor coordination has improved. It consists of following a pattern on the screen with the sphere on your hand. The test will end when the user returns to the point at which he started drawing (Figure 34).

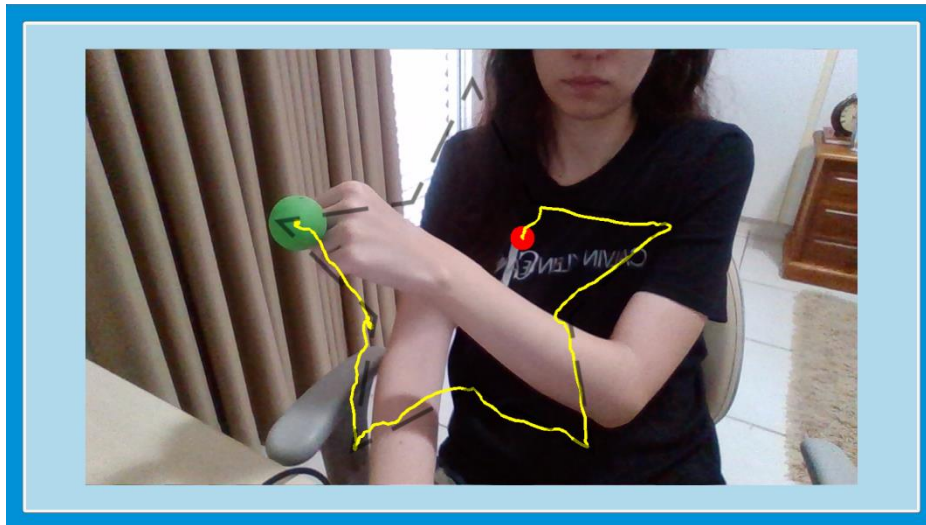
After finishing the drawing, a warning will appear on the screen, indicating that the progress report has been generated and sent to the registered email.

Figure 33 – Exergame – 3D version.



Source: The author.

**Figure 34** – Drawing coordination test.



Source: The author.

#### 4.2.4 Difficulty adjustment

Due to being at different recovery stages, each post-stroke player has a different range of elbow extension, at a different speed. This has to be translated into the game. If the adjustment is not made, the patient with little amplitude will not be able to move the character correctly and achieve the objective of the game.

The difficulty setting of the game has an automatic and a customizable part. The customizable part consists of the player choosing, on the presented Likert scale (Likert, 1932) ([Figure 31](#)), a difficulty level from 1 (extremely easy) to 7 (extremely difficult). The automatic part uses the angle range and velocity values to modulate the character's movement ([Table 10](#)).

**Table 10** – Variables that are used to adjust the difficulty.

Variable	Description	Influence – 2D game	Influence – 3D game
<i>levelChoice</i>	Option selected by the user on the Likert scale of difficulty	<ul style="list-style-type: none"> <li>• Character's range of motion</li> <li>• Rate of appearance of new columns</li> <li>• Distance between columns on the y axis</li> </ul>	<ul style="list-style-type: none"> <li>• Number of fruits in the scene</li> <li>• Size of help to find the fruits</li> <li>• Score from each fruit</li> </ul>
<i>angleRange</i>	Angular amplitude measured during calibration before the session	<ul style="list-style-type: none"> <li>• Character's range of motion</li> <li>• Rate of appearance of new columns</li> </ul>	<ul style="list-style-type: none"> <li>• Character's range of motion</li> </ul>

---

<i>velocity</i>	Movement speed measured during calibration before the session	• Rate of appearance of new columns	---
-----------------	--	--	-----

---

Source: the author.

### a) Character's range of motion

For this adjustment, first, the angular amplitude of the elbow (*angleRange*) is calculated, through the measured maximum (*maxAngle*) and minimum (*minAngle*) angles:

$$angleRange = maxAngle - minAngle.$$

Then, the ratio (*angPosRatio*) between the position of the bird on the y axis (*birdPosRange*) and the angular amplitude is calculated:

$$angPosRatio = birdPosRange / angleRange.$$

This ratio is then used in the following formula:

$$newPos = angPosRatio * (angle - minAngle),$$

being *newPos* the bird's next position and *angle* the current angle of the elbow. This formula allows the bird to move from top to bottom of the scene, regardless of the patient's range of motion.

Also, an additional challenge is offered so that the patient is encouraged to extend/flex the elbow beyond its current range and, therefore, gain more amplitude, which is the goal of therapy. For this, the following calculation is made:

$$maxAngle = maxAngle + 0,1 * levelChoice * maxAngle$$

$$minAngle = minAngle - 0,1 * levelChoice * minAngle,$$

where *levelChoice* is the difficulty chosen on the Likert scale. Through these calculations, a proportional value to the chosen difficulty is added to the maximum angle and, likewise, removed from the minimum angle. This means that the patient has to extend or flex the elbow more to reach the required position of the character, encouraging him to move beyond his current range.

### b) Rate of appearance of new columns

The rate of appearance of new columns in the scene (*spawnRate*) is impacted by the elbow angle amplitude and speed calibrated at the beginning of the session and by the selected difficulty, through the formula:



$$spawnRate = (2 * angleRange) / (difficultyAnswer * velocity),$$

This rate indicates in how many seconds a new column will appear on the scene. Note that, the greater the chosen difficulty and the user's velocity, the faster the columns will appear. Also, the greater the patient's movement amplitude, the slower the columns will appear, as the patient must move the arm further to reach a certain position.

### c) Distance between columns on the Y axis

According to the difficulty chosen by the patient, a distance is selected between the columns on the Y axis. Therefore, there is a possibility to choose from seven pre-selected distances in the game. The shorter this distance, the more precise the movement must be, thus, the greater the difficulty. For this reason, the column distance is chosen inversely proportional to the Likert scale value, and that column is instantiated in the scene.

### d) Number of fruits in the scene

The number of fruits in the scene (*fruitCount*) is decided by the Likert scale answer, that is, the *levelChoice* variable. The fruit count is calculated by the formula:

$$fruitCount = 5 * (-levelChoice + 8),$$

which means 35 fruits at level 1 and 5 fruits at level 7, so it's easier to find fruits and score at the easier levels.

### e) Size of help to find the fruits

The fruits are all instantiated with animated concentric circles around them ([Figure 33](#)), which makes them easier to find. These circles are bigger to easier the level.

### f) Score from each fruit

There are 9 types of fruit possible to capture. The score attributed to each fruit is a number from 1 to 9 (the rarer the fruit, the higher this number) times the *levelChoice*. This was done so that, at level 7, even with only 5 fruits, they will be so valuable that the total possible score will be higher than the one possible at level 1, when the fruits are much easier to capture.

#### 4.2.5 Collected data and progress report

During the game, some relevant data about the patient and a specific therapy session are collected. They are:

- ID: a unique and fixed number, randomly generated, to identify the user, maintaining his anonymity;
- Session number: how many sessions have been made so far;
- Session duration (minutes): the current session duration;
- Days of playing: the number of days on which the user had a therapy session;
- Angle range ( $^{\circ}$ ): the angular amplitude of the elbow, measured by the system;
- Velocity: the elbow extension speed, measured by the system;
- Difficulty choice: the difficulty chosen on the Likert scale;
- Number of flexions: the number of elbow flexions during a session;
- Score: score on that session;
- Number of errors: the number of errors (hitting an obstacle);
- First e-mail and Second e-mail: the e-mails to which the patient wishes to send the progress report; and
- Drawing test: the drawing test image.

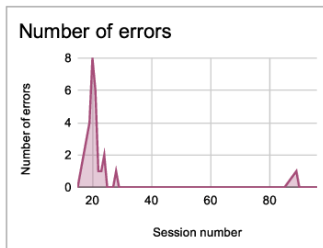
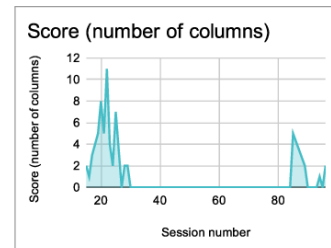
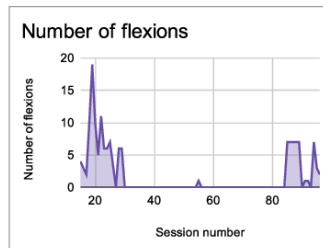
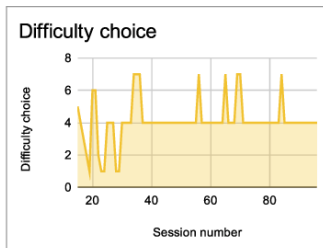
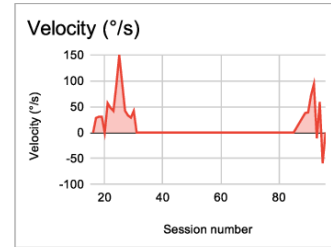
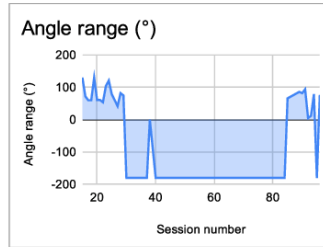
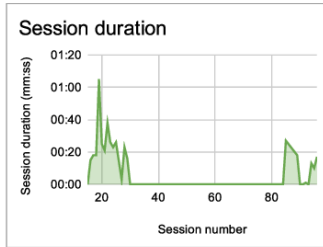
This data is collected and stored in the cloud automatically, through the services of the Google platform, with no need for a local database. A progress report is also generated with the data collected over several sessions ([Figure 35](#)), which can be sent via email to two people, for example, the patient and his therapist. This makes the therapy as remote as possible.

Figure 35 – Example of progress report generated by the game.

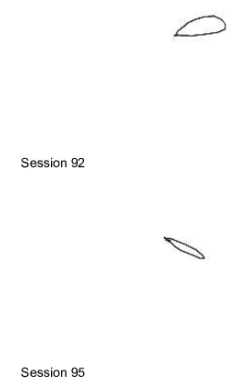
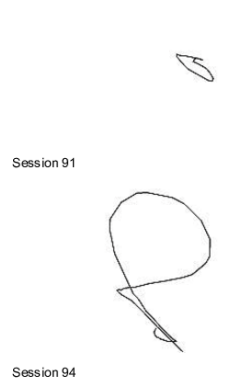
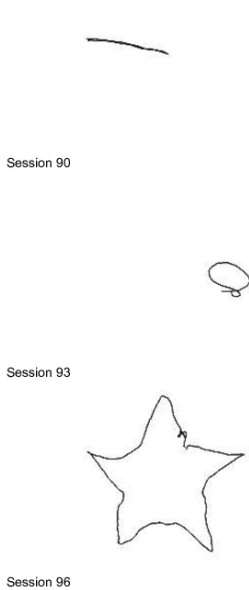
### Sessions report

**ID:** 473  
**Session Number:** 96  
**Days of Playing:** 16

**Date/Time:** 04/11/2020 08:41:35



### Drawing tests



Source: The author.

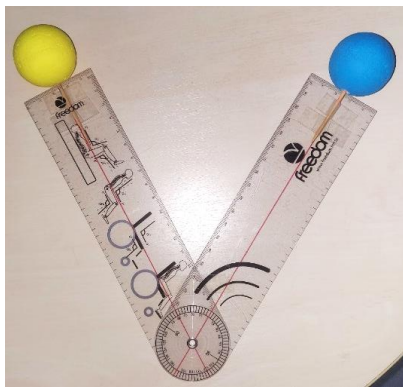
### 4.3 System Tests

In the following tests, the accuracy of the angle measured by the system was tested by changing the following variables:

#### *a) Angle value*

To test the accuracy of the angles measured through the game, a comparison between these angles and those of a gold standard measurement instrument, a goniometer (angle measurement instrument used by health professionals) has been chosen. For this, two 4 cm polystyrene balls with different colors were attached to a goniometer, one at the end of each arm, as if it were the patient's upper limb ([Figure 36](#)). Then, it was positioned parallel to a laptop, 40 cm away, with the spheres approximately in the center of the image. Then, the laptop webcam (standard HD - 1280x720), calibrated with 50 photos, was used to measure the value of the angle read by the game at every 10 degrees of the goniometer, from 10 to 180°, obtaining 200 samples per angle. The distance in centimeters between the spheres was also measured. After that, the values obtained were plotted, highlighting the arithmetic mean for every 200 samples. Also, the error of the mean was calculated for every angle and plotted. The environment was a furnished room with controlled artificial lighting.

**Figure 36** – Goniometer with spheres attached.



Source: The author.

#### *b) Number of photos in calibration*

To test how many photos are needed for a good calibration of the system, sets of 46, 25, 10, 5, 3, 2 and 1 photos were made. The calibration parameters for each set were calculated.

Then, the goniometer was positioned at  $60^\circ$  in front of a webcam, 40 cm away, and 200 samples of the value measured by the system were collected for each set of calibration parameters. Afterwards, the average error of the angle obtained was calculated, as well as the standard deviation, the reprojection error and the optical center errors. The reprojection error is an estimation of how precise the calibration parameters are. First, the object point is projected to image points using the OpenCV function *projectPoints()*. Then, the absolute norm between this result and the chessboard corner finding algorithm is calculated. The average error is the arithmetic mean of the errors calculated for all the calibration images. The optical center errors can be known because the webcam frame size is known and they are the coordinates of the center of the frame. The results were plotted on graphs.

*c) Sphere diameter and distance from camera*

For this test, the goniometer was positioned at  $60^\circ$ . Two spheres of 3, 3.5, 4, 5 and 6 cm in diameter were placed in each goniometer arm at a time. The distance (z axis) from the goniometer to the webcam was also varied, taking measurements at 40, 80, 120 and 160 cm distances. For each distance and sphere size, 100 samples were obtained. The mean and standard deviation of each 100 samples were calculated and then the absolute error from the desired value ( $60^\circ$ ). Then, they were classified in a ranking with the lowest errors of the mean and placed in a table.

*d) Sphere X and Y center pixel coordinates*

For this test, the goniometer was positioned at  $60^\circ$ , with two spheres of 4 cm in diameter, one in each arm. First, both spheres were placed in the same x coordinates, on the far left of the frame, near the  $x = 0$  coordinate for the centers of both spheres. Then, they were slowly translated to the far right of the frame, close to  $x = 1280$  pixels, keeping y constant and measuring the angle. Subsequently, the goniometer was placed in the upper coordinate, close to  $y = 0$  for both spheres and translated to near  $y = 720$  slowly, measuring the angle. The objective was to find out if the proximity of the sphere to the corners of the picture, where there are more distortions, influenced the values of the angles.

*e) Sphere velocity*

For this test, the goniometer was positioned at  $60^\circ$ , with two spheres of 4 cm in diameter, one in each arm. The goniometer was moved up and down (y axis), at different speeds. The y velocity was measured in cm/s and correlated with the angle readings.

*f) Frame rate*

It is known, among game developers, that an ideal frame rate is greater than 30 frames per second (fps), because, at around 10 to 15 fps, the human eye is able to distinguish the separate frames of the video game. It has been shown, in the “algorithm choice” section, that the color algorithm is much faster than fiducial markers and Deep Learning, but now it has the addition of the Perspective-n-Point and graphics calculations. Therefore, the average frame rate of the final game was collected, both in the 3D and 2D versions, on a laptop (i7-9750H CPU, 32 GB of RAM and a NVIDIA GTX 1660 Ti graphics card) and on a mobile phone (Samsung M51).

#### **4.4 Final Considerations**

This chapter focused on the logical organization behind the research, in order to present the sequence of steps necessary for the development of the proposed tool, as well as showing what was done in each of the stages of the project. The method used to support the creation of the system proposed in the research was also shown.

---

## RESULTS AND DISCUSSION

---

This chapter shows the results of the development stage that culminated in the creation of the “Free to Fly” rehabilitation exergame with a novel tracking methodology, which aims to be simple yet effective alternative to exercise, while playing an entertainment game and capturing important data, such as joint angles estimation and, perhaps, clinical progression over time, yet to be tested. This chapter shows the results of the preliminary system tests discussed previously, in order to get a sense of the quality of system capture before further tests with patients. Therefore, the angle accuracy, the number of photos in calibration, the sphere diameter and distance from camera, the sphere  $x$  and  $y$  pixel coordinates, the sphere velocity and frame rate of the system were investigated.

### *a) Angle value*

The tests generated the charts in [Figure 37](#) (angle readings) and [Figure 38](#) (distance readings). It must be remembered that the distance is the triangle’s side opposite to the joint angle, which the law of cosines should be applied to. In the figures, it can be noted that there is a pattern: instead of a straight line, which was expected by the author, at high angle values, both the accuracy and precision of the measurement get worse.

Therefore, the circumferences properties were further investigated. Firstly, the objective: to calculate the joint angle. Then, the data: the coordinates of two 3D points in the same circumference, of which the joint is the central point. It is possible to be noticed that, without the arc length or the radius of the circumference, it is only possible to get the joint angle by calculating the distance between the points in a straight line first, which is called the chord. A way to obtain the chord between two points in a circumference is to use the following formula (Beck, 2020):

$$c = 2r \sin\left(\frac{\theta}{2}\right),$$

where  $c$  is the chord length and  $r$  the circle radius. Replacing  $r$  with 21 cm, which is the length from the pole of the goniometer to the center of the sphere, we have:

$$c = 2 * 21 * \sin\left(\frac{\theta}{2}\right) = 42 \sin\left(\frac{\theta}{2}\right),$$

which generates the graph of [Figure 39](#). Taking into account that the x axis of this graph is in radians, we have the answer to the pattern found in [Figure 37](#) and [Figure 38](#).

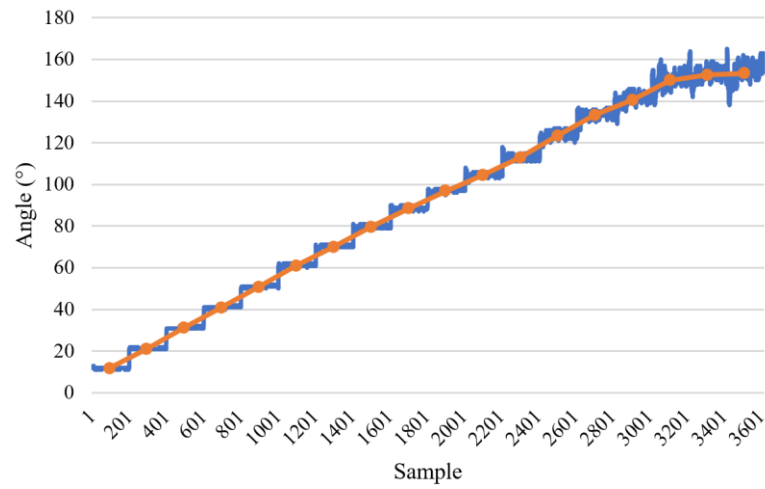
This property can also be visualized by measuring the distance in a straight line between the markings of the angles of a protractor, with a ruler, which generates a graph with the same pattern ([Figure 40](#)). In other words, the variation rate of the distance, especially from approximately  $110^\circ$ , becomes noticeably faster, interfering in the accuracy and precision of the system, since a small error in the distance calculations will result in a big error in the angle.

Apparently, this is a mathematical property, and, in this work, no way was found to work around the problem of lower accuracy on obtuse angles. The graph of the average error of the 200 samples from each angle can be seen in [Figure 41](#). Therefore, due to this property, it is possible to see that, at large angles, the measurement becomes less and less reliable. So, ideally, the system should be used by patients with lower joint amplitudes, under around  $110^\circ$ , that is where the error increases above  $5^\circ$ .

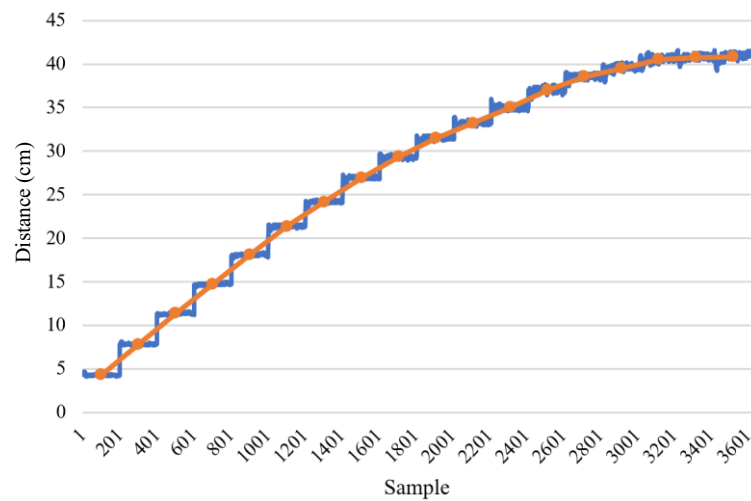
#### *b) Number of photos in calibration*

This test was done to find out if the number of photos using during calibration phase interfered with angle accuracy during the game. The methods used were described previously. The results can be seen in [Figure 42](#). All variables seem to follow a constant projection, until the set with only 1 photo, which had a big error, because only one photo does not seem to provide enough distortion data. The mean error of the average of all sets but the photo set 1 was  $1.57^\circ$ , with a standard deviation of  $0.48^\circ$ , confirming that the values were close. No correlation was found between any of the values. As a conclusion, it can be affirmed that 2 photos are enough to calibrate the system under the test conditions.

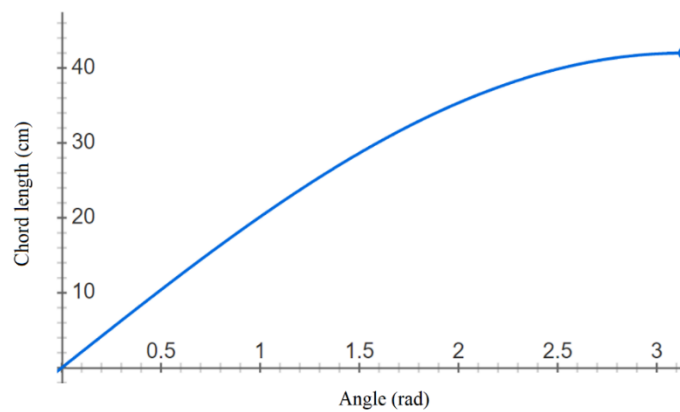


**Figure 37** – Angle readings chart.

Source: The author.

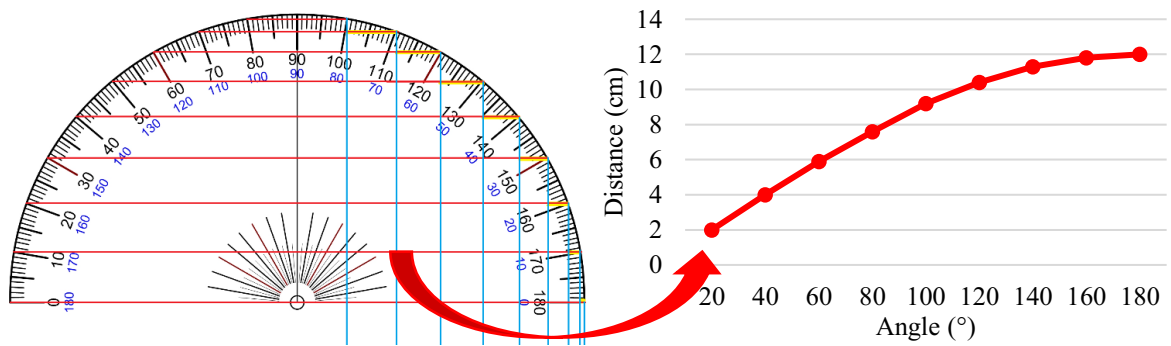
**Figure 38** – Distance readings chart.

Source: The author.

**Figure 39** –  $42\sin\left(\frac{\theta}{2}\right)$  plot from chord length formula.

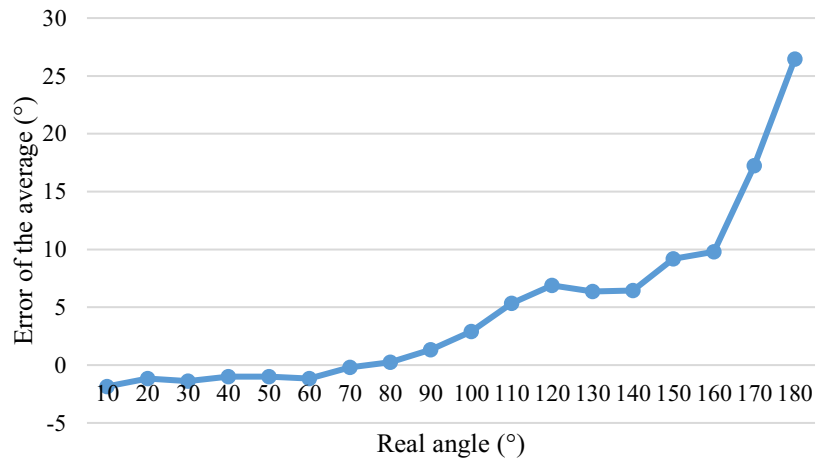
Source: The author.

**Figure 40** – Experimental results of measuring the distance (in red) between angles in a protractor.



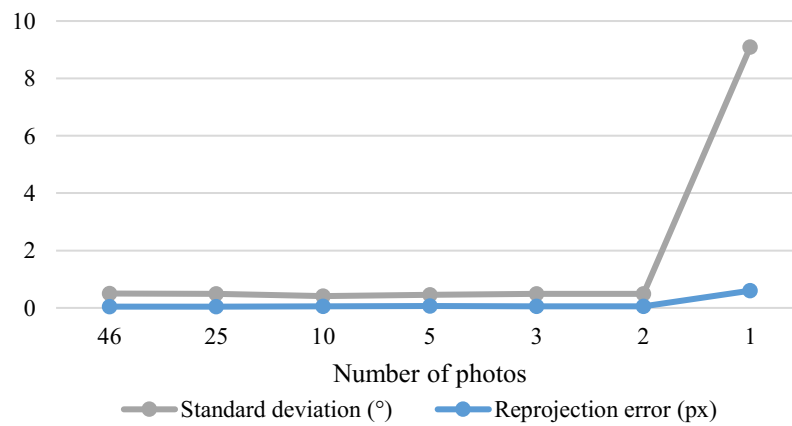
Source: The author.

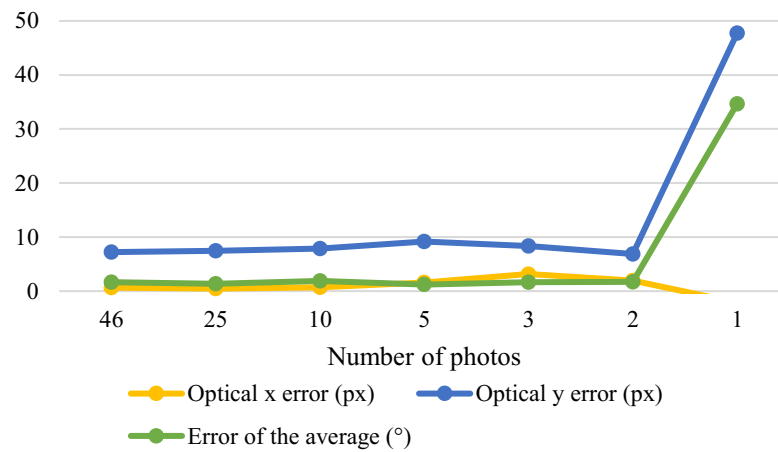
**Figure 41** – Error of the mean of each angle.



Source: The author.

**Figure 42** – Interference of number of photos on the accuracy.





Source: The author.

### c) Sphere diameter and distance from camera

This test was done to find out if the sphere diameter, whether 3, 3.5, 4, 5 or 6, influenced the accuracy of the angle. At the same time, if the distance from camera, whether 40, 80, 120 or 160 cm improved the capture or not. This is to find out the ideal distance that the patient should be from the camera and the ideal apparatus size. The methods were described in the previous chapter. The results are shown in [Table 11](#). It can be seen that the top 10 values gave an error below  $2.86^\circ$ , which probably will not be very noticed while playing, thus not interfering severely with the usability of the system. However, this can be problematic for obtaining reliable clinical progress data. These values were all at the lowest distances tested: 40 and 80 cm. Also, in the top 10 values, all ball sizes appeared twice, so it can be inferred that any size from 3.5 to 6 cm can be used, with the best values being 5 and 4 cm.

**Table 11** – Influence of sphere diameter and distance from camera on accuracy.

Ranking	Absolute error of the mean (°)	Distance from camera (cm)	Sphere diameter (cm)
1 <sup>st</sup>	0.09901	80	5
2 <sup>nd</sup>	0.188119	40	4
3 <sup>rd</sup>	0.257426	40	3
4 <sup>th</sup>	0.356436	40	5
5 <sup>th</sup>	0.356436	40	6
6 <sup>th</sup>	0.554455	80	4
7 <sup>th</sup>	0.653465	40	3.5
8 <sup>th</sup>	1.445545	80	3.5

<b>9<sup>th</sup></b>	1.712871	80	6
<b>10<sup>th</sup></b>	2.861386	80	3
<b>11<sup>th</sup></b>	3.564356	120	5
<b>12<sup>th</sup></b>	6.188119	120	3
<b>13<sup>th</sup></b>	6.514851	120	6
<b>14<sup>th</sup></b>	6.746988	120	4
<b>15<sup>th</sup></b>	8.742574	120	3.5
<b>16<sup>th</sup></b>	10.86	160	6
<b>17<sup>th</sup></b>	13.20792	160	5
<b>18<sup>th</sup></b>	19.16832	160	4
<b>19<sup>th</sup></b>	43.06931	160	3.5
<b>20<sup>th</sup></b>	51.85149	160	3

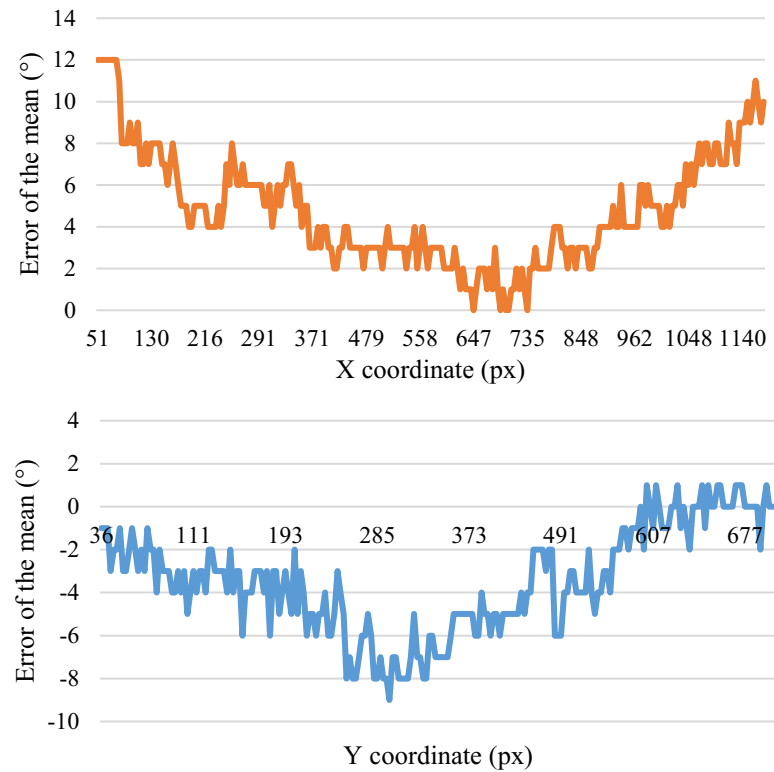
Source: The author.

*d) Sphere X and Y center pixel coordinates*

This test was done to find out if the error in the estimation of the  $(x,y)$  coordinates of the center of the sphere was related to the  $(x,y)$  pixel coordinates of the frame captured by the camera. It is important to remember that the frame captured by the camera has stronger radial and tangent distortions along the lowest and highest  $x$  and  $y$  pixel coordinates. The methods used in this test are described in the previous section. The results of this test can be seen in [Figure 43](#). They show that the  $x$  and  $y$  coordinates can influence the angle error, especially when closer to the corners of the frame, even with the distortion correction made in the calibration step. In this particular camera, there was a more significant error when near the corners on the  $x$  axis (up to  $12^\circ$ ), while on the  $y$  axis, the maximum absolute error was  $9^\circ$ . In both cases, there was an increase in the angle value when closer to the corner coordinates.

This was expected, due to the radial and tangent distortions of the camera. Even with the algorithm calculating distortion coefficients and correction, this does not seem to work well with spheres, only with the chessboard pattern, as seen in [Figure 44](#). It can be seen that the straight lines were undistorted, but the sphere still looks distorted, as evidenced by its elliptical shape. This is read by the system as a larger diameter than the real one. This results in the difference related to the angle.

**Figure 43** – Influence of the sphere x and y coordinates on the angle error.



Source: The author.

**Figure 44** – Original (left) and corrected (right) images.



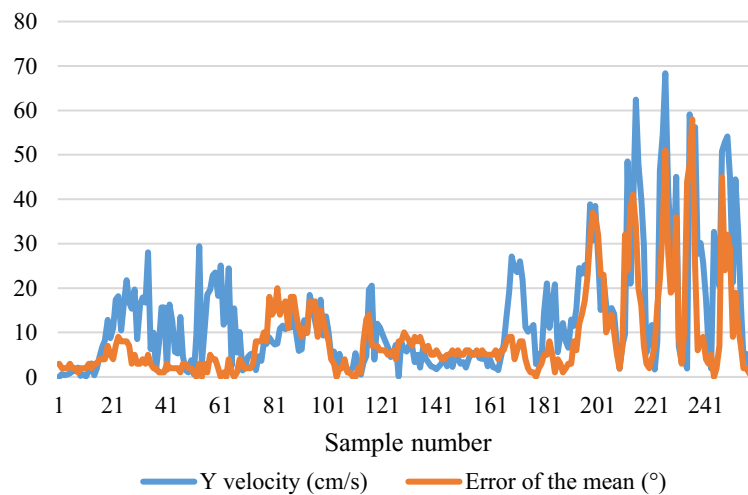
Source: The author.

*e) Sphere's velocity*

This test was done in order to find if the sphere's velocity, as manipulated by the movement of the user, interferes with the accuracy of the angle obtained. The methods used in this test are described in the previous chapter. The results of this test can be seen in [Figure 45](#).

There was a 0.70 correlation between the speed and the error of the mean of the angle readings. As expected, the lower the speed, the smaller the error. In addition, with a comfortable movement speed, the error is less noticeable than the 3D predictions of fiducial markers, for example. The velocity interferes in the readings only because of the motion blur, which occurs while the image stabilizes, making the outlines blurred, and is a property of all regular cameras.

**Figure 45** – Influence of the speed on the angle error.



Source: The author.

Other sources of error not tested include illumination variation and occlusions. These two factors strongly influence the capture, but are easily controllable. First, the system is better played in a room with artificial lighting only. Second, to avoid occlusions, there are several alternatives, such as positioning the user a little sideways.

#### *f) Frame rate*

This test was done to find out if the frame rate was ideally above 30 fps. The methods utilized in this test are described in the previous chapter. The results show that, on the laptop, the 3D game reached an average of 40 frames per second (fps) in the HD webcam resolution and webcam shown in the frame, which is the heaviest setting possible. On the mobile phone, under the same conditions, the system achieved 21 fps. On the laptop, the highest setting in the 2D game achieved 65 fps on average and, on mobile, 26 fps. While the laptop frame rates were permissive, the mobile ones were not very much, considering the 30 fps standard. However, they were still above the fps that the human eye begins to differentiate from frame to frame (the

exact frame rate that this happens is not very well documented), because it was not possible to notice any frames “jumping” yet. It is important to remember that the game has settings that help to increase the fps. Thus, it was considered that the frame rate could improve a little for mobile, but, considering that the game is rendering, being processed, the webcam capture being shown and the angles calculated, it was considered satisfactory by the author in order to further test it.

## **5.1 Final Considerations**

This chapter presented the results obtained from the tests carried out to find the main variables that influence the accuracy of the angle capture and what was the frame rate of the system, indicating if it was light enough to be processed on mobile devices. All information and pertinent impressions of “Free to Fly” were collected throughout the experiments, analyzed and subsequently documented. The tests showed some usability problems that, after being solved, should improve the applicability of “Free to Fly” as a tool for rehabilitation exergaming, so that it can be effectively used as an assistive technology tool to help people with severe motor impairments during activities of daily living.



---

## CONCLUSIONS AND FUTURE WORK

---

This chapter shows the conclusions of the research presented in this dissertation. In addition, due to the knowledge acquired during the work, some suggestions for future work are also presented, which may improve the tool proposed here.

### 6.1 Research Conclusions

In this work, a system for post-stroke rehabilitation was developed, comprising of an exercise game (exergame), which has an innovative form of 3D motion capture, that utilizes only a regular camera, which can be built into the processing and display device itself, such as the front camera of a smartphone or the webcam of a notebook, for example. This differentiates it from other 3D motion capture systems which use methods such as infrared, depth cameras, electromagnetic, mechanical, inertial sensors, etc. Also, the motion capture uses an innovative Computer Vision strategy, that utilizes colored spheres, which could be made from craft materials, to estimate the body parts position and the joint angles in 3D in real-time, while processing the game and displaying the camera capture. The fact that the spheres can be made from craft materials makes possible for the user to produce its own control at home, only needing the distribution of the software of the game to be able to readily play anytime, anywhere he/she desires to, thus, perhaps, helping in the motor rehabilitation of the patient.

It was expected that the fact of not having a specialized electronic device would interfere with the accuracy of capturing the moving position of the body parts and the angle between the joints. However, it was also expected that, in this way, the system would be an accessible possibility for therapists and private users who are unable to obtain a specialized sensor. It was attempted, then, to verify whether, even with the accuracy limitations, the system could still be promising and could advance to tests with patients. All this, in order to facilitate access to this assistive technology for people with severe motor disabilities who do not have access to devices commonly used in exergames for motor rehabilitation.



Therefore, the tests have shown that the system has limitations, such as lower accuracy (error above  $5^\circ$ ) at angles above  $110^\circ$ ; sensitivity to variations in ambient lighting, such as opening a window; lower accuracy when the spheres used are smaller (below 4 cm); sensitivity to occlusions caused by the patient himself when, for example, there is a sphere in his shoulder; the variation in accuracy due to distortions in the camera lens; and the motion blur, which occurs when there is very fast movement, during which the camera cannot detect the sphere and loses its capture. However, it is important to remember that this method can be faster than using fiducial markers, due to the latter algorithm being heavier than the one developed here, as well as Deep Learning, which requires an even greater amount of calculations. The method presented here, being lighter, would perhaps be suitable for a wider range of playback and processing devices.

Positive points of the system include its very low cost, the ease of playing anywhere, anytime, and perhaps data capture that has some clinical importance, as it calculates the angle of joints, which would be important for checking the progress of spasticity in such clinical patients. Finally, it appears that the objective proposed at the beginning of this work was achieved, since the tool developed in the research was able to successfully capture angles and has the potential to present good usability. Although it is possible to notice, based on the graphs presented, the inaccuracy of the angles under certain conditions and/or other limiting factors discussed above.

However, the "Free to Fly" system developed may provide post-stroke patients hope of having a useful and motivating entertainment tool to perform their physical therapy with greater pleasure and autonomy. Thus, in the long term, the proposed tool can be used by people with severe motor disabilities in their own homes, thus promoting an improvement in quality of life, self-esteem, as well as other emotional and physical aspects.

## **6.2 Future Works**

For future works, even though the users' best performance with "Free to Fly" will depend a lot on their skills and previous training, it was possible to see that it is needed to improve the development of the system prior to testing, as there are some variables that could be improved. Thus, to serve a greater number of potential "Free to Fly" users, it is necessary to include tools that provide improvements in the areas of lighting, calibration and angle of

capture. In order to obtain more data on the study in question, it is also intended to further collaborate with more therapists and volunteers to identify improvements to be made.

In this sense, it is intended to use a collection protocol where volunteers are instructed to perform pre-established tasks, enabling the generation of data that provide a more detailed statistical analysis, such as the application of the instrument to assess the gold standard angle measurement in the patient, in real-time, while also collecting the system estimation. Finally, it is planned to test whether the position and angle capture achieved with the system can be accurate enough and have a good correlation with clinical standard measurements of post-stroke rehabilitation progress.

## BIBLIOGRAPHY

- Adams, R J, Lichter, M. D., Ellington, A., White, M., Armstead, K., Patrie, J. T., & Diamond, P. T. (2018). Virtual Activities of Daily Living for Recovery of Upper Extremity Motor Function. *IEEE Transactions on Neural Systems and Rehabilitation Engineering*, 26(1), 252–260. <https://doi.org/10.1109/TNSRE.2017.2771272>
- Adams, Richard J, Ellington, A. L., Armstead, K., Sheffield, K., Patrie, J. T., & Diamond, P. T. (2019). Upper Extremity Function Assessment Using a Glove Orthosis and Virtual Reality System. *OTJR: Occupation, Participation and Health*, 39(2), 81–89. <https://doi.org/10.1177/1539449219829862>
- Afsar, S. I., Mirzayev, I., Yemisci, O. U., Saracgil, S. N. C., Ikbali Afsar, S., Mirzayev, I., Umit Yemisci, O., & Cosar Saracgil, S. N. (2018). Virtual Reality in Upper Extremity Rehabilitation of Stroke Patients: A Randomized Controlled Trial. *Journal of Stroke and Cerebrovascular Diseases: The Official Journal of National Stroke Association*, 27(12), 3473–3478. <https://doi.org/10.1016/j.jstrokecerebrovasdis.2018.08.007>
- Ahmed, N., Mauad, V. A. Q., Gomez-Rojas, O., Sushea, A., Castro-Tejada, G., Michel, J., Liñares, J. M., Pedrosa Salles, L., Candido Santos, L., Shan, M., Nassir, R., Montañez-Valverde, R., Fabiano, R., Danyi, S., Hassan Hosseyni, S., Anand, S., Ahmad, U., Casteleins, W. A., Sanchez, A. T., ... Halalau, A. (2020). The Impact of Rehabilitation-oriented Virtual Reality Device in Patients With Ischemic Stroke in the Early Subacute Recovery Phase: Study Protocol for a Phase III, Single-Blinded, Randomized, Controlled Clinical Trial. *Journal of Central Nervous System Disease*, 12, 117957351989947. <https://doi.org/10.1177/1179573519899471>
- Askin, A., Atar, E., Kocyigit, H., & Tosun, A. (2018). Effects of Kinect-based virtual reality game training on upper extremity motor recovery in chronic stroke. *Somatosensory & Motor Research*, 35(1), 25–32. <https://doi.org/10.1080/08990220.2018.1444599>
- Assis, G. A. de, Correa, A. G. D., Martins, M. B. R., Pedrozo, W. G., Lopes, R. de D., de Assis, G. A., Dionisio Correa, A. G., Rodrigues Martins, M. B., Pedrozo, W. G., & Lopes, R. de D. (2016). An augmented reality system for upper-limb post-stroke motor rehabilitation: a feasibility study. *Disability and Rehabilitation. Assistive Technology*, 11(6), 521–528. <https://doi.org/10.3109/17483107.2014.979330>
- Aung, Y. M., & Al-Jumaily, A. (2011). Rehabilitation exercise with real-time muscle simulation based EMG and AR. *2011 11th International Conference on Hybrid Intelligent Systems (HIS)*, 641–646. <https://doi.org/10.1109/HIS.2011.6122181>
- Ballester, B Rubio, Badia, S. B. i, & Verschure, P. F. M. J. (2012). Including Social Interaction in Stroke VR-Based Motor Rehabilitation Enhances Performance: A Pilot Study. *Presence*, 21(4), 490–501. [https://doi.org/10.1162/PRES\\_a\\_00129](https://doi.org/10.1162/PRES_a_00129)
- Ballester, Belen Rubio, Maier, M., San Segundo Mozo, R. M., Castaneda, V., Duff, A., & M J Verschure, P. F. (2016). Counteracting learned non-use in chronic stroke patients with reinforcement-induced movement therapy. *Journal of Neuroengineering and Rehabilitation*, 13(1), 74. <https://doi.org/10.1186/s12984-016-0178-x>
- Ballester, Belen Rubio, Nirme, J., Duarte, E., Cuxart, A., Rodriguez, S., Verschure, P., & Duff, A. (2015). The visual amplification of goal-oriented movements counteracts acquired non-use in hemiparetic stroke patients. *Journal of Neuroengineering and Rehabilitation*, 12, 50. <https://doi.org/10.1186/s12984-015-0039-z>
- Baniña, M. C., Mullick, A. A., & Levin, M. F. (2013). Deficits in obstacle avoidance behaviour in individuals with good arm recovery after stroke. *2013 International Conference on Virtual Rehabilitation (ICVR)*, 190–191. <https://doi.org/10.1109/ICVR.2013.6662122>
- Bank, P. J. M., Cidota, M. A., Ouwehand, P. E. W., & Lukosch, S. G. (2018). Patient-Tailored

- Augmented Reality Games for Assessing Upper Extremity Motor Impairments in Parkinson's Disease and Stroke. *Journal of Medical Systems*, 42(12), 246. <https://doi.org/10.1007/s10916-018-1100-9>
- Baran, M., Lehrer, N., Duff, M., Venkataraman, V., Turaga, P., Ingalls, T., Rymer, W. Z., Wolf, S. L., & Rikakis, T. (2015). Interdisciplinary concepts for design and implementation of mixed reality interactive neurorehabilitation systems for stroke. *Physical Therapy*, 95(3), 449–460. <https://doi.org/10.2522/ptj.20130581>
- Beck, K. (2020). *How to Calculate Arc Lengths Without Angles*. Sciencing. <https://sciencing.com/calculate-arc-lengths-angles-8059022.html>
- Bensenor, I. M., Goulart, A. C., Szwarcwald, C. L., Vieira, M. L. F. P., Malta, D. C., & Lotufo, P. A. (2015). Prevalence of stroke and associated disability in Brazil: National Health Survey - 2013. *Arquivos de Neuro-Psiquiatria*, 73, 746–750. [http://www.scielo.br/scielo.php?script=sci\\_arttext&pid=S0004-282X2015000900746&nrm=isso](http://www.scielo.br/scielo.php?script=sci_arttext&pid=S0004-282X2015000900746&nrm=isso). <https://doi.org/10.1590/0004-282X20150115>
- Billinghurst, M. (2013). *2013 Lecture3: AR Tracking*. SlideShare. <https://pt.slideshare.net/marknb00/2013-lecture3-ar-tracking>
- Blender. (2021). *Blender*. <https://www.blender.org/>
- Boone, A. E., Wolf, T. J., & Engsborg, J. R. (2019). Combining Virtual Reality Motor Rehabilitation With Cognitive Strategy Use in Chronic Stroke. *The American Journal of Occupational Therapy: Official Publication of the American Occupational Therapy Association*, 73(4), 7304345020p1-7304345020p9. <https://doi.org/10.5014/ajot.2019.030130>
- Borstad, A. L., Crawfis, R., Phillips, K., Lowes, L. P., Maung, D., McPherson, R., Siles, A., Worthen-Chaudhari, L., & Gauthier, L. V. (2018). In-Home Delivery of Constraint-Induced Movement Therapy via Virtual Reality Gaming. *Journal of Patient-Centered Research and Reviews*, 5(1), 6–17. <https://doi.org/10.17294/2330-0698.1550>
- Brokaw, E. B., Eckel, E., & Brewer, B. R. (2015). Usability evaluation of a kinematics focused Kinect therapy program for individuals with stroke. *Technology and Health Care: Official Journal of the European Society for Engineering and Medicine*, 23(2), 143–151. <https://doi.org/10.3233/THC-140880>
- Brown, D. (1966). *Decentering distortion of lenses*.
- Brunnstrom, S. (1966). Motor Testing Procedures in Hemiplegia: Based on Sequential Recovery Stages. *Physical Therapy*, 46(4), 357–375. <https://doi.org/10.1093/ptj/46.4.357>
- Cameirao, M. S., Faria, A. L., Paulino, T., Alves, J., & Bermudez I Badia, S. (2016). The impact of positive, negative and neutral stimuli in a virtual reality cognitive-motor rehabilitation task: a pilot study with stroke patients. *Journal of Neuroengineering and Rehabilitation*, 13(1), 70. <https://doi.org/10.1186/s12984-016-0175-0>
- Cameirão, M. S., Faria, A. L., Paulino, T., Alves, J., & Bermúdez I Badia, S. (2016). The impact of positive, negative and neutral stimuli in a virtual reality cognitive-motor rehabilitation task: a pilot study with stroke patients. *Journal of Neuroengineering and Rehabilitation*, 13(1), 70. <https://doi.org/10.1186/s12984-016-0175-0>
- Cargnin, D. J., Cordeiro d'Ornellas, M., & Cervi Prado, A. L. (2015). A Serious Game for Upper Limb Stroke Rehabilitation Using Biofeedback and Mirror-Neurons Based Training. *Studies in Health Technology and Informatics*, 216, 348–352.
- Castano, J. B., Hoyos Escobar, J. D., Munoz Cardona, J. E., Lopez Herrera, J. F., Bedoya Castano, J., Hoyos Escobar, J. D., Munoz Cardona, J. E., & Lopez Herrera, J. F. (2014). Shoulder flexion rehabilitation in patients with monoparesia using an exergame. *2014 IEEE 3rd International Conference on Serious Games and Applications for Health (SeGAH)*, 1–5. <https://doi.org/10.1109/SeGAH.2014.7067072>
- Chen, C., Lee, S., Wang, W., Chen, H., Liu, J., Huang, Y., & Su, M. (2017). The changes of

- improvement-related motor kinetics after virtual reality based rehabilitation. *2017 International Conference on Applied System Innovation (ICASI)*, 683–685. <https://doi.org/10.1109/ICASI.2017.7988517>
- Chen, X., Ma, C., Xu, S., & He, J. (2007). Virtual Reality Based on Stereotypical RUPERT for Stroke Functional Rehabilitative Training Scenarios. *5th ACIS International Conference on Software Engineering Research, Management Applications (SERA 2007)*, 639–644. <https://doi.org/10.1109/SERA.2007.134>
- Chen, Y., Abel, K. T., Janecek, J. T., Chen, Y., Zheng, K., & Cramer, S. C. (2019). Home-based technologies for stroke rehabilitation: A systematic review. *International Journal of Medical Informatics*, *123*, 11–22. <https://doi.org/https://doi.org/10.1016/j.ijmedinf.2018.12.001>
- Cheng, Y. (1995). Mean shift, mode seeking, and clustering. *IEEE Transactions on Pattern Analysis and Machine Intelligence*, *17*(8), 790–799. <https://doi.org/10.1109/34.400568>
- Choi, H.-S., Shin, W.-S., & Bang, D.-H. (2019). Mirror Therapy Using Gesture Recognition for Upper Limb Function, Neck Discomfort, and Quality of Life After Chronic Stroke: A Single-Blind Randomized Controlled Trial. *Medical Science Monitor: International Medical Journal of Experimental and Clinical Research*, *25*, 3271–3278. <https://doi.org/10.12659/MSM.914095>
- Cidota, M. A., Bank, P. J. M., & Lukosch, S. G. (2019). Design Recommendations for Augmented Reality Games for Objective Assessment of Upper Extremity Motor Dysfunction. *2019 IEEE Conference on Virtual Reality and 3D User Interfaces (VR)*, 1430–1438. <https://doi.org/10.1109/VR.2019.8797729>
- Conrady, A. E. (1919). Decentred Lens-Systems. *Monthly Notices of the Royal Astronomical Society*, *79*(5), 384–390. <https://doi.org/10.1093/mnras/79.5.384>
- Cyrino, G., Tannus, J., Lamounier, E., Cardoso, A., & Soares, A. (2018). *Serious Game with Virtual Reality for Upper Limb Rehabilitation after Stroke*. 2018 20th Symposium on Virtual and Augmented Reality (SVR). <https://doi.org/10.1109/SVR.2018.00006>
- da Silva Cameirão, M., Bermúdez I Badia, S., Duarte, E., & Verschure, P. F. M. J. (2011). Virtual reality based rehabilitation speeds up functional recovery of the upper extremities after stroke: a randomized controlled pilot study in the acute phase of stroke using the rehabilitation gaming system. *Restorative Neurology and Neuroscience*, *29*(5), 287–298. <https://doi.org/10.3233/RNN-2011-0599>
- Demers, M, Kong, D. C. C., & Levin, M. F. (2017). Acceptability of using a Kinect-based virtual reality intervention to remediate arm motor impairments in subacute stroke. *2017 International Conference on Virtual Rehabilitation (ICVR)*, 1–2. <https://doi.org/10.1109/ICVR.2017.8007496>
- Demers, Marika, Chan Chun Kong, D., & Levin, M. F. (2019). Feasibility of incorporating functionally relevant virtual rehabilitation in sub-acute stroke care: perception of patients and clinicians. *Disability and Rehabilitation. Assistive Technology*, *14*(4), 361–367. <https://doi.org/10.1080/17483107.2018.1449019>
- Dias, J., Veloso, A. I., & Ribeiro, T. (2019). “A Priest in the Air.” *2019 14th Iberian Conference on Information Systems and Technologies (CISTI)*, 1–7. <https://doi.org/10.23919/CISTI.2019.8760748>
- Dias, P., Silva, R., Amorim, P., Lains, J., Roque, E., Serodio, I., Pereira, F., & Santos, B. S. (2019). Using Virtual Reality to Increase Motivation in Poststroke Rehabilitation. *IEEE Computer Graphics and Applications*, *39*(1), 64–70. <https://doi.org/10.1109/MCG.2018.2875630>
- Dibia, V. (2019). *SkyFall: Gesture Controlled Web based Game using Tensorflow Object Detection Api*. GitHub. <https://github.com/victordibia/skyfall>
- Ding, W. L., Zheng, Y. Z., Su, Y. P., & Li, X. L. (2018). Kinect-based virtual rehabilitation and

- evaluation system for upper limb disorders: A case study. *Journal of Back and Musculoskeletal Rehabilitation*, 31(4), 611–621. <https://doi.org/10.3233/BMR-140203>
- Duff, M., Chen, Y., Attygalle, S., Herman, J., Sundaram, H., Qian, G., He, J., & Rikakis, T. (2010). An Adaptive Mixed Reality Training System for Stroke Rehabilitation. *IEEE Transactions on Neural Systems and Rehabilitation Engineering*, 18(5), 531–541. <https://doi.org/10.1109/TNSRE.2010.2055061>
- Duff, M., Chen, Y., Attygalle, S., Sundaram, H., & Rikakis, T. (2010). Mixed reality rehabilitation for stroke survivors promotes generalized motor improvements. *2010 Annual International Conference of the IEEE Engineering in Medicine and Biology*, 5899–5902. <https://doi.org/10.1109/IEMBS.2010.5627537>
- Duff, Margaret, Chen, Y., Cheng, L., Liu, S.-M., Blake, P., Wolf, S. L., & Rikakis, T. (2013). Adaptive mixed reality rehabilitation improves quality of reaching movements more than traditional reaching therapy following stroke. *Neurorehabilitation and Neural Repair*, 27(4), 306–315. <https://doi.org/10.1177/1545968312465195>
- Dukes, P. S., Hayes, A., Hodges, L. F., & Woodbury, M. (2013). Punching ducks for post-stroke neurorehabilitation: System design and initial exploratory feasibility study. *2013 IEEE Symposium on 3D User Interfaces (3DUI)*, 47–54. <https://doi.org/10.1109/3DUI.2013.6550196>
- Faith, A., Chen, Y., Rikakis, T., & Iasemidis, L. (2011). Interactive rehabilitation and dynamical analysis of scalp EEG. *Conference Proceedings: ... Annual International Conference of the IEEE Engineering in Medicine and Biology Society. IEEE Engineering in Medicine and Biology Society. Annual Conference, 2011*, 1387–1390. <https://doi.org/10.1109/IEMBS.2011.6090326>
- Faria, A L, Cameirao, M. S., Paulino, T., & Bermudez i Badia, S. (2015). The benefits of emotional stimuli in a virtual reality cognitive and motor rehabilitation task: Assessing the impact of positive, negative and neutral stimuli with stroke patients. *2015 International Conference on Virtual Rehabilitation (ICVR)*, 65–71. <https://doi.org/10.1109/ICVR.2015.7358584>
- Faria, Ana L, Cameirao, M. S., Couras, J. F., Aguiar, J. R. O., Costa, G. M., & Bermudez I Badia, S. (2018). Combined Cognitive-Motor Rehabilitation in Virtual Reality Improves Motor Outcomes in Chronic Stroke - A Pilot Study. *Frontiers in Psychology*, 9, 854. <https://doi.org/10.3389/fpsyg.2018.00854>
- Feigin, V., Nguyen, G., Cercy, K., Johnson, C., Alam, T., Parmar, P., Abajobir, A., Abate, K., Abd-Allah, F., Abejie, A., Abyu, G., Ademi, Z., Agarwal, G., Beshir, M., Akinyemi, R., Al-Raddadi, R., Aminde, L., Amlie-Lefond, C., Ansari, H., & Roth, G. (2018). Global, Regional, and Country-Specific Lifetime Risks of Stroke, 1990 and 2016. *New England Journal of Medicine*, 379, 2429–2437. <https://doi.org/10.1056/NEJMoa1804492>
- Fischler, M. A., & Bolles, R. C. (1981). Random Sample Consensus: A Paradigm for Model Fitting with Applications to Image Analysis and Automated Cartography. *Commun. ACM*, 24(6), 381–395. <https://doi.org/10.1145/358669.358692>
- FreeMusicArchive. (2021). *FreeMusicArchive*.
- Freire Bastos Filho, T., Jacobo Valencia Jimênes, N., De Oliveira Muniz Lyra, J., Frizera Neto, A., & Cardoso, V. F. (2017). *Sistema integrado de Realidade Virtual e eletromiografia para reabilitação*.
- Funabashi, A. M. M., Aranha, R. V., Silva, T. D., Monteiro, C. B. M., Silva, W. S., & Nunes, F. L. S. (2017). AGaR: A VR Serious Game to Support the Recovery of Post-Stroke Patients. *2017 19th Symposium on Virtual and Augmented Reality (SVR)*, 279–288. <https://doi.org/10.1109/SVR.2017.15>
- Gauthier, L. V, Kane, C., Borstad, A., Strahl, N., Uswatte, G., Taub, E., Morris, D., Hall, A., Arakelian, M., & Mark, V. (2017). Video Game Rehabilitation for Outpatient Stroke

- (VIGoROUS): protocol for a multi-center comparative effectiveness trial of in-home gamified constraint-induced movement therapy for rehabilitation of chronic upper extremity hemiparesis. *BMC Neurology*, 17(1), 109. <https://doi.org/10.1186/s12883-017-0888-0>
- George, S. H., Rafiei, M. H., Borstad, A., Adeli, H., & Gauthier, L. V. (2017). Gross motor ability predicts response to upper extremity rehabilitation in chronic stroke. *Behavioural Brain Research*, 333, 314–322. <https://doi.org/10.1016/j.bbr.2017.07.002>
- GestureTek. (2016). *IREX*. <http://www.gesturetekhealth.com/products/irex>
- GIMP. (2021). *GIMP*. <https://www.gimp.org/>
- Goldman, J. (2020). *Best cheap gaming laptops under \$1,000 for 2021*. CNET. <https://www.cnet.com/news/best-cheap-gaming-laptop-under-1000-for-2021/>
- Gomes, A. L. S., Mello, F. F. de, Cocicov Neto, J., Benedeti, M. C., Modolo, L. F. M., & Riberto, M. (2019). Can the positions of the spastic upper limb in stroke survivors help muscle choice for botulinum toxin injections? *Arquivos de Neuro-Psiquiatria*, 77, 568–573. [http://www.scielo.br/scielo.php?script=sci\\_arttext&pid=S0004-282X2019000800568&nrm=iso](http://www.scielo.br/scielo.php?script=sci_arttext&pid=S0004-282X2019000800568&nrm=iso). <https://doi.org/10.1590/0004-282x20190087>
- Guina, R. (2020). *How Much Does a Nintendo Wii Cost?* Cash Money Life. <https://cashmoneylife.com/how-much-does-a-nintendo-wii-cost/>
- Gutiérrez-Celaya, J. A., Leder, R., Carrillo, R., Hawayek, A., Hernández, J., & Sucar, E. (2011). fMRI-based inverse analysis of stroke patients' motor functions. *2011 Pan American Health Care Exchanges*, 1–6. <https://doi.org/10.1109/PAHCE.2011.5871831>
- Hefter, H., Jost, W. H., Reissig, A., Zakine, B., Bakheit, A. M., & Wissel, J. (2012). Classification of posture in poststroke upper limb spasticity: a potential decision tool for botulinum toxin A treatment? *International Journal of Rehabilitation Research*, 35(3). [https://journals.lww.com/intjrehabilres/Fulltext/2012/09000/Classification\\_of\\_posture\\_in\\_poststroke\\_upper\\_limb.7.aspx](https://journals.lww.com/intjrehabilres/Fulltext/2012/09000/Classification_of_posture_in_poststroke_upper_limb.7.aspx). <https://doi.org/10.1097/MRR.0b013e328353e3d4>
- Heller, A., Wade, D. T., Wood, V. A., Sunderland, A., Hower, R. L., & Ward, E. (1987). Arm function after stroke: measurement and recovery over the first three months. *Journal of Neurology, Neurosurgery, and Psychiatry*, 50(6), 714–719. <https://doi.org/10.1136/jnnp.50.6.714>
- Hienz, H., Grobel, K., & Offner, G. (1996). Real-time hand-arm motion analysis using a single video camera. *Proceedings of the Second International Conference on Automatic Face and Gesture Recognition*, 323–327. <https://doi.org/10.1109/AFGR.1996.557285>
- Hoermann, S., Ferreira Dos Santos, L., Morkisch, N., Jettkowski, K., Sillis, M., Devan, H., Kanagasabai, P. S., Schmidt, H., Kruger, J., Dohle, C., Regenbrecht, H., Hale, L., & Cutfield, N. J. (2017). Computerised mirror therapy with Augmented Reflection Technology for early stroke rehabilitation: clinical feasibility and integration as an adjunct therapy. *Disability and Rehabilitation*, 39(15), 1503–1514. <https://doi.org/10.1080/09638288.2017.1291765>
- Hondori, H. M., Khademi, M., Dodakian, L., McKenzie, A., Lopes, C. V., & Cramer, S. C. (2016). Choice of Human-Computer Interaction Mode in Stroke Rehabilitation. *NEUROREHABILITATION AND NEURAL REPAIR*, 30(3), 258–265. <https://doi.org/10.1177/1545968315593805>
- Hondori, H. M., Khademi, M., Dodakian, L., McKenzie, A., Lopes, C. V., Cramer, S. C., Mousavi Hondori, H., Khademi, M., Dodakian, L., McKenzie, A., Lopes, C. V., & Cramer, S. C. (2016). Choice of Human-Computer Interaction Mode in Stroke Rehabilitation. *Neurorehabilitation and Neural Repair*, 30(3), 258–265. <https://doi.org/10.1177/1545968315593805>
- House, G., Burdea, G., Polistico, K., Roll, D., Kim, J., Grampurohit, N., Damiani, F., Keeler, S., Hundal, J., & Pollack, S. (2016). Integrative rehabilitation of residents chronic post-

- stroke in skilled nursing facilities: the design and evaluation of the BrightArm Duo. *Disability and Rehabilitation. Assistive Technology*, 11(8), 683–694. <https://doi.org/10.3109/17483107.2015.1068384>
- Huang, L., & Chen, M. (2016). The effectiveness of gardening game design for the upper extremity function of stroke patients. *2016 International Conference on Advanced Materials for Science and Engineering (ICAMSE)*, 110–112. <https://doi.org/10.1109/ICAMSE.2016.7840249>
- Hung, C.-T., Croft, E. A., & Van der Loos, H. F. M. (2015). A wearable vibrotactile device for upper-limb bilateral motion training in stroke rehabilitation: A case study. *Conference Proceedings: ... Annual International Conference of the IEEE Engineering in Medicine and Biology Society. IEEE Engineering in Medicine and Biology Society. Annual Conference, 2015*, 3480–3483. <https://doi.org/10.1109/EMBC.2015.7319142>
- IBGE. (2018). *PNAD Contínua 2018 - Acesso à Internet e à televisão e posse de telefone móvel celular para uso pessoal*. [https://biblioteca.ibge.gov.br/visualizacao/livros/liv101705\\_informativo.pdf](https://biblioteca.ibge.gov.br/visualizacao/livros/liv101705_informativo.pdf)
- Janku, P., Koplik, K., Dulík, T., & Szabo, I. (2016). Comparison of tracking algorithms implemented in OpenCV. *MATEC Web of Conferences*, 76, 4031. <https://doi.org/10.1051/mateconf/20167604031>
- Jayasree-Krishnan, V., Gamdha, D., Goldberg, B. S., Ghosh, S., Raghavan, P., & Kapila, V. (2019). A Novel Task-Specific Upper-Extremity Rehabilitation System with Interactive Game-Based Interface for Stroke Patients. *2019 International Symposium on Medical Robotics (ISMR)*, 1–7. <https://doi.org/10.1109/ISMR.2019.8710184>
- Ji, E.-K., & Lee, S.-H. (2016). Effects of virtual reality training with modified constraint-induced movement therapy on upper extremity function in acute stage stroke: a preliminary study. *Journal of Physical Therapy Science*, 28(11), 3168–3172. <https://doi.org/10.1589/jpts.28.3168>
- Johnson, L., Bird, M.-L., Muthalib, M., & Teo, W.-P. (2018). Innovative STRoke Interactive Virtual thErapy (STRIVE) online platform for community-dwelling stroke survivors: a randomised controlled trial protocol. *BMJ Open*, 8(1), e018388. <https://doi.org/10.1136/bmjopen-2017-018388>
- Kairy, D., Veras, M., Archambault, P., Hernandez, A., Higgins, J., Levin, M. F., Poissant, L., Raz, A., & Kaizer, F. (2016). Maximizing post-stroke upper limb rehabilitation using a novel telerehabilitation interactive virtual reality system in the patient's home: study protocol of a randomized clinical trial. *Contemporary Clinical Trials*, 47, 49–53. <https://doi.org/10.1016/j.cct.2015.12.006>
- Karbasi, M., Bilal, S., Aghababaeyan, R., Ehsani Rad, A., Bhatti, Z., & Shah, A. (2016). Analysis and enhancement of the denoising depth data using kinect through iterative technique. *Jurnal Teknologi*, 78. <https://doi.org/10.11113/jt.v78.5348>
- Kato, N., Tanaka, T., Sugihara, S., Shimizu, K., & Kudo, N. (2016). Trial operation of a cloud service-based three-dimensional virtual reality tele-rehabilitation system for stroke patients. *2016 11th International Conference on Computer Science & Education (ICCSE)*, 285–290. <https://doi.org/10.1109/ICCSE.2016.7581595>
- Kelly, K. M., Borstad, A. L., Kline, D., & Gauthier, L. V. (2018). Improved quality of life following constraint-induced movement therapy is associated with gains in arm use, but not motor improvement. *Topics in Stroke Rehabilitation*, 25(7), 467–474. <https://doi.org/10.1080/10749357.2018.1481605>
- Kim, B. R., Chun, M. H., Kim, L. S., & Park, J. Y. (2011). Effect of virtual reality on cognition in stroke patients. *Annals of Rehabilitation Medicine*, 35(4), 450–459. <https://doi.org/10.5535/arm.2011.35.4.450>
- Kimyoon-young. (2020). *centerNet + deep sort with pytorch*. GitHub.



- <https://github.com/kimyoon-young/centerNet-deep-sort>
- Kizony, R., Weiss, P. L., Feldman, Y., Shani, M., Elion, O., Kizony, R., Weiss, P. L., Kizony, R., Harel, S., & Baum-Cohen, I. (2013). Evaluation of a Tele-Health System for upper extremity stroke rehabilitation. *2013 International Conference on Virtual Rehabilitation (ICVR)*, 80–86. <https://doi.org/10.1109/ICVR.2013.6662096>
- Kutlu, M., Freeman, C. T., Hallewell, E., Hughes, A.-M., & Laila, D. S. (2016). Upper-limb stroke rehabilitation using electrode-array based functional electrical stimulation with sensing and control innovations. *Medical Engineering & Physics*, *38*(4), 366–379. <https://doi.org/10.1016/j.medengphy.2016.01.004>
- Kutlu, M., Freeman, C. T., Hallewell, E., Hughes, A., & Laila, D. S. (2015). FES-based upper-limb stroke rehabilitation with advanced sensing and control. *2015 IEEE International Conference on Rehabilitation Robotics (ICORR)*, 253–258. <https://doi.org/10.1109/ICORR.2015.7281208>
- Kwon, J.-S., Park, M.-J., Yoon, I.-J., & Park, S.-H. (2012). Effects of virtual reality on upper extremity function and activities of daily living performance in acute stroke: a double-blind randomized clinical trial. *NeuroRehabilitation*, *31*(4), 379–385. <https://doi.org/10.3233/NRE-2012-00807>
- Lauterbach, S. A., Foreman, M. H., & Engsberg, J. R. (2013). Computer Games as Therapy for Persons with Stroke. *Games for Health Journal*, *2*(1), 24–28. <https://doi.org/10.1089/g4h.2012.0032>
- Lee, G. (2013). Effects of training using video games on the muscle strength, muscle tone, and activities of daily living of chronic stroke patients. *Journal of Physical Therapy Science*, *25*(5), 595–597. <https://doi.org/10.1589/jpts.25.595>
- Lee, K.-H. (2015). Effects of a virtual reality-based exercise program on functional recovery in stroke patients: part 1. *Journal of Physical Therapy Science*, *27*(6), 1637–1640. <https://doi.org/10.1589/jpts.27.1637>
- Lee, M., Pyun, S.-B., Chung, J., Kim, J., Eun, S.-D., & Yoon, B. (2016). A Further Step to Develop Patient-Friendly Implementation Strategies for Virtual Reality-Based Rehabilitation in Patients With Acute Stroke. *Physical Therapy*, *96*(10), 1554–1564. <https://doi.org/10.2522/ptj.20150271>
- Lee, S. J., & Chun, M. H. (2014). Combination Transcranial Direct Current Stimulation and Virtual Reality Therapy for Upper Extremity Training in Patients With Subacute Stroke. *Archives of Physical Medicine and Rehabilitation*, *95*(3), 431–438. <https://doi.org/10.1016/j.apmr.2013.10.027>
- Levin, M. F., Snir, O., Liebermann, D. G., Weingarden, H., & Weiss, P. L. (2012). Virtual reality versus conventional treatment of reaching ability in chronic stroke: clinical feasibility study. *Neurology and Therapy*, *1*(1), 3. <https://doi.org/10.1007/s40120-012-0003-9>
- Likert, R. (1932). A Technique for the Measurement of Attitudes. *Archives of Psychology*, *140*, 1–55.
- Lin, J., Kelleher, C. L., & Engsberg, J. R. (2013). Developing Home-Based Virtual Reality Therapy Interventions. *Games for Health Journal*, *2*(1), 34–38. <https://doi.org/10.1089/g4h.2012.0033>
- Lu, X. (2018). A Review of Solutions for Perspective-n-Point Problem in Camera Pose Estimation. *Journal of Physics: Conference Series*, *1087*, 52009. <https://doi.org/10.1088/1742-6596/1087/5/052009>
- Lukezic, A., Vojir, T., Čehovin Zajc, L., Matas, J., & Kristan, M. (2017). Discriminative correlation filter with channel and spatial reliability. *Proceedings of the IEEE Conference on Computer Vision and Pattern Recognition*, 6309–6318. <https://doi.org/10.1109/CVPR.2017.515>

- Mack, E. (2015). *Myo gesture control armband review: Pointless or ahead of its time?* New Atlas. <https://newatlas.com/myo-gesture-control-armband-review/39103/#:~:text=If you want more gesture,the Myo armband in action.>
- Maiya, S. R. (2019). *Single object tracking*. Nanonets. <https://nanonets.com/blog/object-tracking-deepsort/>
- MatLab. (2021). *Ground Truth Labeler*. <https://www.mathworks.com/help/driving/ref/groundtruthlabeler-app.html>
- Mauro, A., Azzaro, C., Albani, G., Ferraris, C., Nerino, R., Chimienti, A., Pettiti, G., & Contin, L. (2014). *System and method for motion capture*. <https://patents.google.com/patent/US10092220B2/>
- McDermott, E. J., & Himmelbach, M. (2019). Effects of arm weight and target height on hand selection: A low-cost virtual reality paradigm. *PloS One*, 14(6), e0207326. <https://doi.org/10.1371/journal.pone.0207326>
- Microsoft. (2021). *Azure Kinect DK*. <https://www.microsoft.com/en-us/d/azure-kinect-dk/8pp5vxmd9nhq?activetab=pivot:overviewtab>
- Mobini, A., Behzadipour, S., & Saadat, M. (2015). Test-retest reliability of Kinect's measurements for the evaluation of upper body recovery of stroke patients. *Biomedical Engineering Online*, 14, 75. <https://doi.org/10.1186/s12938-015-0070-0>
- Moher, D., Liberati, A., Tetzlaff, J., & Altman, D. G. (2009). Preferred reporting items for systematic reviews and meta-analyses: the PRISMA statement. *PLoS Medicine*, 6(7), e1000097. <https://doi.org/10.1371/journal.pmed.1000097>
- Nakayama, H., Jørgensen, H. S., Raaschou, H. O., & Olsen, T. S. (1994). Recovery of upper extremity function in stroke patients: the Copenhagen Stroke Study. *Archives of Physical Medicine and Rehabilitation*, 75(4), 394–398. [https://doi.org/10.1016/0003-9993\(94\)90161-9](https://doi.org/10.1016/0003-9993(94)90161-9)
- Norouzi-Gheidari, N, Levin, M. F., Fung, J., & Archambault, P. (2013). Interactive virtual reality game-based rehabilitation for stroke patients. *2013 International Conference on Virtual Rehabilitation (ICVR)*, 220–221. <https://doi.org/10.1109/ICVR.2013.6662126>
- Norouzi-Gheidari, Nahid, Hernandez, A., Archambault, P. S., Higgins, J., Poissant, L., & Kairy, D. (2020). Feasibility, Safety and Efficacy of a Virtual Reality Exergame System to Supplement Upper Extremity Rehabilitation Post-Stroke: A Pilot Randomized Clinical Trial and Proof of Principle. *INTERNATIONAL JOURNAL OF ENVIRONMENTAL RESEARCH AND PUBLIC HEALTH*, 17(1). <https://doi.org/10.3390/ijerph17010113>
- Ogun, M. N., Kurul, R., Yasar, M. F., Turkoglu, S. A., Avci, S., & Yildiz, N. (2019). Effect of Leap Motion-based 3D Immersive Virtual Reality Usage on Upper Extremity Function in Ischemic Stroke Patients. *Arquivos de Neuro-Psiquiatria*, 77(10), 681–688. <https://doi.org/10.1590/0004-282X20190129>
- OpenCV. (2020a). *OpenCV - About*. <https://opencv.org/about/>
- OpenCV. (2020b). *OpenCV modules*. <https://docs.opencv.org/master/index.html>
- Prange, G., Krabben, T., Molier, B., van der Kooij, H., & Jannink, M. (2008). A low-tech virtual reality application for training of upper extremity motor function in neurorehabilitation. *2008 Virtual Rehabilitation*, 8–12. <https://doi.org/10.1109/ICVR.2008.4625113>
- Proffitt, R. M., Henderson, W., Scholl, S., & Nettleton, M. (2018). Lee Silverman Voice Treatment BIG((R)) for a Person With Stroke. *The American Journal of Occupational Therapy : Official Publication of the American Occupational Therapy Association*, 72(5), 7205210010p1-7205210010p6. <https://doi.org/10.5014/ajot.2018.028217>
- Pyae, A., Luimula, M., & Smed, J. (2015). Rehabilitative Games for Stroke Patients. *EAI Endorsed Trans. Serious Games*, 1(4), e2. <https://doi.org/10.4108/sg.1.4.e2>
- Rabin, B., Burdea, G., Hundal, J., Roll, D., & Damiani, F. (2011). Integrative motor, emotive and cognitive therapy for elderly patients chronic post-stroke A feasibility study of the

- BrightArm rehabilitation system. *2011 International Conference on Virtual Rehabilitation*, 1–8. <https://doi.org/10.1109/ICVR.2011.5971852>
- Rand, D., Katz, N., & Weiss, P. L. (2009). Intervention using the VMall for improving motor and functional ability of the upper extremity in post stroke participants. *European Journal of Physical and Rehabilitation Medicine*, *45*(1), 113–121.
- Rand, Debbie, Weingarden, H., Weiss, R., Yacoby, A., Reif, S., Malka, R., Shiller, D. A., & Zeilig, G. (2017). Self-training to improve UE function at the chronic stage post-stroke: a pilot randomized controlled trial. *Disability and Rehabilitation*, *39*(15), 1541–1548. <https://doi.org/10.1080/09638288.2016.1239766>
- Reinthal, A., Szirony, K., Clark, C., Swiers, J., Kellicker, M., & Linder, S. (2012). ENGAGE: Guided Activity-Based Gaming in Neurorehabilitation after Stroke: A Pilot Study. *Stroke Research and Treatment*, *2012*, 784232. <https://doi.org/10.1155/2012/784232>
- Reis, A., Lains, J., Paredes, H., Filipe, V., Abrantes, C., Ferreira, F., Mendes, R., Amorim, P., & Barroso, J. (2016). *Developing a System for Post-Stroke Rehabilitation: An Exergames Approach BT - Universal Access in Human-Computer Interaction. Users and Context Diversity* (M. Antona & C. Stephanidis (eds.); pp. 403–413). Springer International Publishing. [https://doi.org/10.1007/978-3-319-40238-3\\_39](https://doi.org/10.1007/978-3-319-40238-3_39)
- Rosebrock, A. (2020). *Start Here with Computer Vision, Deep Learning, and OpenCV. PyImageSearch*. <https://www.pyimagesearch.com/start-here/>
- Roy, A. K., Soni, Y., & Dubey, S. (2013). Enhancing effectiveness of motor rehabilitation using kinect motion sensing technology. *2013 IEEE Global Humanitarian Technology Conference: South Asia Satellite (GHTC-SAS)*, 298–304. <https://doi.org/10.1109/GHTC-SAS.2013.6629934>
- Rubio Ballester, B., Bermudez i Badia, S., & Verschure, P. F. M. J. (2012). Including Social Interaction in Stroke VR-Based Motor Rehabilitation Enhances Performance: A Pilot Study. *Presence*, *21*(4), 490–501. [https://doi.org/10.1162/PRES\\_a\\_00129](https://doi.org/10.1162/PRES_a_00129)
- Sampson, M., Shau, Y.-W., & King, M. J. (2012). Bilateral upper limb trainer with virtual reality for post-stroke rehabilitation: case series report. *Disability and Rehabilitation. Assistive Technology*, *7*(1), 55–62. <https://doi.org/10.3109/17483107.2011.562959>
- Saposnik, G. (2016). Virtual reality in stroke rehabilitation. In *Ischemic stroke therapeutics* (pp. 225–233). Springer. [https://doi.org/10.1007/978-3-319-17750-2\\_22](https://doi.org/10.1007/978-3-319-17750-2_22)
- Saposnik, G., & Levin, M. (2011). Virtual reality in stroke rehabilitation: a meta-analysis and implications for clinicians. *Stroke*, *42*(5), 1380–1386. <https://doi.org/10.1161/STROKEAHA.110.605451>
- Schaham, N. G., Zeilig, G., Weingarden, H., Rand, D., Givon Schaham, N., Zeilig, G., Weingarden, H., & Rand, D. (2018). Game analysis and clinical use of the Xbox-Kinect for stroke rehabilitation. *International Journal of Rehabilitation Research. Internationale Zeitschrift Fur Rehabilitationsforschung. Revue Internationale de Recherches de Readaptation*, *41*(4), 323–330. <https://doi.org/10.1097/MRR.0000000000000302>
- Schüler, T., Drehlmann, S., Kane, F., & Piekartz, H. von. (2013). Abstract virtual environment for motor rehabilitation of stroke patients with upper limb dysfunction. A pilot study. *2013 International Conference on Virtual Rehabilitation (ICVR)*, 184–185. <https://doi.org/10.1109/ICVR.2013.6662117>
- Schweighofer, N. (2019). *Method and system for motion measurement and rehabilitation*. <https://patents.google.com/patent/US20200197744A1/>
- Seyedebrahimi, A., Khosrowabadi, R., & Hondori, H. M. (2019). Brain Mechanism in the Human-Computer Interaction Modes Leading to Different Motor Performance. *2019 27th Iranian Conference on Electrical Engineering (ICEE)*, 1802–1806. <https://doi.org/10.1109/IranianCEE.2019.8786750>
- Shin, J.-H., Bog Park, S., & Ho Jang, S. (2015). Effects of game-based virtual reality on health-

- related quality of life in chronic stroke patients: A randomized, controlled study. *Computers in Biology and Medicine*, 63, 92–98. <https://doi.org/10.1016/j.compbiomed.2015.03.011>
- Shin, J.-H., Ryu, H., & Jang, S. H. (2014). A task-specific interactive game-based virtual reality rehabilitation system for patients with stroke: a usability test and two clinical experiments. *Journal of Neuroengineering and Rehabilitation*, 11, 32. <https://doi.org/10.1186/1743-0003-11-32>
- Shiri, S., Feintuch, U., Lorber-Haddad, A., Moreh, E., Twito, D., Tuchner-Arieli, M., & Meiner, Z. (2012a). Novel virtual reality system integrating online self-face viewing and mirror visual feedback for stroke rehabilitation: rationale and feasibility. *Topics in Stroke Rehabilitation*, 19(4), 277–286. <https://doi.org/10.1310/tsr1904-277>
- Shiri, S., Feintuch, U., Lorber-Haddad, A., Moreh, E., Twito, D., Tuchner-Arieli, M., & Meiner, Z. (2012b). A Novel Virtual Reality System Integrating Online Self-Face Viewing and Mirror Visual Feedback for Stroke Rehabilitation: Rationale and Feasibility. *Topics in Stroke Rehabilitation*, 19(4), 277–286. <https://doi.org/10.1310/tsr1904-277>
- Sin, H., & Lee, G. (2013). Additional virtual reality training using Xbox Kinect in stroke survivors with hemiplegia. *American Journal of Physical Medicine & Rehabilitation*, 92(10), 871–880. <https://doi.org/10.1097/PHM.0b013e3182a38e40>
- Subramanian, S., Knaut, L. A., Beaudoin, C., McFadyen, B. J., Feldman, A. G., & Levin, M. F. (2006). Virtual Reality Environments for Rehabilitation of the Upper Limb after Stroke. *2006 International Workshop on Virtual Rehabilitation*, 18–23. <https://doi.org/10.1109/IWVR.2006.1707520>
- Sucar-Succar, L. E., Luis-Valasquez, R., Azcarate-Hernandez, G., Leder, R. S., & Reinkensmeyer, D. (2011). *3d monocular visual tracking therapy system for the rehabilitation of human upper limbs* (Patent No. CA2731775A1). <https://patents.google.com/patent/CA2731775A1/>
- Sucar, L. E., Leder, R., Hernandez, J., Sanchez, I., & Azcarate, G. (2009). Clinical evaluation of a low-cost alternative for stroke rehabilitation. *2009 IEEE International Conference on Rehabilitation Robotics*, 863–866. <https://doi.org/10.1109/ICORR.2009.5209526>
- Sucar, L. E., Orihuela-Espina, F., Velazquez, R. L., Reinkensmeyer, D. J., Leder, R., & Hernandez-Franco, J. (2014). Gesture Therapy: An Upper Limb Virtual Reality-Based Motor Rehabilitation Platform. *IEEE Transactions on Neural Systems and Rehabilitation Engineering*, 22(3), 634–643. <https://doi.org/10.1109/TNSRE.2013.2293673>
- Sunderland, A., Tinson, D., Bradley, L., & Hewer, R. L. (1989). Arm function after stroke. An evaluation of grip strength as a measure of recovery and a prognostic indicator. *Journal of Neurology, Neurosurgery, and Psychiatry*, 52(11), 1267–1272. <https://doi.org/10.1136/jnnp.52.11.1267>
- Thielbar, K. O., Triandafilou, K. M., Barry, A. J., Yuan, N., Nishimoto, A., Johnson, J., Stoykov, M. E., Tsoupikova, D., & Kamper, D. G. (2020). Home-based Upper Extremity Stroke Therapy Using a Multiuser Virtual Reality Environment: A Randomized Trial. *Archives of Physical Medicine and Rehabilitation*, 101(2), 196–203. <https://doi.org/10.1016/j.apmr.2019.10.182>
- Thomson, K., Pollock, A., Bugge, C., & Brady, M. C. (2016). Commercial gaming devices for stroke upper limb rehabilitation: a survey of current practice. *Disability and Rehabilitation. Assistive Technology*, 11(6), 454–461. <https://doi.org/10.3109/17483107.2015.1005031>
- TreeIt. (2021). *TreeIt*. <https://www.evolved-software.com/treeit/treeit>
- Unity. (2021a). *OpenCV Plus Unity*. <https://assetstore.unity.com/packages/tools/integration/opencv-plus-unity-85928>
- Unity. (2021b). *Unity*. <https://unity.com/>

- Vanbellinghen, T., Filius, S. J., Nyffeler, T., & van Wegen, E. E. H. (2017). Usability of Videogame-Based Dexterity Training in the Early Rehabilitation Phase of Stroke Patients: A Pilot Study. *Frontiers in Neurology*, *8*, 654. <https://doi.org/10.3389/fneur.2017.00654>
- Vectr. (2021). *Vectr*.
- Virani, S. S., Alonso, A., Benjamin, E. J., Bittencourt, M. S., Callaway, C. W., Carson, A. P., Chamberlain, A. M., Chang, A. R., Cheng, S., Delling, F. N., Djousse, L., Elkind, M. S. V, Ferguson, J. F., Fornage, M., Khan, S. S., Kissela, B. M., Knutson, K. L., Kwan, T. W., Lackland, D. T., ... Tsao, C. W. (2020). Heart Disease and Stroke Statistics-2020 Update: A Report From the American Heart Association. *Circulation*, *141*(9), e139–e596. <https://doi.org/10.1161/CIR.0000000000000757>
- Vourvopoulos, A., Faria, A. L., Cameirao, M. S., & Bermudez i Badia, S. (2013). RehabNet: A distributed architecture for motor and cognitive neuro-rehabilitation. *2013 IEEE 15th International Conference on E-Health Networking, Applications and Services (Healthcom 2013)*, 454–459. <https://doi.org/10.1109/HealthCom.2013.6720719>
- Wade, D. T., Langton-Hewer, R., Wood, V. A., Skilbeck, C. E., & Ismail, H. M. (1983). The hemiplegic arm after stroke: measurement and recovery. *Journal of Neurology, Neurosurgery, and Psychiatry*, *46*(6), 521–524. <https://doi.org/10.1136/jnnp.46.6.521>
- Wairagkar, M., McCrindle, R., Robson, H., Meteyard, L., Sperrin, M., Smith, A., & Pugh, M. (2017). MaLT - Combined Motor and Language Therapy Tool for Brain Injury Patients Using Kinect. *Methods of Information in Medicine*, *56*(2), 127–137. <https://doi.org/10.3414/ME16-02-0015>
- Wang, Q., Markopoulos, P., Yu, B., Chen, W., & Timmermans, A. (2017). Interactive wearable systems for upper body rehabilitation: a systematic review. *Journal of Neuroengineering and Rehabilitation*, *14*(1), 20. <https://doi.org/10.1186/s12984-017-0229-y>
- Wang, R., Paris, S., & Popović, J. (2011). Practical Color-Based Motion Capture. *Proceedings of the 2011 ACM SIGGRAPH/Eurographics Symposium on Computer Animation*, 139–146. <https://doi.org/10.1145/2019406.2019425>
- Warren, T. (2019). *Microsoft shrinks Kinect into a \$399 cloud-powered PC peripheral*. The Verge. <https://www.theverge.com/2019/2/24/18237244/microsoft-azure-kinect-developer-kit-price-release-date-mwc-2019>
- Wii. (2021). *Wii | Nintendo*. <https://www.nintendo.pt/Wii/Wii-94559.html>
- Willmann, R. D., Lanfermann, G., Bongers, E. G. J. M., & Vrugt, J. T. (2007). *Health management device*. <https://patents.google.com/patent/US20090259148A1/>
- Wu, Y., Lim, J., & Yang, M. (2013). Online Object Tracking: A Benchmark. *2013 IEEE Conference on Computer Vision and Pattern Recognition*, 2411–2418. <https://doi.org/10.1109/CVPR.2013.312>
- Xbox. (2021). *Xbox Official Site: Consoles, Games, and Community | Xbox*. <https://www.xbox.com/>
- Yang, Z., Rafiei, M. H., Hall, A., Thomas, C., Midtlien, H. A., Hasselbach, A., Adeli, H., & Gauthier, L. V. (2018). A Novel Methodology for Extracting and Evaluating Therapeutic Movements in Game-Based Motion Capture Rehabilitation Systems. *Journal of Medical Systems*, *42*(12), 255. <https://doi.org/10.1007/s10916-018-1113-4>
- Yaqin Tao, & Huosheng Hu. (2004). Colour based human motion tracking for home-based rehabilitation. *2004 IEEE International Conference on Systems, Man and Cybernetics (IEEE Cat. No.04CH37583)*, *1*, 773–778 vol.1. <https://doi.org/10.1109/ICSMC.2004.1398396>
- Yavuzer, G., Senel, A., Atay, M. B., & Stam, H. J. (2008). “Playstation eyetoy games” improve upper extremity-related motor functioning in subacute stroke: a randomized controlled clinical trial. *European Journal of Physical and Rehabilitation Medicine*, *44*(3), 237–244. <https://doi.org/10.1016/j.apmr.2007.08.162>

- Yeh, S., Lee, S., Chan, R., & Chen, S. (2019). A Kinect-Based System for Stroke Rehabilitation. *2019 Twelfth International Conference on Ubi-Media Computing (Ubi-Media)*, 192–198. <https://doi.org/10.1109/Ubi-Media.2019.00045>
- Yilmaz, A., Javed, O., & Shah, M. (2006). Object tracking: A Survey. *ACM Computing Surveys*, 38, 1–45. <https://doi.org/10.1145/1177352.1177355>
- Zhang, Z. (2014). *Camera Calibration*. *Computer Vision*. [https://doi.org/10.1007/978-0-387-31439-6\\_164](https://doi.org/10.1007/978-0-387-31439-6_164). [https://doi.org/10.1007/978-0-387-31439-6\\_164](https://doi.org/10.1007/978-0-387-31439-6_164)